Pre-trial of hepatocellular carcinoma on cirrhosis in a rat model

Ayça Zeybek

THÈSE

Pour obtenir le grade de

DOCTEUR DE LA COMMUNAUTE UNIVERSITE GRENOBLE ALPES

préparée dans le cadre d'une cotutelle entre la Communauté Université Grenoble Alpes et Izmir Institute of Technology, Turquie

Spécialité : **Chimie Biologie**

Arrêté ministériel : le 6 janvier 2005 - 7 août 2006

Présentée par

«Ayça ZEYBEK KUYUCU»

Thèse dirigée par **« Patrice MARCHE »** et **« Thomas DECAENS»** et codirigée par **« Gülşah ŞANLI »**

préparée au sein du **Laboratoire Immunologie Analytique des Pathologies Chroniques, IAB**
de **l'École Doctorale Chimie et Science du Vivant**

Essai du traitement pré-clinique du carcinome hépatocellulaire sur la cirrhose dans le modèle de rat

Thèse soutenue publiquement le **« 22/12/2016 »**,
devant le jury composé de :

M, Serdar, ÖZÇELİK (Président)
M, Hervé , LERAT (Rapporteur)
Mme, Şenay, ŞANLIER (Rapporteur)
M, Mehmet, ÖZTÜRK (Rapporteur)
Mme, Neşe, ATABEY(Membre)
Mme, Gülşah, ŞANLI (Membre)
M, Patrice, MARCHE (Membre)

PRE-CLINICAL TRIAL TREATMENT OF HEPATOCELLULAR CARCINOMA ON CIRRHOSIS IN A RAT MODEL

by
Ayça ZEYBEK KUYUCU

December 2016

ACKNOWLEDGEMENTS

Firstly, I would like to express my sincere gratitude to my supervisors Prof. Dr. Patrice MARCHE and Assoc. Dr. Gülşah ŞANLI for the continuous support of my Ph.D. study and related research which is the first step of my academic career. I would also like to thank them for encouraging my research and allowing me to grow as a research scientist. Their advice on both research as well as on my career has been priceless. From the beginning of my academic life, their incomparable guidance, understanding, encouragement, confidence and everlasting support have maximized my motivation and have helped me to carry out this project by keeping warm the love of science in my heart. It is a big honor to work with such a wonderful person.

I would like to express my gratitude to my advisors Prof. Thomas Decaens and Dr. Zuzana Macek Jílková for their insightful comments and encouragement, but also for the hard question which incented me to widen my research from various perspectives. Their guidance helped me in all the time of research and writing of this thesis.

During my Ph.D at Grenoble in Institute for Advanced Biosciences (IAB), I would like to thank Team Marche members, especially Ph.D. students Keerthi Kurma and Gael Roth, who were able to give me a real human dimension and share their experiences and culture.

I would also like to express my appreciations to my thesis committee, Prof. Dr. Serdar Özçelik and Prof. Dr. Neşe Atabey for their kindly help and advice. Besides this, I would also like to thank to Hervé LERAT for his suggestions to writing thesis.

I am grateful to my dear friends Murat Delman, Ayşegül Örs, and Şanlı Laboratory members for their good friendship, encouragements, and constructive comments.

My special thanks; I owe my parents a great debt of gratitude for their everlasting support, motivation, patience, and limitless love. Especially my husband Arif Yiğit Kuyucu has been a constant source of support and encouragement during the challenges of graduate school and life. I am truly thankful for having him in my life.

I would also like to thank the Scientific and Technological Research Council of Turkey (TÜBİTAK 2214/B International Joint PhD Fellowship Programme) and Campus France for their financial support.

The Institute for Advanced Biosciences (IAB) is an internationally renowned institute in basic biomedical and translational research in the areas of epigenetic, chronic diseases and cancer. The IAB is supported jointly by the National Institute of Health and Medical Research (INSERM), the University of Grenoble Alpes (UGA) and the National Centre for Scientific Research (CNRS).

My study was conducted in the Prevention and Therapy of chronic diseases Department in the IAB in collaboration with an IRMaGE platform in the Grenoble Institute of Neuroscience (GIN, INSERM, and University of Grenoble-Alpes, France).

ABSTRACT

PRE-CLINICAL TRIAL TREATMENT OF HEPATOCELLULAR CARCINOMA ON CIRRHOSIS IN A RAT MODEL

Hepatocellular carcinoma (HCC) is the second most common cause of cancerrelated mortality worldwide. AKT pathway has been found activated in 50% of HCC cases, making it promising target. Therefore we assess efficacy of the allosteric AKT inhibitor or the combination of Sorafenib with AKT inhibitor compared to untreated control and to standard treatment, Sorafenib, in vitro and in vivo. AKT inhibitor blocked phosphorylation of AKT in vitro and strongly inhibited cell growth and migration with significantly higher potency than Sorafenib. Similarly, apoptotic cell was strongly increased by AKT inhibitor in vitro. To mimic human advanced HCC, we used diethylnitrosamine-induced cirrhotic rat model with fully developed HCC. MRI analyses showed that AKT inhibitor significantly reduced overall tumor size. Furthermore, number of tumors was decreased by AKT inhibitor, which was associated with increased apoptosis and decreased proliferation. Tumor contrast enhancement was significantly decreased in the AKT inhibitor group. Moreover, on tumor tissue sections, we observed a vascular normalization and a significant decrease in fibrosis in surrounding liver of animals treated with AKT inhibitor. Finally, pAKT/AKT levels in AKT inhibitor treated tumors were reduced, followed by down regulation of actors of AKT downstream signalling pathway: pmTOR, pPRAS40, pPLCγ1 and pS6K1. In conclusion, we demonstrated that AKT inhibitor blocks AKT phosphorylation in vitro and in vivo. In HCC-rat model, AKT inhibitor was well tolerated, showed anti-fibrotic effect and had stronger antitumor effect than Sorafenib. Our results confirm the importance of targeting AKT in HCC.

Key words: HCC, Sorafenib, AKT inhibitor, PI3K/AKT/mTOR pathway, target therapy, DEN, cirrhosis, rat, animal model.

RESUME

Le carcinome hépatocellulaire (CHC) est l'un des cancers les plus courants dans le monde entier avec la deuxième plus forte mortalité parmi tous les cancers. PI3K/AKT/mTOR et MAPK/ERK sont les deux grandes voies de signalisation reconnues comme cibles pour la thérapie du cancer du foie. Le Sorafenib, étant le seul traitement systémique approuvé, cible plusieurs voies de signalisation conduisant à l'inhibition de la voie MAPK. En revanche, une exposition long terme au Sorafénib influence la voie PI3K et régularise positivement la phosphorylation de ses cibles en aval, notamment AKT, qui provoque la résistance du CHC du Sorafénib. Ainsi, étant une nouvelle stratégie thérapeutique, la combinaison du Sorafénib avec des inhibiteurs AKT est étudiée dans un modèle de rats cirrhotiques induit par DEN développant le CHC.

Nos résultats de IRM ont montré une faible progression tumorale, un nombre de tumeurs réduit et une taille plus faible des tumeurs chez les rats traités avec une nouvelle stratégie thérapeutique associant inhibiteur d'AKT et Sorafenib. En outre, notre analyse western blot a montré une inhibition forte et sélective de la voie d'AKT soit pour le seul inhibiteur d'AKT soit pour un traitement de combinaison, ce qui indique la spécificité de cette molécule. En conclusion, nos résultats confirment l'importance du ciblage d'AKT dans le développement et la progression du CHC.

TABLE OF CONTENTS

LIST OF FIGURES

Figure **Page**

LIST OF TABLES

Table **Page**

CHAPTER 1

INTRODUCTION

1.1. Cancer

Cancer is a disease that means abnormal cell growth with the potential to invade or spread to other parts of the body. Normal cells grow, divide and die because they have many control mechanisms. Cancer cells have disorders in control mechanisms that manage how often they divide, and in the feedback systems that regulate these control mechanisms (Evan and Vousden 2001). Cancer cell genotypes share six common traits in cell physiology that govern the transformation of normal cells to cancer cells, as shown in figure 1.1 (Hanahan and Weinberg 2000).

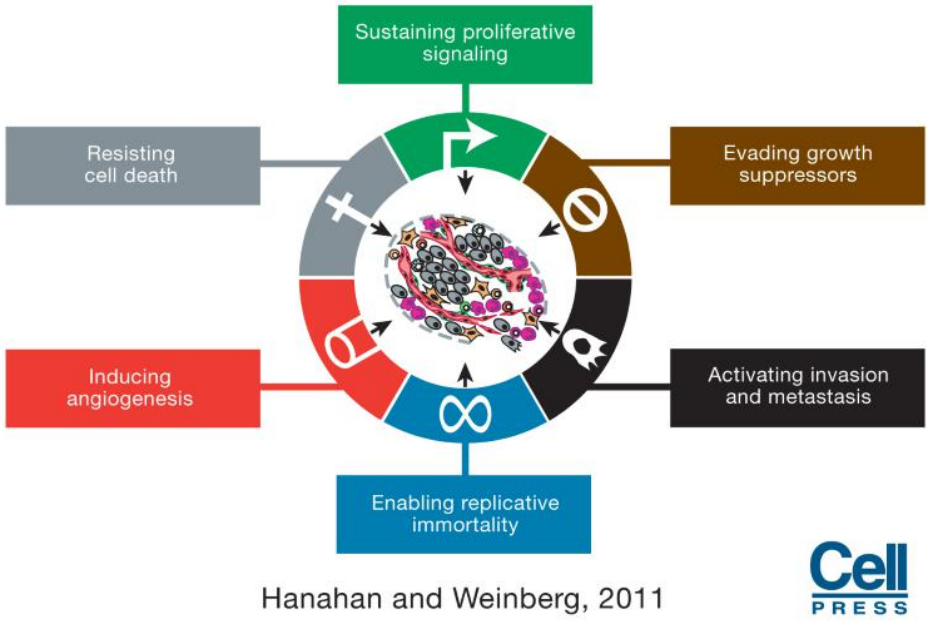

Figure 1.1. Acquired Capabilities of Cancer (Source: (Hanahan and Weinberg 2011)).

First hallmark of cancer is “sell-sufficiency in growth signal”. When normal cells move from a quiescent state into an active proliferative state, they have need for mitogenic growth signals. No type of normal cell can proliferate in the absence of such

stimulatory signal. However, cancer cells do not require stimulation to grow from external signal. Second hallmark of it is “insensitivity to antigrowth signals”. Multiple anti-proliferative signals act to maintain cellular quiescence and tissue homeostasis within a normal tissue. If cells are forced out of the active proliferative cycle into the G_0 state or cells are induced to permanently abdicate their proliferative potential, antigrowth signals can block proliferation. Cancer cells are usually resistant to these signals. Third hallmark of it is “evading apoptosis”. Apoptosis is controlled by a complex network of proliferation and survival genes that is frequently disrupted during tumor evolution (Wendel, Stanchina et al. 2004). Cancer cells are able to be resistant to this mechanism. For example, when p53 tumor suppressor gene is inactivated or the PI3 kinase–AKT/PKB pathway, which transmits antiapoptotic survival signal is activated, cell cycle progression increases and control cell death decreases (Vivanco and Sawyers 2002). A fourth hallmark of it is “limitless replicative potential”. Cell populations that have progressed through a certain number of doubling, stop growing— and end up in a process termed senescence (Hayflick 1997). On the other hand, cancer cells have the ability to divide indefinitely. Due to damage chromosomes, immortal cells can become cancerous (Hanahan and Weinberg 2011). Fifth hallmark of cancer is “sustained angiogenesis”. The oxygen and nutrients supplied by the vasculature are crucial for cell function and survival. When a tissue is formed, the process of angiogenesis that is the growth of new blood vessels is transitory and carefully regulated. During tumor development, sustain angiogenesis seems to be acquired in a discrete step via an “angiogenic switch” from vascular quiescence (Bergers and Benjamin 2003). Final hallmark of cancer is “tissue invasion and metastasis”. Later during the development of most of cancer, cancer cells move out, and invade adjacent tissue. They travel to distant sites or organs, where they succeed in creating new colonies (van Zijl, Krupitza et al. 2011).

1.2. Liver Cancer

Liver is the largest glandular organ in the body and it is responsible for various critical functions to keep the body free of toxins and harmful substances. Liver cancer is classified primary cancer which begins in the cells of the liver and secondary cancer that develops from cells from other organs that spread to the liver. Unfortunately, it is

the second leading cause of cancer related mortality worldwide (Siegel, Miller et al. 2016). According to GLOBAL statistic, liver cancer is largely a problem of the less developed regions and showed in table 1. Most primary liver cancers are classified as hepatocellular carcinoma (HCC). Current evidence indicates that during hepatocarcinogenesis, two main pathogenic mechanisms prevail: (1) cirrhosis associated with hepatic regeneration after tissue damage caused by hepatitis infection, toxins (for example, alcohol or aflatoxin) or metabolic influences, and (2) mutations occurring in single or multiple oncogenes or tumor suppressor genes. Approximately 90 % of HCC are associated with underlying cirrhosis, which corresponds to the latest stage of liver fibrosis (Shibata and Aburatani 2014). HCC is followed by intrahepatic cholangiocarcinoma (IHCC) (Jemal, Bray et al. 2011).

Table 1. Estimated liver cancer cases, mortality and 5-year prevalence worldwide in 2012 for men and women.

Estimated numbers (thousands)	**Men**			**Women**		
	Cases	Deaths	5-year prev.	Cases	Deaths	5-year prev.
World	554	521	453	228	224	180
More developed regions	92	80	112	42	43	51
Less developed regions	462	441	341	186	182	129
WHO Africa region (AFRO)	25	24	17	14	13	9
WHO Americas region (PAHO)	40	35	35	23	23	18
WHO East Mediterranean region (EMRO)	20	19	12	10	9	6
WHO Europe region (EURO)	47	44	42	23	25	20
WHO South-East Asia region (SEARO)	55	52	33	25	24	15
WHO Western Pacific region (WPRO)	368	347	314	133	129	112
IARC membership (24 countries)	120	104	135	56	55	60
United States of America	23	17	21	8	7	7
China	293	282	220	101	101	71
India	17	17	8	10	10	5
European Union (EU-28)	36	32	33	16	17	14

Chronic liver damage, such as that caused by chronic hepatitis, liver cirrhosis and fatty liver disease, is closely associated with the occurrence of liver cancer (Forner, Llovet et al. 2012) (El-Serag 2012). Liver cirrhosis is the end-stage disease of chronic liver injury. A growing number of studies show that cirrhosis is caused by different factor such as hepatitis B and C, chronic alcoholism, or non-alcoholic steato-hepatitis (NASH) due to dysmetabolism (Poynard, Bedossa et al. 1997). Besides this, parasites such as liver fluke are associated with IHCC in Southeast Asian countries (Shaib and El-Serag 2004). Interindividual variation of time span from normal liver to fibrotic and cirrhotic stages suggested potential influence of congenital variations. Advances in genotyping techniques allowed to identify the relation of liver fibrosis and cirrhosis to different etiologies (Kitamoto, Kitamoto et al. 2013) (Zimmer and Lammert 2011). Inflammation of the liver is also a cause of HCC (Haybaeck, Zeller et al. 2009).

HCC is the leading cause of death among patients with cirrhosis (Forner, Llovet et al. 2012) (Siegel, Ma et al. 2014). Several pathways have been showed to be involved in HCC pathogenesis (Figure 1.2.) (Shibata and Aburatani 2014), such as PI3K/Akt/mTOR, EGFR, Ras/Raf/mitogen activated protein kinase (MEK)/extracellular signal regulated kinase (ERK), and IGFR pathways (Finn 2013).

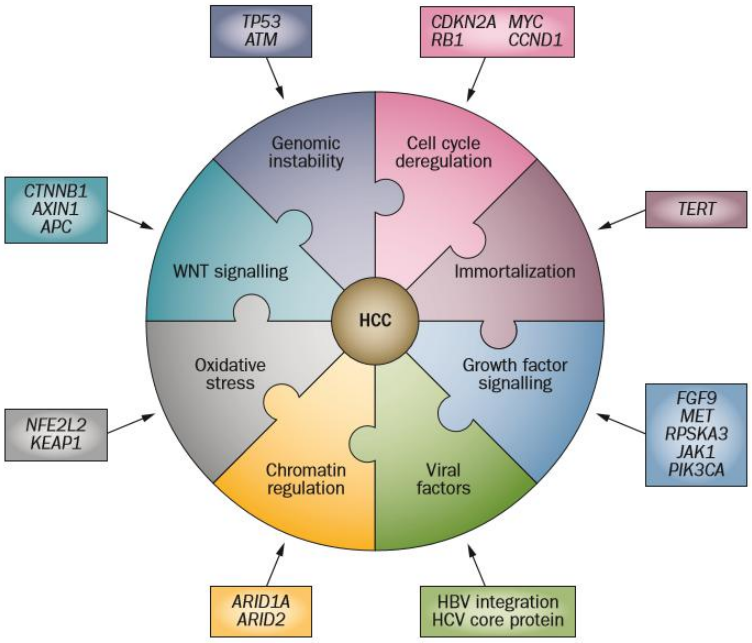

Figure 1.2. Oncogenic pathways in hepatocarcinogenesis (Source: (Shibata and Aburatani 2014)).

1.2.1. Signaling Pathways Involved in HCC Pathogenesis

HCC is highly vascularized tumor, and the central role of angiogenesis in its initiation, growth, and subsequent dissemination to other tissues is well recognized. Angiogenesis in HCC is dependent on endothelial cell activation, proliferation, and migration, which occur in response to angiogenic cues (e.g., inflammation) and involves several molecular effectors such as growth factors, extra-cellular matrix proteins, and proteases (Sanz-Cameno, Trapero-Marugán et al. 2010).

HCCs usually have an intermediate number of mutations genome (Li and Mao 2013). TP53 is the top gene among recurrently mutated genes in HCC, and its mutation frequency varies approximately 25.9% of HCCs (Hussain, Schwank et al. 2007). In addition, upstream regulator of TP53 activation, ATM and target of TP53, CDKN1A genes have also been reported as mutation genes (Shiloh and Ziv 2013). Moreover, mutations of the IRF2 gene, which encodes a positive regulator of TP53 protein expression, are mutually exclusive to the TP53 mutation with HCC (Guichard, Amaddeo et al. 2012). Cell senescence is regulated by RB and CDKN2A. In HCC cases, RB and CDKN2A genes mutations have been reported (Zhang, Guo et al. 2008). Activation of telomerase (encoded by the TERT gene), which is physiologically silenced in most normal cells, is required for infinite replication in cancer cells. TERT promoter mutations have been seen in 54% of human HCCs and 25% of cirrhotic preneoplastic nodules, and this case could be the earliest recurrent genetic event in hepatocarcinogenesis (Nault, Mallet et al. 2013). WNT signalling is a driving molecular event in a wide range of tumours, including liver cancers (Polakis 2000). CTNNB1, also APC and AXIN1, which are tumour suppressor genes are frequently reported in HCC (10.0−32.8%) and hepatoblastoma (Oda, Imai et al. 1996) (Shibata and Aburatani 2014). The NFE2L2 gene encodes a sequence-specific transcript ional factor that upregulates genes associated with oxidative stress and other metabolic pathways (Taguchi, Motohashi et al. 2011). Activating mutations of this gene have been recurrently reported in HCC (Guichard, Amaddeo et al. 2012). Protein-phosphorylation enzymes are activated via binding of growth factors to their receptor proteins, thus activating proliferative signaling pathway to transfer signals into the nucleus. Growth factor, such as epidermal growth factor (EGF), transforming growth factor (TGF)-α/-β, insulin-like growth factor (IGF) and vascular endothelial growth factor (VEGF), also

function in liver regeneration after injury, while fibroblast growth factor (FGF) and the platelet-derived growth factor (PDGF) family are involved in liver fibrosis and HCC growth (Höpfner, Schuppan et al. 2008). The lost of the growth factor reseptor and oncogenes include tyrosine kinase activity. The tyrosine kinases are classified into transmembrane receptor tyrosine kinases such as the EGFR and VEGFR. However, Raf, MAP kinase/ERK kinase (MEK) and mammalian target of rapamycin (mTOR) are serine/threonine kinases. In general, the mitogen-activated protein kinase (MAPK), phosphoinositide 3-kinase (PI3K)/Akt/mTOR signaling pathways, and the VEGFR (VEGFR -1, -2, and -3) and PDGFR signaling cascades show altered activity in HCC. These cascades is demonstrated in figure 1.3 (Whittaker, Marais et al. 2010).

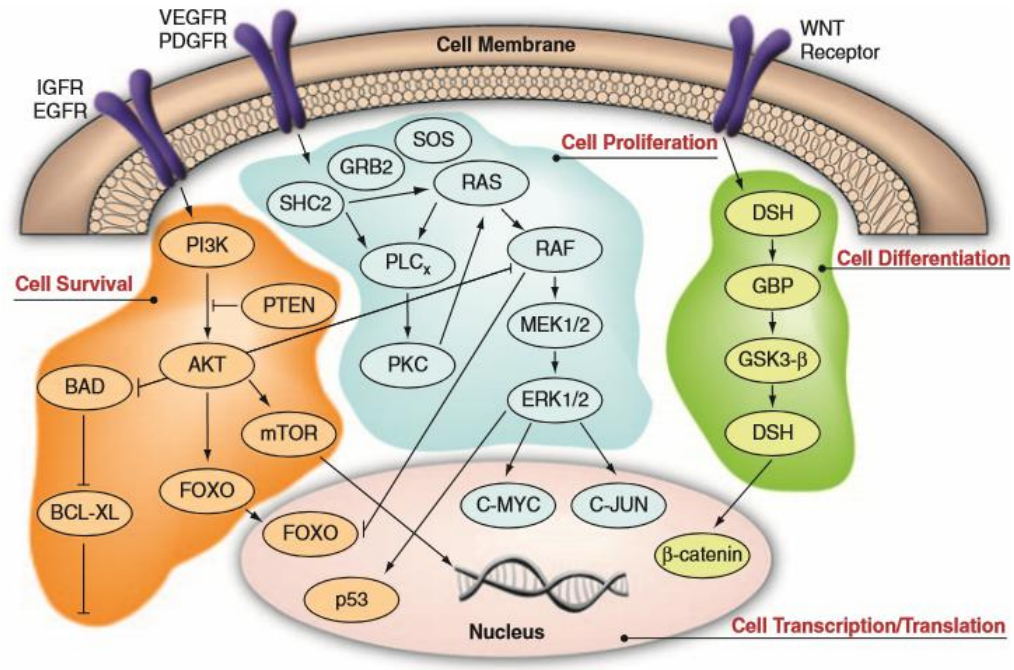

Figure 1.3. Cellular signaling pathways implicated in the pathogenesis of HCC (Source: (Whittaker, Marais et al. 2010))

1.2.2. MAPK Pathway (Ras/Raf/MEK/ERK)

Important intro-cellular signaling pathways that are involved in cell growth and survival, and regulate cell differentiation, are upregulated in cancer cells. Due to these properties, many researchers have studied MAPK pathway as a therapeutic target. The

MAPK pathway is a common downstream pathway for the EGFR, PDGFR and VEGFR, and is universally used for signal transduction downstream of cytokine receptors, integrin complexes and G-protein receptors to Ras (Figure 1.4). Besides, the MAPK pathway is responsible for HCC growth and survival (Llovet , Ricci et al. 2008). The downstream extracellular signaling-regulated kinase (ERK) is activated by two upstream protein kinases, which are coupled to growth factor receptors by Ras proteins. Ras, which is activated by ligand binding, activates Raf serine/threonine kinases and MEK (MAP kinase/ERK kinase), while MEK phosphorylates and activates ERK, which phosphorylates proteins involved in cell growth, apoptosis resistance, extracellular matrix production and angiogenesis (Andersen, Spee et al. 2012). Raf inhibitors such as Sorafenib, have been developed in HCC therapy. It exhibits strong inhibitory activity against Raf-1 (C-Raf) kinase, B-Raf (wild-type B-Raf and mutant V600E B-Raf) serine/threonine kinase, the pro-angiogenic receptor tyrosine kinases VEGFR, PDGFR and FGFR1, and tyrosine kinases which are involved in tumor progression and overall prognosis (Wilhelm, Adnane et al. 2008).

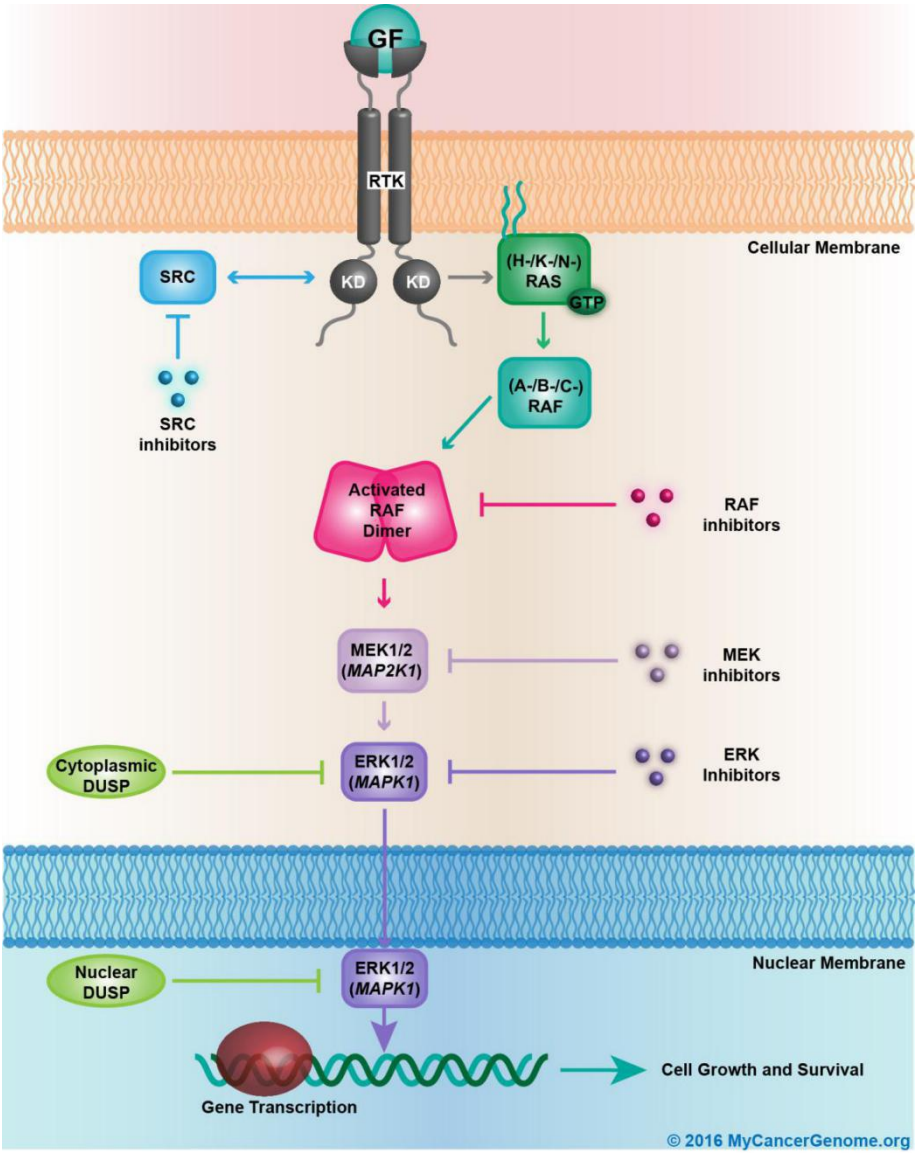

Figure 1.4. Summary of MAP kinases pathway (Source: www. mycancergenome. org)

1.2.3. PI3K/Akt/mTOR Pathway

The PI3K/Akt/mTOR pathway is a major intracellular signaling cascade involved in the regulation of cell growth, proliferation, and survival. The activation of the AKT/mTOR pathways is seen nearly in 50% of patients with HCC (Yuzugullu, Benhaj et al. 2009). When the membrane lipid phosphatidylinositol 4,5-bisphosphate (PIP2) is phosphorylated by phosphatidylinositol 3-kinase (PI3K), it converts into phosphatidylinositol 3,4,5-triphosphate (PIP3). Then it binds and activates the serine/threonin kinase AKT. The serine/threonine kinase mTOR is an important

mediator in the PI3K/Akt pathway which is activated downstream of Akt; thus, both molecules regulate protein synthesis (Zhai and Sun 2013). In addition to regulating various transcription factors such as FOXO, activated Akt also phosphorylates several cytoplasmic protein, most notables mTOR and BCL-2-assosiated death promoter (Avila, Berasain et al. 2006). the activation of mTOR increases cellular proliferation and inactivation of BCL-2-assosiated death promoter (BAD) not only decreases apoptosis but also increases cell survival. This pathway is negatively regulated by the phosphatase and tumor suppressor phosphatase on chromosome 10, PTEN which targets the lipid products of PI3K for dephosphorylation in normal tissue. (Whittaker, Marais et al. 2010). Anomalies PTEN function may lead to over-activation of the PI3K/AKT/mTOR pathway in HCC. Importantly, downregulation of PTEN expression has been shown to correlate with increased tumor grade, advanced disease stage with HCC (Zhou, Liu et al. 2006).

The PI3K/AKT/mTOR signaling pathway can be overactivated by enhanced stimulation of receptor tyrosine kinases, particularly the IGF receptor and EGFR. Expression of both IGF and IGF receptor is upregulated in HCC and human cirrhotic liver (Alexia, Fallot et al. 2004).

mTOR plays a pivotal role in HCC. mTORC1 and mTORC2 pathways, including pRPS6, p-AKT, IGF-1R and RICTOR are up-regulated in 40-50% of HCC (Matter, Decaens et al. 2014). mTOR pathway and its upstream pathways PI3K and AKT occupy a central position in the network of deregulated signaling pathways in HCC. mTORC1 induces the negative feedback loop, which in turn activates PI3K-AKT with MAPK and RAS signaling and thus may actually increase growth of cancer cells (Carracedo, Ma et al. 2008). PRAS40 and Deptor have been characterized as distinct negative regulators of mTORC1 (Peterson, Park et al. 2009). Upon activation, mTORC1 directly phosphorylates PRAS40 and Deptor, which reduces their physical interaction with mTORC1 and further activates mTORC1 signaling (Wang, Zeng et al. 2007). mTORC2 also plays key roles in various biological processes, including cell survival, metabolism, proliferation and cytoskeleton organization (Laplante and Sabatini 2012). Ablation of various mTORC2 components specifically blocks Akt phosphorylation at Ser473 and the downstream phosphorylation of some Akt substrates (Guertin, Stevens et al. 2006). Inhibition of AKT following mTORC2 depletion reduces the phosphorylation of, and therefore activates, the FOXO1 and FOXO3a transcription factors (Salih and Brunet 2008).

Overall, growing evidence shows that AKT as an essential actor in liver cancer tumorigenesis, progression and a potential target in the management of HCC. Therefore, we suggest that a therapy with an AKT inhibitor will be able to treat fully developed HCC by inhibiting the PI3K/Akt/mTOR pathway (Figure 1.5). Moreover, it is thought that AKT inhibitor may overcome Sorafenib resistance in HCC. Thus, the combination of Sorafenib with Akt-inhibitor represents new therapeutic strategy which can improve treatment effectiveness in HCC.

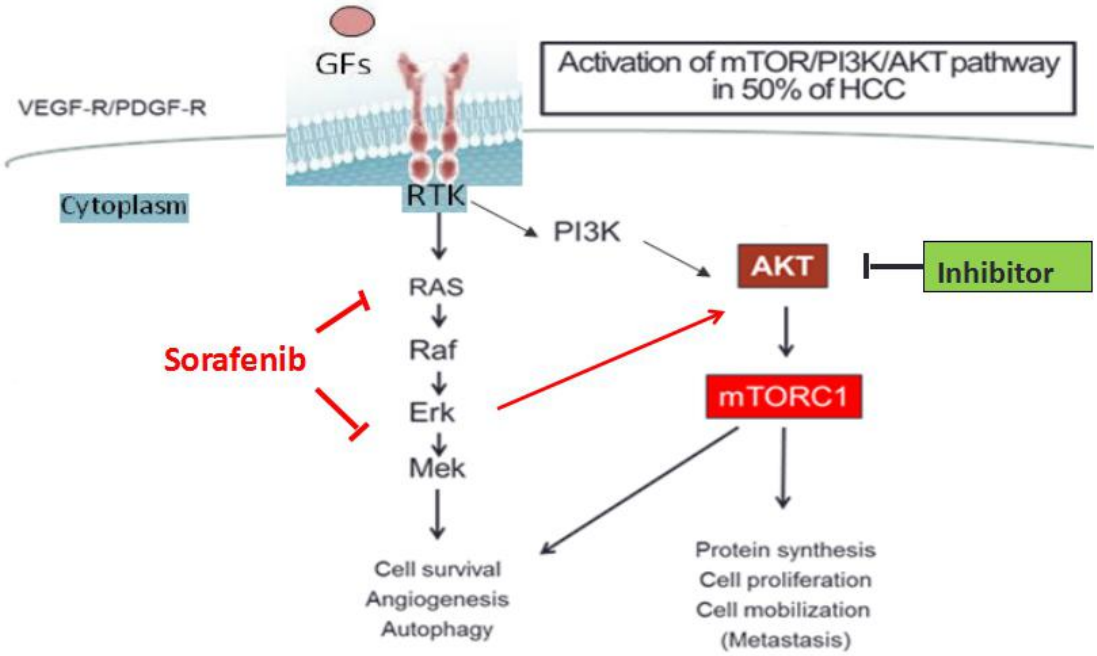

Figure 1.5. Major molecular pathway in HCC

1.3. Treatment of Liver Cancer _ HCC

Staging of HCC is essential to determine the treatment modality as well as the prognosis. Tumor stage, liver function, factional status and patient's symptoms should be investigated. The Barcelona Clinic Liver Cancer (BCLC) classification system is used worldwide, and takes into account all these variables (Ravi and Singal 2014).

Apart from being extensively validated, this system connects between the staging and treatment options, providing well-laid out algorithms for managing HCC (Figure 1.6).

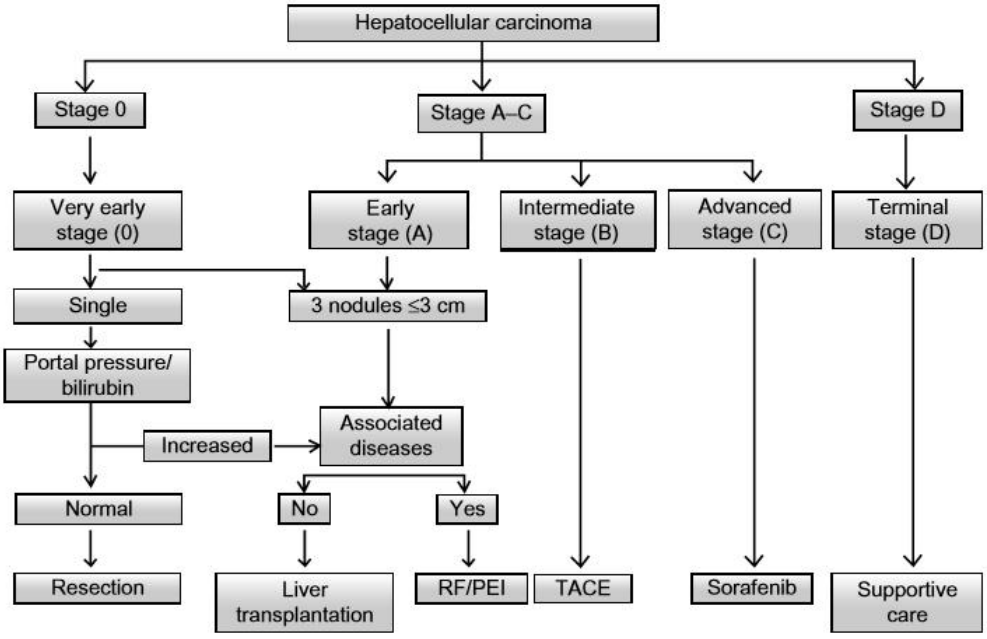

Figure 1.6. Barcelona Clinic Liver Cancer staging system and treatment strategy.RF, radiofrequency ablation; PEI, percutaneous ethanol injection; TACE, transcatheter arterial chemoembolization. (Source: (Bruix and Sherman 2011)).

Surgery is used to diagnose, stage and treat cancer, and certain cancer-related symptoms. Liver cancers are classified based on whether or not they can be removed. Depending on the size and location of the tumor, part of liver can be removed. This operation is considered for a single tumor that has not grown into blood vessels. Unfortunately, most liver cancers can not be completed removed. Often the cancer is in too many different parts of the liver, is too large or has spread beyond the liver. Also, there are possible risks and side effects after surgery. As a lot of blood vessels pass through the liver, blending may occur. Other possible problems are similar to those seen with other major surgeries and can include infections, complications from anesthesia, blood clots, and pneumonia. Besides these, new liver cancer can develop (Ang, Ng et al. 2015).

The other treatment of liver cancer is liver transplantation. Sometimes it can be the best option for some people. Unfortunately, the opportunities for liver transplant are limited. After transplantation, the patients are treated by drugs that help to suppress their immune systems to prevent their bodies from rejecting the new organ. These drugs increase risk of infection, can cause high blood pressure, high cholesterol, and diabetes; can weaken the bones and kidneys; and can even lead to new cancer (Obed, Tsui et al. 2008) (Cillo, Vitale et al. 2004). Although surgery and liver transplantation are considered the optimal curative treatment for diseases, there is a significant shortage of organ donors, and surgical complications, recurrence and metastasis are common.

Transcatheter arterial chemoembolization (TACE) is another method for HCC patients who are not convenient for surgery (Brown, Geschwind et al. 2006). Chemotherapy drugs which are coated with small embolic particles are injected by through a catheter into an artery directly supplying the tumor (Miraglia, Pietrosi et al. 2007). However, TACE is not suitable for big tumors and tumors with portal-systemic shunt and patients with poor liver function.

Chemotherapy is a category of cancer treatment that uses one or more anti-cancer drugs. Sorafenib, a multi kinase inhibitor, has been shown to improve the overall survival (OS) of patients with advanced HCC and the time represented a breakthrough in the clinical management of this cancer (Llovet , Ricci et al. 2008). Sorafenib is an inhibitor of Raf serine/threonine kinases, inducing cell apoptosis and blocking tumor angiogenesis (Liu, Cao et al. 2006) and receptor tyrosine kinases associated with VEGFR2 and 3, platelet-derived growth factor receptor (PDGFR)-β, Flt-3 and c-Kit (Wilhelm, Carter et al. 2004) and other pathways such as STAT3 that is a major kinase independent target of Sorafenib (Jiang, Feng et al. 2015). In 2007, a pair of phase III studies indicated that Sorafenib improved survival and the time to radiological progression, leading to its approval for the treatment of advanced HCC (Llovet , Ricci et al. 2008) (Cheng, Kang et al. 2009). However, benefits of Sorafenib are unfortunately modest, with upfront (innate/intrinsic) and acquired (evasive/secondary) drug resistance being major contributing factors (Li, Gao et al. 2015). The other important problem is toxicity leading to a high rate of dose reductions and treatment interruptions in patients (Gomez and Lacouture 2011). Therefore, the response rate of Sorafenib is actually quite low and the median extension of survival is three months for advanced HCC cases. Furthermore, this treatment often causes side effects altering the quality of patient's life. Moreover, long-term exposure to Sorafenib often results in

reduced sensitivity of the tumor cells, leading to acquired resistance. Interestingly, Sorafenib has been demonstrated to activate AKT kinase and upregulate the phophorylation of its downstream targets, such as mTOR (Figure 1.5). This over-activation of Akt pathway is considered to be the main mechanisms of resistance to Sorafenib (Zhai, Hu et al. 2014).

1.3.1. Inhibitor of PI3K/AKT/mTOR pathway

The phosphoinositide 3-kinase (PI3K)/AKT/mTOR pathway is one of the most frequently dysregulated signaling cascades in human malignancies (Weigelt and Downward 2012). Since the activation of PI3K pathway in cancer plays crucial role in cell growth and survival, this pathway is attractive target for pharmacological intervention. The first PI3K pathway-target agents approved for the treatment of cancer were the Rapamycin Analogs Everolimus and Temsirolimus, which allosterically inhibit mTORC1 (Wallin, Edgar et al. 2011).

Dienstmann et all. summarized all the target agents which inhibit to PI3K/AKT/mTOR pathway in table 2 (Dienstmann, Rodon et al. 2014).

Table 2. A summary of PI3K/AKT/mTOR pathway inhibitors in clinical development (Source: (Dienstmann, Rodon et al. 2014)).

Agent (company)	Target	Phase[a]	Tumor types currently under investigation[a]
Everolimus (Novartis)	mTORC1	Approved	Approved for the treatment of renal cell carcinoma, subependymal giant cell astrocytoma associated with tuberous sclerosis, pancreatic neuroendocrine tumors, and ER+ breast cancer (in combination with exemestane)
Temsirolimus (Pfizer)	mTORC1	Approved	Approved for the treatment of renal cell carcinoma
BEZ235 (Novartis)	PI3K/mTOR	Phase II	Advanced solid tumors, breast cancer, castration-resistant prostate cancer, renal cell carcinoma, leukemias, pancreatic neuroendocrine tumors, urothelial transitional cell carcinoma
GDC-0980 (Genentech)	PI3K/mTOR	Phase II	Solid cancers, non-Hodgkin lymphoma, breast cancer, prostate cancer
PF-05212384 (Pfizer)	PI3K/mTOR	Phase I/II	Advanced solid tumors, colorectal cancer, endometrial neoplasms
SAR245409 (XL-765; Sanofi/Exelixis)	PI3K/mTOR	Phase II	Advanced solid tumors, CLL, indolent non-Hodgkin lymphoma, mantle cell lymphoma, ovarian cancer
BAY80-6946 (Bayer)	Pan-class I PI3K	Phase II	Advanced solid tumors, non-Hodgkin lymphoma
Buparlisib (BKM120; Novartis)	Pan-class I PI3K	Phase IV	Advanced solid tumors, breast cancer (ER+, HER2+, and HER2−), cervical cancer, colorectal cancer, endometrial cancer, esophageal cancer, GIST, glioblastoma, head & neck neoplasms, leukemias and lymphomas, melanoma, NSCLC, ovarian cancer, prostate cancer, renal cell carcinoma, urothelial transitional cell cancer
Pictilisib (GDC-0941; Genentech)	Pan-class I PI3K	Phase II	Breast cancer, NSCLC
PX-866 (Oncothyreon)	Pan-class I PI3K	Phase II	Advanced *BRAF*-mutant cancers, NSCLC, prostate cancer
SAR245408 (XL-147; Sanofi/Exelixis)	Pan-class I PI3K	Phase I/II	Advanced solid tumors
ZSTK474 (Zenyaku Kogyo)	Pan-class I PI3K	Phase I/II	Advanced solid tumors
BYL719 (Novartis)	PI3K p110α	Phase II	Advanced solid tumors (including those with *PIK3CA* alteration), breast cancer, colorectal cancer, esophageal cancer, gastrointestinal cancer, GIST, head & neck squamous cell cancer
GDC-0032 (Genentech)	PI3K p110α, δ, and γ inhibitor	Phase I	Advanced solid tumors and metastatic breast cancer (ER+)
MLN01117 (INK1117; Intellikine)	PI3K p110α	Phase I	Advanced solid tumors with *PIK3CA* mutation
GSK2636771 (GSK)	PI3K p110β	Phase I	Advanced solid tumors with PTEN deficiency
SAR260301 (Sanofi)	PI3K p110β	Phase I	Advanced solid tumors
Idelalisib (CAL-101; GS-1101; Gilead/Calistoga)	PI3K p110δ	Phase III	CLL, lymphomas

(cont. on next page)

Table 2 (cont).

Agent (company)	Target	Phase[a]	Tumor types currently under investigation[a]
AMG319 (Amgen)	PI3K p110δ	Phase I	Hematologic malignancies
Perifosine (KRX-0401; Keryx)	AKT	Phase I/II	Advanced solid tumors, multiple myeloma
MK2206 (Merck)	AKT	Phase II	Advanced solid tumors, breast cancer, colorectal cancer, endometrial cancer, head & neck cancer, lung cancer, lymphomas, pancreatic cancer, prostate cancer
GDC-0068 (Genentech)	AKT	Phase II	Advanced solid tumors, gastric cancer, prostate cancer
GSK2110183 (GSK)	AKT	Phase II	Advanced solid tumors, CLL, multiple myeloma, ovarian cancer
GSK2141795 (GSK)	AKT	Phase II	Advanced solid tumors, breast cancer, cervical cancer, endometrial cancer, leukemias, melanoma, multiple myeloma
ARQ 092 (ArQule/Daiichi Sankyo)	AKT	Phase I	Advanced solid tumors
AZD5363 (AstraZeneca)	AKT	Phase I/II	Advanced solid tumors, breast cancer, prostate cancer
AZD2014 (AstraZeneca)	mTORC1/2	Phase II	Advanced solid tumors, breast cancer, renal cell carcinoma
MLN0128 (INK128; Intellikine)	mTORC1/2	Phase I	Advanced solid tumors, hematologic malignancies
CC-223 (Celgene)	mTORC1/2	Phase I/II	Breast cancer, glioblastoma, hematologic malignancies, liver cancer, NSCLC, neuroendocrine tumors

Currently, allosteric and catalytic AKT inhibitors are being investigated as an advances in drug design in clinical studies (Josephs and Sarker 2015). The allosteric inhibitor (ARQ 092 or ARQ 751) bind to both the active and inactive forms of AKT. They appear to suppress AKT activation of active form and block the cell cycle progression and proliferation, cell metabolism, cell survival and protein translation and growth and also suppress the AKT activation of in active form by disrupting membrane translocation in shown figure1.7 (Yu, Savage et al. 2015).

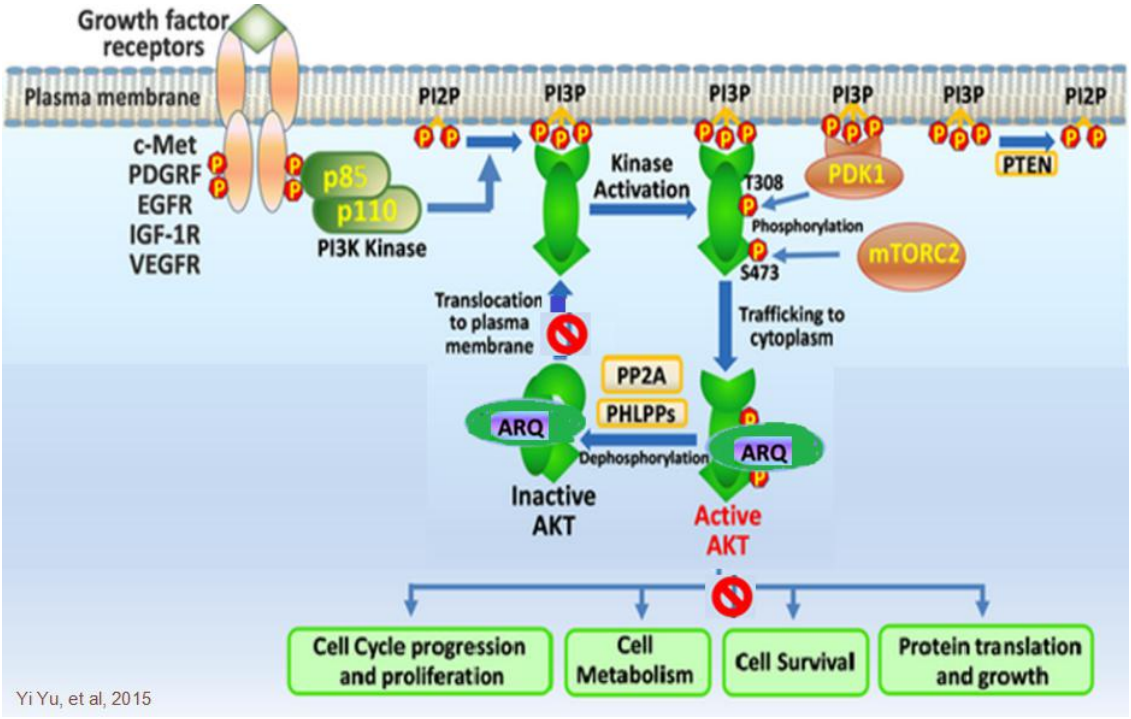

Figure 1.7. AKT pathway inhibition by ARQ inhibitors: ARQ 092 and ARQ 751 (Source: (Yu, Savage et al. 2015)).

1.4. Animal model of hepatocellular carcinoma

To gain better functional insight into the molecular mechanisms of hepatocarcinogenesis, several studies were performed using human HCC tissue. On the basis of these studies, a collection of genetic and epigenetic alterations, chromosomal aberrations, gene mutations and altered molecular pathways were described (Zender, Villanueva et al. 2010). However, in many cases, it was difficult to consider whether these variations depicted a correlative occurrence or if they were causally linked to HCC pathogenesis. From this perspective, animal models of HCC offer a unique possibility to study mechanistic and cellular aspects of tumor biology, including the genetics of tumor initiation and promotion, tumor progression and metastasis *in vivo*. Moreover, animal models also represent a valuable tool to test wide spectrum of therapeutic compounds for their efficacy to inhibit particular signaling pathways and thus to prevent or decelerate HCC development and growth (Vucur, Roderburg et al. 2010).

Several rodent HCC models have been developed to investigate the pathogenesis, treatment and prevention of liver cancer (HCC), which can be broadly divided into (1) xenograft models, (2) chemically induced models and (3) genetically modified mouse models (Heindryckx, Colle et al. 2009). Whereas, tumors are formed by injecting human cancer cells into immune deficient mice in xenograft models, HCC in chemically induced and genetic models arise in their natural cellular and intercellular context, allowing researchers to study molecular mechanisms and cellular interactions during tumor initiation. Xenograft models are, in fact, used in 90% of cases. Chemically-induced hepatocarcinogenesis provides a valuable model for investigating the molecular biology of hepatocarcinogenesis, particularly in its early stages, for various reasons cited previously (Ogawa 2009). Diethylnitrosamine (DEN) is a potent hepatocarcinogenic dialkyl nitrosamine used in animal models of HCC. Among several chemically induced, genetically modified mice, DEN-induced HCC was most similar to the expression patterns of the poor survival group of human HCCs (Lee, Chu et al. 2004). Firstly, it can be easily administered to mice/rats from different genotypes. Second, it has a high HCC incidence and is highly reproducible (Heindryckx, Colle et al. 2009) (Lim 2002) (Hann and Balmain 2001). Importantly, this model is extremely well-tolerated by rodents and is not associated with serious side effects.

As fibrosis/cirrhosis modifies liver vascularization, extracellular matrix composition, and drugs metabolism, it is essential to use a cirrhotic animal model to test drugs for advance HCC, in order to test efficacy on tumors but also tolerance of the treatment. Indeed most of HCC models have background of normal surrounding liver or moderately fibrotic liver. The animal that is mostly used is mouse but mice are not able to develop severe fibrosis or cirrhosis. Here we have chosen a rat model because rats are able to develop extensive fibrosis, compensated cirrhosis, decompensated cirrhosis and HCC after chronic administration of DEN (Schiffer, Housset et al. 2005). In fact, in male Fischer 344 rats (150-170g), chronic weekly intra-peritoneal injection of 50 mg/kg of DEN induces moderate (F2) fibrosis after 8 weeks, fully developed cirrhosis (F4) after 12 weeks, and decompensated cirrhosis with ascites and HCC after 14 weeks.

On the basis of the currently limited treatment options for liver cancer, DEN-induced cirrhotic rat model with HCC is essential to test novel drug-targeting approaches that might help to reduce the global challenges associated with advanced HCC.

1.5. ARQ 092 & ARQ 751

ArQule is a biopharmaceutical company engaged in the research and development of targeted therapeutics to treat cancers and certain rare diseases. This company develops and commercializes novel small molecule drugs. To date, five drug candidates were synthesized, all of which are in targeted, biomarker-defined patient populations, making ArQule a leader in precision medicine. We have studied two of them; ARQ 092 and ARQ 751.

ARQ 092 and next generation of ARQ 092 which is ARQ 751 are synthesized by ArQule, Inc. as highly potent and selective allosteric inhibitors of AKT (Yu, Savage et al. 2015) and general chemical structure is shown in figure 1.8 (Yu, Savage et al. 2015). the difference between ARQ 092 and ARQ 751 differs R1, R2 and R3 groups.

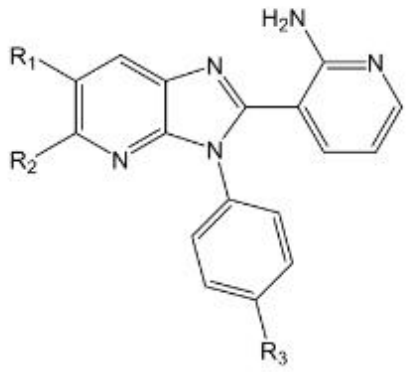

R1, R2 and R3 are substituted or unsubstituted alkyl or aryl groups

Figure 1.8. Chemical structure of the core moiety of ARQ 092 and ARQ 751 (Source: (Yu, Savage et al. 2015)).

It has been recently reported the preclinical characterization of ARQ 092 and it showed strong affinity for unphosphorylated full-length AKT1 and potently inhibited the phosphorylated form of full-length AKT isoforms.Thus, it showed potent antiproliferative activity also exhibited strong anti-tumor activity and the desirable pharmacokinetic properties of ARQ 092 which is under investigation in clinical trials targeting advanced solid tumors. Previously studies demonstrated that AKT activation

entails the translocation of the protein to the cell membrane and the binding of the PH domain of AKT to phosphoinositides, upon which a conformational change permits the phosphorylation of Thr308 (for AKT1) in the activation loop by phosphoinositidedependent kinase 1 (PDK1) (Scheid and Woodgett 2003). For full activation of AKT, Ser473 in the hydrophobic motif (HM) domain is phosphorylated by the mTORC2 complex (Yang, Qiao et al. 2010). ARQ 092 binds to between the allosteric pocket formed by the kinase and PH domains. Cocrystal structure demonstrates in figure 1.9 (Lapierre, Eathiraj et al. 2016).

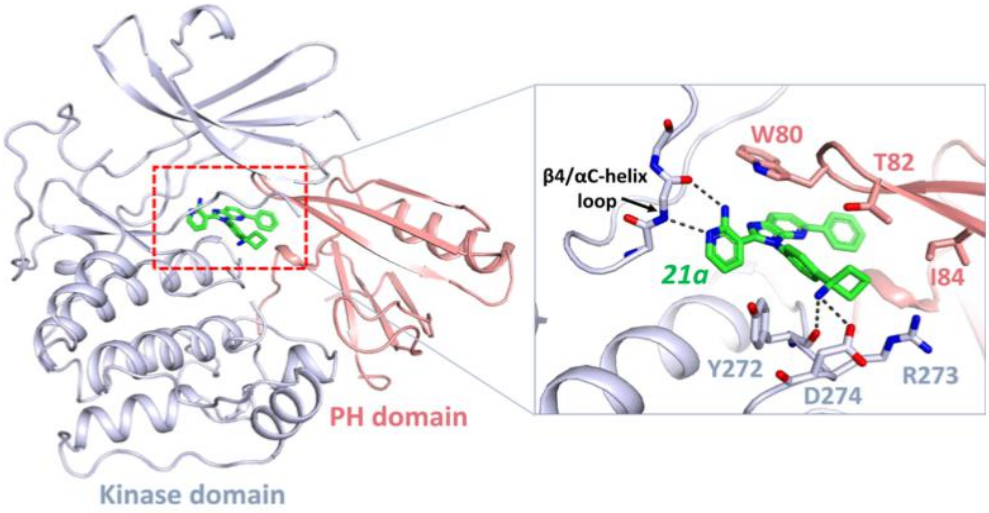

Figure 1.9. Cocrystal structure of ARQ 092 with AKT1 (Source: (Lapierre, Eathiraj et al. 2016)).

ARQ 092 is an oral selective and potent pan-AKT inhibitor that inhibits both wild-type and mutantAKT1, 2 and 3 isoforms. The drug is currently in phase 1b clinical trial.

ARQ 751 is an orally available, selective, next generation pan-AKT inhibitor that potently inhibits AKT1, 2 and 3 isoforms. It is diversified portfolio of AKT inhibitors might provide us the opportunity to best address oncology. Pre-clinical profile for ARQ 751 defines a highly potent and highly selective molecule. ARQ 751 is in pre-clinical trial.

1.6. Aim of Study

The objective of this project is to compare the efficacy of two allosteric inhibitors of AKT i.e. ARQ 092, ARQ751 and combination treatment (Sorafenib plus ARQ 092) with Sorafenib and Control, through *in vitro* and *in vivo* studies, in a cirrhotic rat model with HCC.

Sorafenib molecular side effects might reside, in AKT activation. Targeting AKT signaling in combination seems very promising. The combination of Sorafenib with Akt-inhibitor could represent new therapeutic strategy which can improve treatment effectiveness and overcome Sorafenib resistance in HCC.

CHAPTER 2

MATERILAS & METHODS

2.1. *In Vitro*

2.1.1. Cell Lines

Three different human HCC cell lines (Hep3B, Huh7, and PLC/PRF/5) and hepatoblastoma cell line (HepG2) were used in this study. HepG2 (p53 wild type, ras mutant) and Hep3B (p53 deleted and ras wild type) cells were cultured in Minimum Essential Medium (MEM, GIBCO ™, Life Technologies), with GlutaMAX™ Supplement. Huh7 cells (p53 mutant, ras wild type) were incubated in Dulbecco's Modified Eagle Medium (DMEM, GIBCO ™, Life technologies), with high glucose, and GlutaMAX ™ supplement. PLC/PRF/5 cells (p53 mutant, ras wild type) were cultured in DMEM supplemented with 1% of sodium pyruvate (GIBCO TM, Life technologies).

2.1.2. Treatments

ARQ molecules ARQ 092, ARQ 751 were kindly provided by ArQule Inc (Woburn, MA, USA).

For *in vitro studies,* ARQ compounds and Sorafenib tosylate (Bay 43-9006, Sigma-Aldrich, Germany) were dissolved in pure dimethyl sulfoxide (DMSO, Sigma-Aldrich). 5 mM stock solutions of these agents were stored at - 20°C temperature and protected from light. The maximum tolerated DMSO percentage used in cell culture was 1%.

2.1.3. Cell Viability Assay

Cell viability was examined by MTT colorimetric assay. MTT (3-(4,5-Dimethylthiazol-2-yl)-2,5-diphenyltetrazolium bromide) is a yellow tetrazole and used for assessing cell metabolic activity. Tetrazolium dye reduction depends on the cellular metabolic activity due to NAD(P)H flux. Cells with a low metabolism reduce very little MTT while rapidly dividing cells exhibit high rates of MTT reduction (Mosmann 1983).

For this study, four different cell lines Hep3B, HepG2, HuH7 and PLC/PRF were used. These cell lines were treated with Sorafenib alone, ARQ 092 alone, ARQ 751 alone and combination of Sorafenib and ARQ 092. Firstly, 5000 cells were seeded in 96-well plates and incubated of 24h. After that, ARQ 092, ARQ 751 and Sorafenib at different concentrations (0.01µM – 50µM) were given to cells for 48h. After incubation time, 10 % MTT was added to every well for 4h at 37°C and then medium was removed and replaced by 100µL DMSO. 96-well plates were gently shaken during 15 minutes for an optimal solubilization of Formazan crystals, and absorbance was measured using a multilabel plate reader (Victor 3 1420-014 Multilabel Plate Reader, Perkin Elmer Inc.) at a 544 nm wavelength. As a negative control, cells were incubated in the same medium with 1 % DMSO. For single treatment values of inhibition concentration (IC) 20 and IC50 were calculated.

For combination study (i.e. Sorafenib and ARQ 092), different concentrations of same IC50:IC50 ratio values of Sorafenib and ARQ 092 were used in order to determine the Combination Index (CI) values. Cells were exposed to 11 different concentrations (IC50/1000, IC50/500, IC50/200, IC50/100, IC50/50, IC50/20, IC50/10, IC50/5, IC50/2, 1xIC50, 2xIC50) during 48h. CI values were calculated using CompuSyn software as described previously (Chou 2006). Each sample was analyzed on three replicates and all experiments were repeated three times.

2.1.4. Apoptosis Analysis

Hep3B, HepG2, HuH7 and PLC/PRF/5 cell lines treated with 2 different concentrations of ARQ 092, ARQ 751 or Sorafenib (IC50 and IC20). For combination study two concentrations of ARQ 092 and Sorafenib (IC50/200 and IC50/10) were chosen. Cells (5x105/well) were first incubated 24h alone in 6-well plates with 1.8 mL

of the adequate growth medium per well during 24h. Then, drug was added and cells were treated during 48h. Cells without drug and with 1% DMSO were used as negative control. After the incubation time, cells were detached from wells by using Trypsin-EDTA solution (Gibco ®, Life Technologies), and were centrifuged. The supernatant was removed and the pellet was washed with Dulbecco's phosphate-buffered saline (DPBS, VGibco ®, Life technologies), and resuspended in 300 µL of binding buffer. 3 µL of annexin V conjugated to fluorescein isothiocyanate (FITC) as a marker of early-stage apoptosis (Blankenberg and Strauss 2001). and 7-AAD (7-amino-actinomycin D) as a marker of cell membrane integrity and cell viability, were added. The stained cells were incubated for 15 min at room temperature (25 °C) and then samples were analyzed by flow cytometry (BD Accuri C6, Becton, Dickinson) to quantify annexin V-FITC and 7-AAD positive/negative apoptotic cells.

2.1.5. Cell Migration

Cell migration assay was assessed in Huh7, Hep3B, HepG2 and PLC/PRF by performing a scratch assay (Hulkower and Herber 2011). For each cell line, cells were seeded in 24-well plates and incubated under normal growing conditions in order to obtain a confluent monolayer. After obtaining monolayer a 200 microliter-tip was then used to scratch and remove the cells to form 2 perpendicular straight fine lines in each well. After that, medium was replaced with the new medium in control or with medium mixed with drug of IC20 and IC50 values for Sorafenib, ARQ 092 and ARQ 751, IC50/200 and IC50/10 values for combination. Images of 24 well-plates were captured every hour by time-lapse microscopy at 37°C, 5% CO_2 with Zeiss AxioVert 100M (Zeiss) connected to a MicroMAX B/W (6.7x6.7 µm, -15, ~ 3 im/s) camera using acquisition software MetaMorph (Universal Imaging). The width of the wound was quantified at 0h, 24h, 48h and 72h by ImageJ software (NIH, USA). Data are presented as relative percentage of closed-wound. The experiments were performed with at least three replicates.

2.1.6. Immunoblot Assay

For immunoblot assay, $1x10^6$ human HCC cell lines (HepG2, Hep3B, Huh7, and PLC/PRF/5) were seeded per each Petri dish with suitable medium and incubated for 24h. After 24h, medium in the Petri dish with cells was replaced by the medium combined with drug (Sorafenib alone, ARQ 092 alone, ARQ 751 alone and combination of Sorafenib and ARQ 092) and incubated for 2h, 24h or 48h. After incubation, medium with drug in Petri dishes were removed and cells were scratched with scrapper in RIPA buffer (50 mM Tris; 1% NP40; 0.5% deoxycholic acid sodium salt; 150 mM NaCl; 1 mM EGTA) containing Protease and Phosphatase Inhibitors, and proteins were quantified with NanoDrop ® (Thermofisher scientific). Proteins were then denatured in Laemmli Sample Buffer (Bio-Rad) containing 10% β-mercaptoethanol and separated by gel (Mini Protean Gels ®, Bio-Rad) and transferred to polyvinylidene difluoride (PVDF; Bio- Rad) membranes using a wet blot method. Membranes were blocked in TBS-Tween solution with 5% BSA for 1 h at 4 °C. Primary antibodies against AKT and phosphorylated AKT (p-AKT $^{(Ser473)}$, AKT $^{(pan)}$), ERK and phosphorylated ERK (pERK $^{(Thr202/Tyr204)}$, ERK $^{(p44/42\ MAPK)}$), β-actin (all Cell Signaling Technology, USA) were incubated at 4°C overnight under shaking conditions. Incubation with the secondary antibody (HRP-anti rabbit IgG, 1:2000; Cell Signaling) was performed under shaking conditions for 1 h. Detection was achieved with Clarity™ Western ECL Blotting Substrate (Bio-Rad) using a ChemiDoc™ MP Imaging System (Bio-Rad). Densitometric quantification of the bands was performed using the Image Lab™ Software (Bio-Rad).

2.1.7. Immunocytochemsitry

Cells on Lab-Tek® 8-well Chamber slides were treated with IC50 concentration of ARQ 092 or Sorafenib during only 2h to avoid false positive signal from apoptotic or dead cells. After, cells were fixed with 2% paraformaldehyde and permeabilized with 0.5% Triton X-100. After fixation, cells were blocked with 10% normal goat serum in PBS. Monoclonal rabit p-Akt (Ser473) antibody was applied overnight at 4°C, followed by goat anti-rabbit Alexa 546 (Life Technologies, Carlsbad, CA, USA). Fluorescent images were obtained using ApoTome microscope (Zeiss) with a 20x magnification.

2.2. *In vivo*

2.2.1. Animal Model

8-week-old Fischer 344 male rats (Charles River Laboratories, France) were housed in the animal facility of Plateforme de Haute Technologie Animale (Jean Roget, University of Grenoble-Alpes, France). They were treated weekly with intra-peritoneal injections of 50mg/kg diethylnitrosamine (DEN) (Sigma-Aldrich, Germany), diluted in pure olive oil in order to obtain a fully developed HCC on a cirrhotic liver after 14 weeks (Schiffer, Housset et al. 2005). Figure 2.1. A represents normal rat liver and figure 2.1. B shows rat liver with DEN induced HCC. To perform oral gavages and MRI analyses, rats were transported to the Grenoble Institute of Neuroscience (GIN, INSERM, U1216, University of Grenoble-Alpes, France) equipped by Grenoble MRI facility IRMaGE.

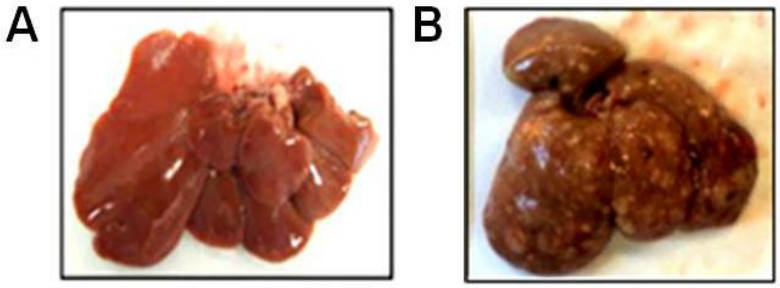

Figure 2.1. Representative pictures of rat liver A) Normal rat liver and B) rat liver with DEN induced HCC.

2.2.2. Preparation of Treatment

For *in vivo* study, 200 mg Sorafenib tosylate tablets (Nexavar®, Bayer HealthCare, Germany) were used. The sugar coating was first dissolved in DMSO and Sorafenib was mixed with 1 mL of poly-oxyl castor oil (Cremophor® EL, Sigma-Aldrich) and 1 mL of 95% ethanol per tablet to emulsify and to solubilize it (Liu, Cao et

al. 2006) (Wilhelm, Carter et al. 2004). To finish, the emulsion was diluted in purified water to obtain a 10 mg/mL solution of Sorafenib suitable for oral gavages.

The dose strategy for ARQ 092 was based on a previous toxicity study. ARQ 092 was dissolved in a 0.01M phosphoric acid solution to obtain a 15 mg/mL ARQ solution suitable for oral gavages with a final pH of 2.25 ± 0.15. For each drug, fresh solution was prepared every week and stored at room temperature, protected from light.

Combination was prepared by mixing the same volume of each drug just before oral gavages.

2.2.3. Treatment of Protocol

After 14 weeks, for the first project, rats were randomized in three different groups as follows: 10 in ARQ 092 group, 10 in Sorafenib group and 6 in the control (untreated) group which is illustrated in figure 2.2.

Both treatments were dispensed by daily oral gavage during six weeks. ARQ 092 was administered for 7 days on 7 days off (for a total of 3 weeks of treatment) at a dose 15 mg/kg/day as recommended by ArQule Inc. However, Sorafenib was administered at a dose of 10 mg/kg/day every days. In fact,during the first week, the dose of Sorafenib was used 20 mg/kg/days but it was immediately reduced to the dose of 10 mg/kg/days due to its toxic effects. From second week, the dose of 10 mg/kg/days of Sorafenib was administered and no adverse effects were observed. For the second project, rats were randomized to 4 groups as follow: ARQ 092 group, Sorafenib group, Combination group (Sorafenib plus ARQ 092) and control group (n= 7 rats /group), which is illustrated in figure 2.3. ARQ 092 alone, Sorafenib alone and Combination (Sorafenib plus ARQ 092) treatments were dispensed by oral gavage for a period of six weeks. ARQ 092 treatment was given during 5 days on 9 days off, at the dose of 15 mg/kg/day as recommended by the ArQule Inc. Sorafenib was administered continuously at the dose of 10 mg/kg/day. Control group was not treated.

For both projects, all rats were daily weighed to monitor the nutritional state and to adapt treatment doses. Protein-rich nutrition was added to the standard food in cages, when a loss of weight was observed. All animals received humane care in accordance with Guidelines on the Humane Treatment of Laboratory Animals, and experiments were approved by the GIN animal Ethic Committee.

2.2.4. MRI Studies

All rats were subjected to three MRI scans. MRI1 was performed before randomization. MRI2 and MRI3 were respectively done after three weeks and six weeks of treatment, which is illustrated in figure 2.2 and 2.3.

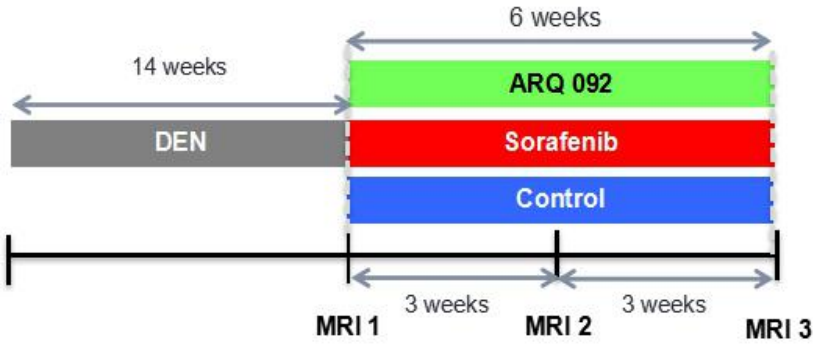

Figure 2.2. *In vivo* treatment protocol. After 14 weeks, DEN injected rats were randomized into 3 groups. Single treated-group Sorafenib (n=10), ARQ 092 (n=10) and control group (n=6). Three MRI scans were performed.

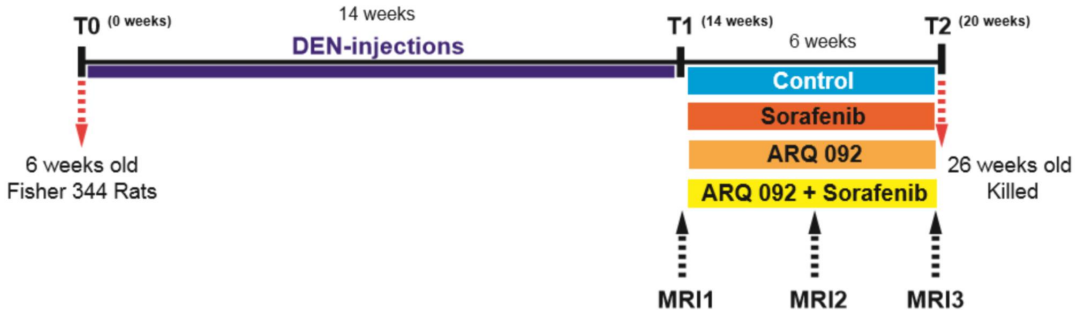

Figure 2.3. *In vivo* treatment protocol. After 14 weeks, DEN injected rats were randomized into 4 groups (n=7) and treated with drugs.. Three MRI scans were performed.

Imaging study was performed with a 4.7 Tesla MR Imaging system (BioSpec 47/40 USR, Bruker Corporation, Germany) and Transmit/Receive Volume Array. Coil for rat body 8x2 (Bruker Corporation, Germany) in the Grenoble MRI facility IRMaGE. Rats were fitted in ventral decubitus position and anesthetized with isoflurane inhalation

(Forane®, Abbott, USA), breathing was continuously monitored to maintain a respiratory rate between 35 and 45 breaths per minute and body temperature was maintained around 37°C.

We used Turbo rapid acquisition with relaxation enhancement T2-weighted (Turbo-RARE T2) sequence (repetition time (TR): 1532.9 msec, echo time (TE): 27.4 msec, flip angle (FA): 180°) and a dynamic contrast enhanced T1-weighted (DCE-MRI) sequence (TR: 265 msec, TE: 4.4 msec, FA: 60°, 20 repetitions). Both sequences had a field of view (FOV) of 55 x 55 mm, 20 slices, a thickness and a slice separation of 2 mm, and were realized with a respiratory triggered acquisition to reduce artefacts.

Gadoterate meglumine (Dotarem®, Guerbet, France) was used for the enhancement at the dose of 0.2 mmol/Kg. Injection was performed 3 min after the beginning of the acquisition through a lateral tail vein catheter.

MRI parameters adjustment and image acquisition were realized by using Paravision 5.1 software.

A morphological analyzes was realized based on the TurboRARE T2 sequences and according to the Response Evaluation Criteria in Solid Tumors (RECIST) criteria. Five liver tumors were selected and measured on MRI1, 2 and 3. Estimated tumor size corresponded to the sum of the largest diameter of these 5 lesions. For each rat, MRI1 was considered as the baseline (i.e.: 0%) and tumor progression corresponded to the comparison between MRI2 or 3 and the baseline, (i.e: "(tumor size $_{MRI2/3}$ - tumor size $_{MRI1}$) / tumor size $_{MRI1}$).

Perfusion analysis was realized based on DCE-MRI sequences. Three tumors were analyzed per rat. The enhancement of one tumor corresponded to the difference between the baseline of the enhancement curve and the maximal value obtained after injection divided by the baseline. Baseline corresponded to the mean of values obtained before injection of the contrast agent and the maximal value of the curve was obtained after realization of a smoothing by a moving average every 3 consecutive values in order to reduce biases due to artefacts. In each rat, every tumor enhancement was normalized on the skin enhancement as a ratio "tumor enhancement / skin enhancement" to reduce biases due to contrast agent injection variations between rats. 5 rats were analyzed by group, i.e. 15 tumors and tumor enhancement were compared between MRI1 and 3 in each group to assess the antiangiogenic effect of drugs.

2.2.5. Histopathological and Morphological Analyses

After the third MRI scan, all rats euthanized with intracardiac blood sampling for haematologic and biochemical analyses. Serum and plasma were taken in order to test biological safety and efficacy parameters. Each liver was weighted, the number of tumors larger than 1 mm at the surface of livers was counted and the largest diameter of the five largest tumors was measured. The sum of these 5 diameters was calculated in order to obtain a histopathological estimation of the tumor size.

2.2.6. Measurement of Liver Triglicerides

Frozen liver fragments (~50 mg) were digested in 0.15 ml of 3 M alcoholic potassium hydroxide (70 °C, 2 h), diluted seven times in distilled water. Amount of liver triglycerides was measured by Triglycerides kit (Erba Mannheim, Czech Republic) and sample absorbance was measured by spectroscopy at 505 nM.

2.2.7. Histopathological, Immunohistochemical and Immunofluorescence Analyses

Liver tissues were fixed in 10% formalin solution neutral buffered (Sigma-Aldrich). Paraffin-embedded four-micrometer sections were then stained with Hematoxylin/Eosin.

In order to detect proliferating cells, paraffin-embedded sections were incubated overnight at 4°C with the primary anti Ki67 antibody (Rabbit, clone SP6, Thermofisher scientific, USA), followed by incubation with the peroxidise-conjugated bovine anti-rabbit IgG (Jackson ImmunoResearch, USA). DAB was used as the chromogen for Ki67 immunodetection. For Ki67+ cells, data are presented as positive cell nuclei per area (high-power fields; 20x magnification).

DNA fragmentation and apoptotic signaling can be detected by TUNNEL (Lozano, Bejarano et al. 2009). Slides were analyzed by ApoBrdU-IHC DNA Fragmentation Assay Kit (Biovision, USA) and methyl green solution was used to counter staining the

cells. Data are presented as apoptotic cells per area (high-power fields; 20x magnification).

To detect vascularisation, paraffin-embedded sections were blocked by 10% donkey serum and then incubated overnight at 4 °C with anti-rat CD34 antibody (Goat, AF4117, R&D Systems; Minneapolis, USA), followed by incubation with Alexa 647-conjugated donkey anti-goat IgG (Life Technologies, Carlsbad, CA, USA). Images were captured using ApoTome microscope (Zeiss) equipped with a camera AxioCam MRm and collected by AxioVision software. Positive area was quantified using ImageJ software on 15 randomly selected fields/section (10x magnification).

Collagen, it was detected on paraffin-embedded sections with Picro-Sirius red stain solution (Sigma-Aldrich) and staining was subsequently quantified by MetaMorph ® software in 10 randomly selected fields/section (10x magnification).

Oil Red O staining was performed on 7μm cryosections, prepared from formalin pre-fixed liver samples. Sections were stained with freshly prepared Oil Red O in isopropanol. Oil Red O staining provides chromogenic as well as fluorescent signals, therefore we used red channel to detect staining as described previously (Macek Jilkova, Afzal et al. 2016). Images were captured using ApoTome microscope equipped with a camera AxioCam MRm, collected by AxioVision software and quantified using ImageJ software. For Oil Red O^+ liver area, data are presented as Oil Red O positive area in percent of total tissue area. Six random areas per each liver section were analyzed.

2.2.8. Immunoblot Analysis

Liver homogenates were prepared in RIPA buffer (50 mM Tris; 1% NP40; 0.5% deoxycholic acid sodium salt; 150 mM NaCl; 1 mM EGTA) containing Proteins were then denatured in Laemmli Sample Buffer (Bio-Rad) containing 5% β-mercaptoethanol and separated by gel electrophoresis (Mini Protean Gels ®, Bio-Rad) and transferred to polyvinylidene difluoride (PVDF; Bio-Rad) membranes using a wet blot method. Membranes were blocked in TBS-Tween solution with 5% BSA for 1 h at 4 °C. Primary antibodies against p-Akt $^{(Ser473)}$, Akt $^{(pan)}$, pERK $^{(Thr202/Tyr204)}$, ERK $^{(p44/42\ MAPK)}$, β-actin (all Cell Signaling Technology, USA) were incubated at 4 °C overnight under shaking conditions. Incubation with the secondary antibody (HRP-anti rabbit IgG, 1:2000; Cell Signaling) was performed under shaking conditions for 1 h. Detection was

achieved with Clarity™ Western ECL Blotting Substrate (Bio-Rad) using a ChemiDoc™ MP Imaging System (Bio-Rad). Densitometric quantification of the bands was performed using the Image Lab™ Software (Bio-Rad)

2.2.9. Real-Time Polymerase Chain Reaction (qPCR)

Total RNA was extracted from frozen rat liver tissue samples. RNA purification was performed with RNeasy Mini Kit ® (Qiagen, USA). Reverse transcription was realized with Transcriptor First Strand cDNA Synthesis Kit ® (Life science, Roche), and amplification reactions were performed in a total volume of 20µL by using a Thermocycler sequence detector (BioRad CFX96, USA) with qPCR kit Mesa Green qPCR MasterMix Plus for SYBR Assay ® (Eurogentec, Belgium).

GADPH was used as housekeeping gene. Primers were designed with Primer 3 software (version 4.0.0) and verified on BLAST. Oligonucleotide sequences were synthesized by Eurofins Genomics ® in 0.01µmol scale, with a Salt Free level of purification. Every analysis was done in duplicates.

2.2.10. Phospho-Kinase Antibody Array Analysis

Extracts from frozen liver tissues from two controls and three ARQ 092 treated rats were analyzed by human phosphokinase antibody array kit (Catalog ARY003B, R&D System, USA) accordingly to the protocol provided by the manufacturer. Dot densities were quantified using Protein Array Analyzer programmed in ImageJ software. Values are expressed as the mean intensity relative to mean intensity of control dots of the respective membrane.

2.3. Statistical Analysis

All comparisons of means were calculated by using ANOVA tests with Tukey HSD correction for multiple means comparisons, and independent T-test only when two means were compared. A p-value of <0.05 was regarded as statistically significant and data are presented as mean values ± standard error mean (SEM). Statistical analyses were performed using Prism 6 (GraphPad Software Inc., CA, USA).

CHAPTER 3

RESULTS

3.1. First Study: Efficacy of AKT Inhibitor ARQ 092 Compared with Sorafenib in a Cirrhotic Rat Model with HCC

3.1.1. ARQ 092 Decreased Cell Viability

In this part, the cell viability was analyzed by MTT assay ising Hep3B, HepG2, HuH7 and PLC/PRF/5 cell lines. Incubation of cells with ARQ-092 or Sorafenib during 48h showed a dose-dependent decreased of cell-viability in these cell lines as shown in figure 3.1.

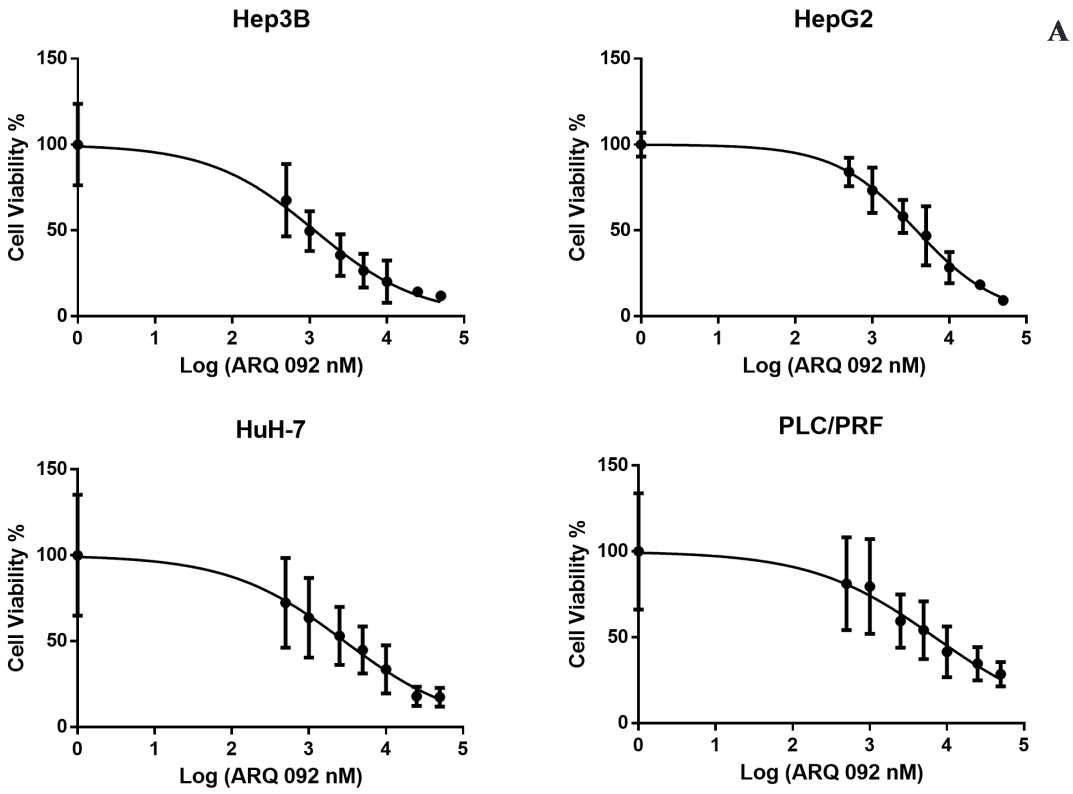

Figure 3.1. MTT assay determining the viability of Hep3B, HepG2, HuH7, PLC/PRF cells treated with different concentrations of Sorafenib **(cont. on next page)**

ARQ 092 incubated during 48 hours. (A) ARQ 092; (B) Sorafenib single treatment on mentioned cell lines. All experiments were done in triplicates and repeated three times. Data are presented as mean ± SD (n=9).

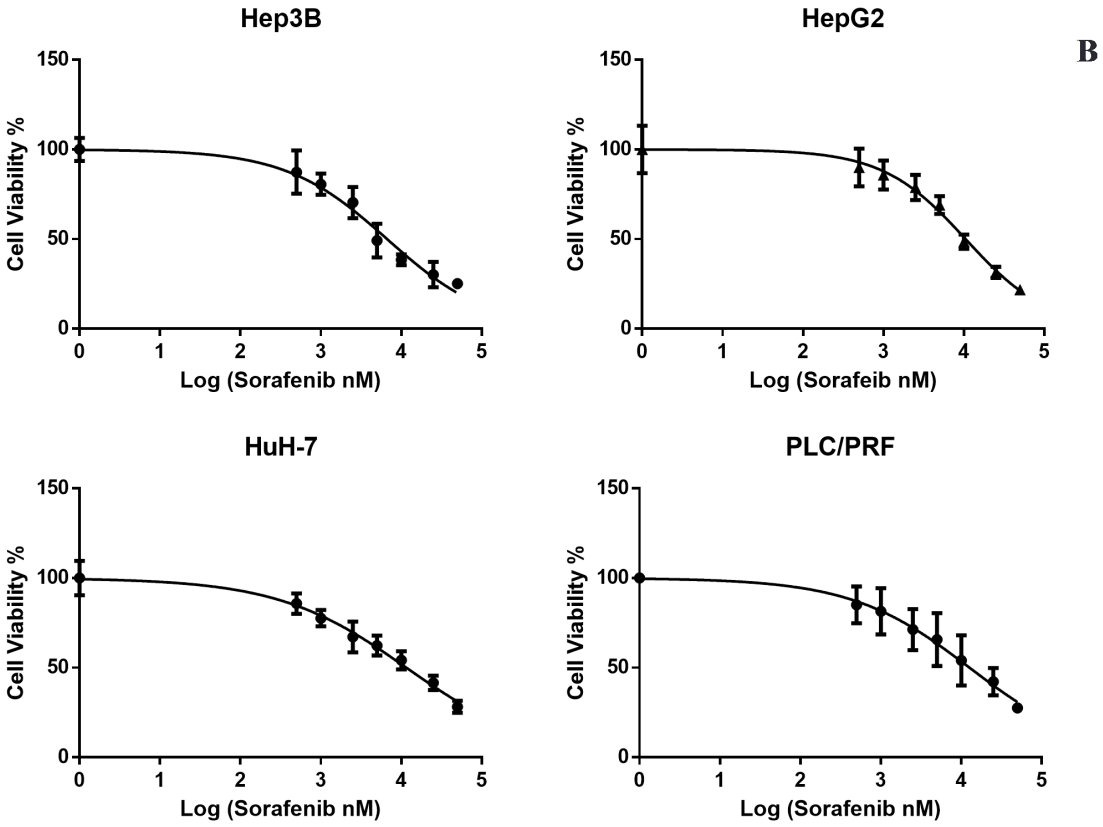

Figure 3.1 (cont.).

From figure 3.1, we can observe that cell viability decreased with increasing concentration of the treatment. Figure 3.1. A represents the single treatment of ARQ 092 and figure 3.1. B represents the single treatment of Sorafenib. Values of IC20 (Inhibitory Concentration 20) were calculated as a growth inhibition 20, where cell viability was 80 % followed by 20 % cell death and IC50 (Inhibitory Concentration 50) as a growth inhibition 50, where cell viability was 50 % followed by 50 % cell death. As expected, when concentration of drugs increased, cell viability of all cell lines decreased.

IC20 and IC50 values of the treatments after 48 hours of incubation are shown in table3.

Table 3. Inhibitory Concentration (IC) 20 and 50 values of Hep3B, HuH7, HepG2 and PLC/PRF cells treated with of ARQ 092 and Sorafenib alone. Values are expressed as the mean ± SD of three independent experiments performed in triplicates.

		Sorafenib	ARQ 092	
		Concentration (μM)		p-value
HepG2	IC20	1.5 ±0.05	0.7 ±0.03	0.2080
	IC50	10.5 ±0.04	3.7 ±0.03	0.0019
Hep3B	IC20	0.9 ±0.03	0.1 ±0.02	0.0268
	IC50	6.7 ±0.03	1.2 ±0.06	< 0.0001
HuH7	IC20	0.9 ±0.01	0.3 ±0.02	0.1514
	IC50	11.6 ±0.03	2.9 ±0.08	0.0027
PLC/PRF/5	IC20	1.1 ±0.06	0.6 ±0.04	0.3091
	IC50	12.7 ±0.04	7.0 ±0.08	0.0830

3.1.2. ARQ 092 Induced Apoptosis

Annexin V FITC and 7AAD staining was used to quantify the apoptosis rate in Hep3B, HepG2, HuH-7 and PLC/PRF cells. The plot has four quadrants: upper left quadrant (Q1-UL) shows necrotic cells (Annexin -, 7AAD+), upper right quadrant (Q1-UR) shows late apoptotic cells (Annexin +, 7AAD+), lower left quadrant (Q1-LL) shows live cells (Annexin -, 7AAD-) and lower right quadrant (Q1-LR) shows early apoptotic cells (Annexin +, 7AAD-) (Figure 3.2).

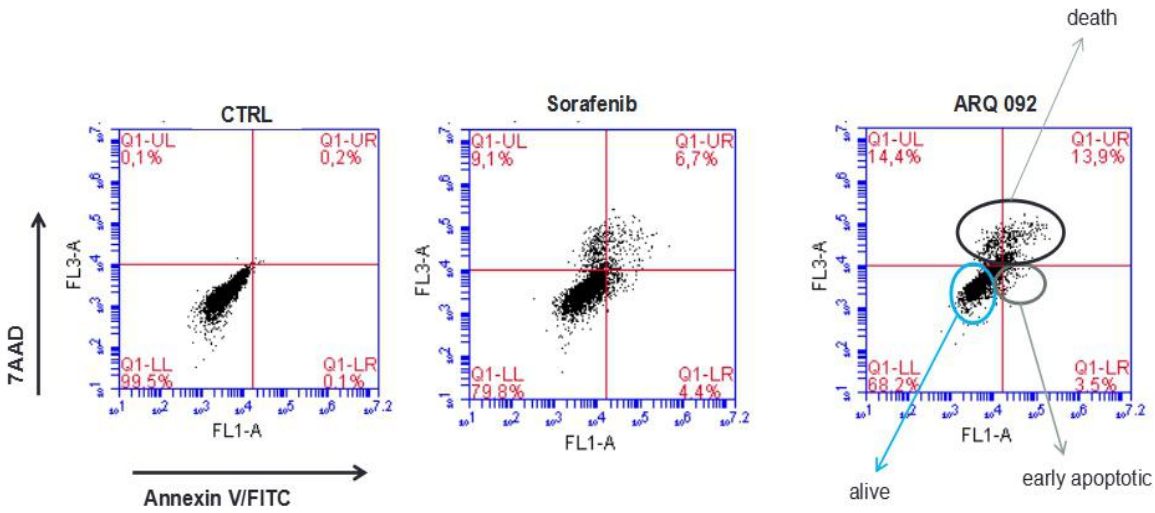

Figure 3.2. Represantative pictures for flow cytometry analysis of cell apoptosis using Annexin V-FITC and 7AAD stainings.

Flow cytometry analysis revealed that ARQ 092 had a dose-dependent effect on apoptosis induction as shown in figure 3.3. Its effect on apoptosis induction was superior to Sorafenib in every cell lines and this superiority was always significant at IC50 concentration as illustrated by figure 3.3.

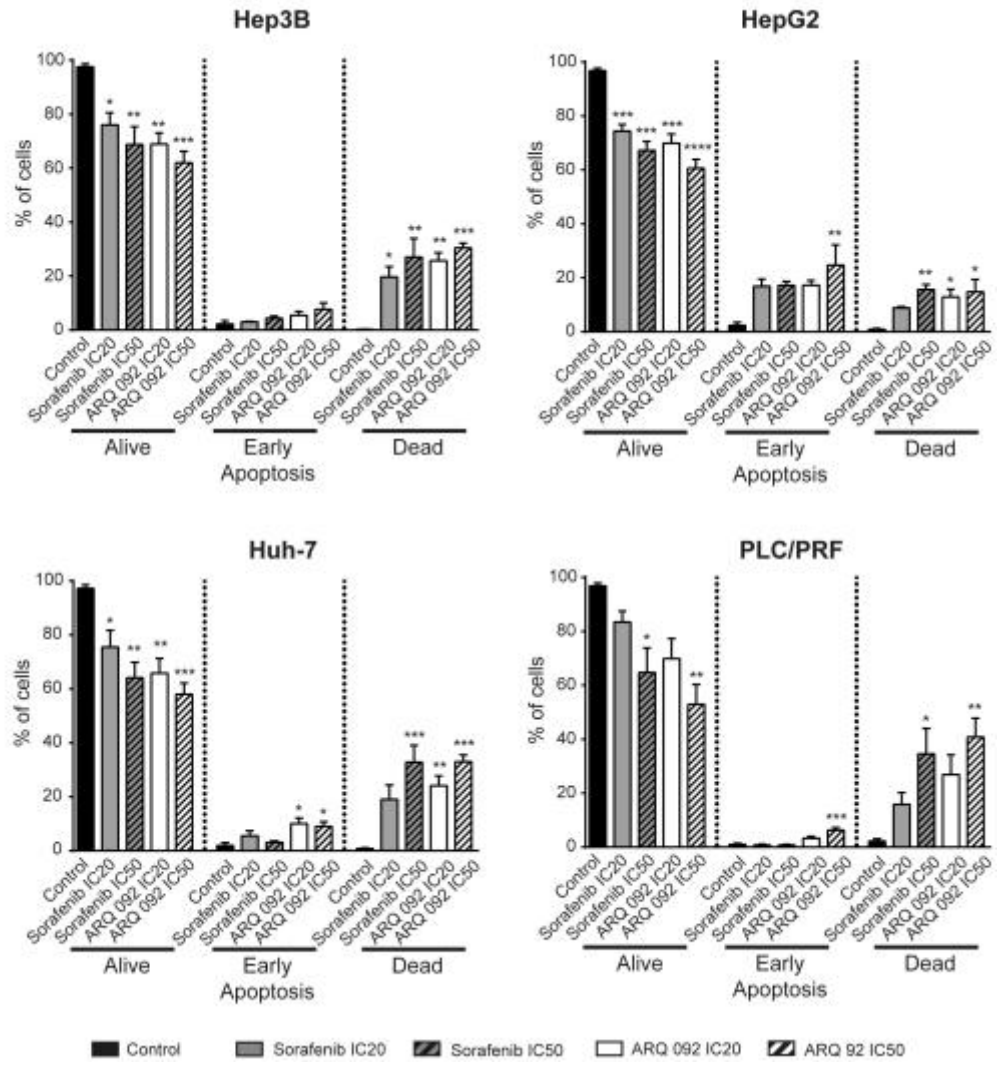

Figure 3.3. Dose-dependent effects of Sorafenib and ARQ 092 on apoptosis in Hep3B (upper left), HepG2 (upper right), Huh-7 (lower left), PLC/PRF (lower right) after 48h of exposure. Values are expressed as means ± SD of three independent experiments performed in duplicates. *p ≤ 0.05, **p ≤ 0.01, ***p ≤ 0.001, ****p ≤ 0.0001 vs. control.

3.1.3. ARQ 092 Inhibited Cell Migration

By wound healing assay, we investigated whether ARQ 092 affect migratory behavior of human HCC cells. Cells were monitored every 24 hours for three days to evaluate the rate of migration into the scratched ares. After 24h incubation times, both IC20 and IC50 concentrations of ARQ 092 strongly reduced migration of Hep3B while Sorafenib had significant effect at IC50 only (Figure 3.4). ARQ 092 or Sorafenib

reduced migration of these cells compared to control with high statistical differences between the groups as illustrated by figure 3.4.

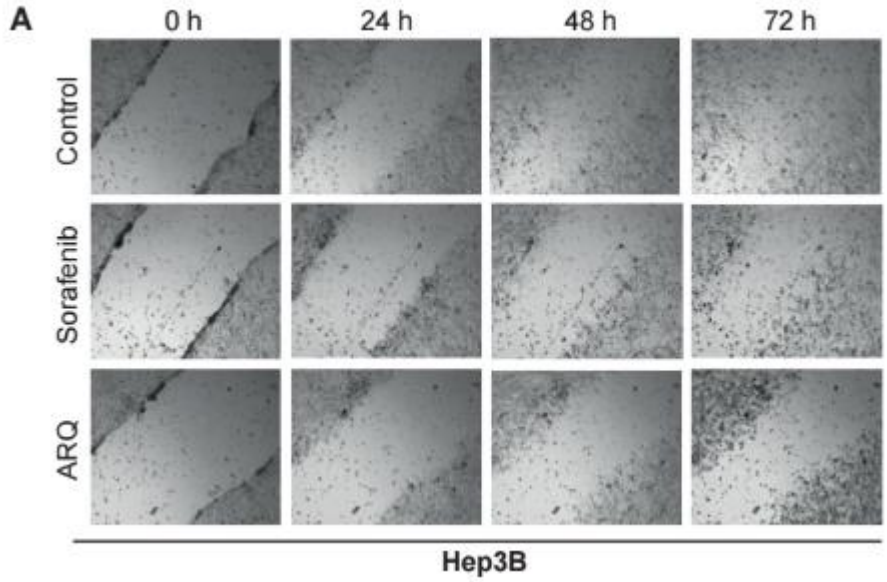

Figure 3.4. Effects of Sorafenib and ARQ 092 on migration of HCC cells. (A) Representative pictures of wound-healing assay at baseline, after 24h, 48h and 72h on Hep3B cell line. (B) Quantification of migration (decrease of width of the wound after first 24h) in Hep3B (upper left), HepG2 (upper right), PLC/PRF (lower left) and Huh-7 cell lines (lower right). Control was set as 100%, values are expressed as means ± SEM from three independent determinations. **(cont. on next page)**

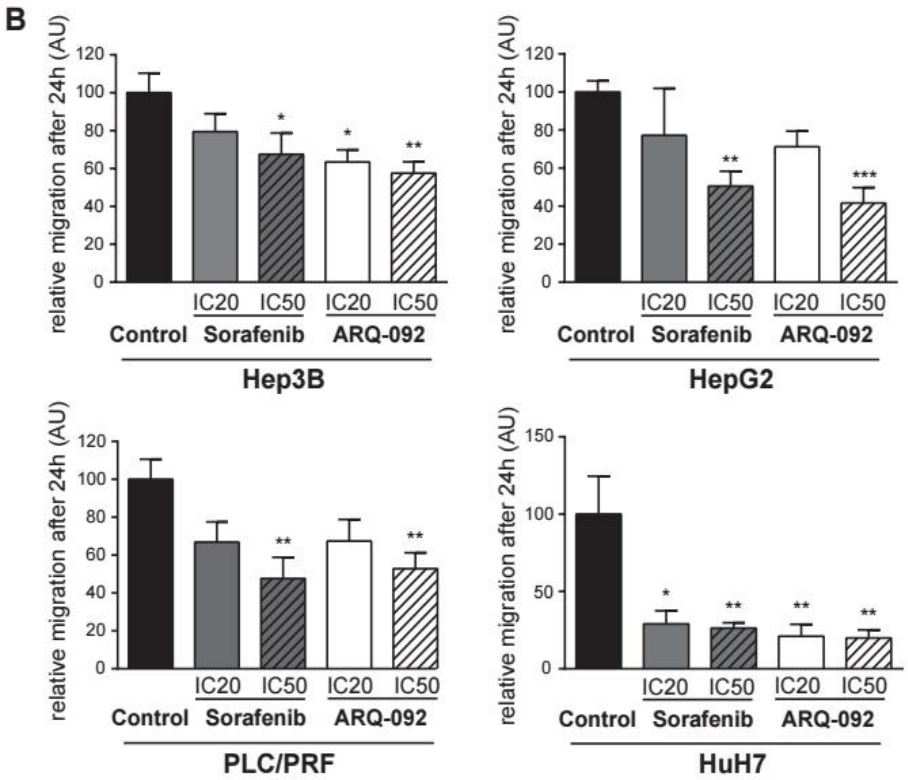

Figure 3.4. (cont.).

3.1.4. Pathway Analysis

Western blot analysis of following proteins, AKT, phosphorylated AKT (pAKT) $^{(Ser473)}$ and β actin, was performed on cell lysates of Hep3B, HepG2, HuH7 and PLC/PRF human cell lines. ARQ 092 treatment completely blocked phosphorylation of AKT as observed at two concentrations of IC20 and IC50 shown in figure 3.5. To statistic analysis, not only IC50 concentration but also IC20 concentration were found significantly decreased phosphorylation of AKT compared to control and sorafenib group for Hep3B and HepG2 cell lines, compered to control for HuH7 and PLC/PRF cell lines.

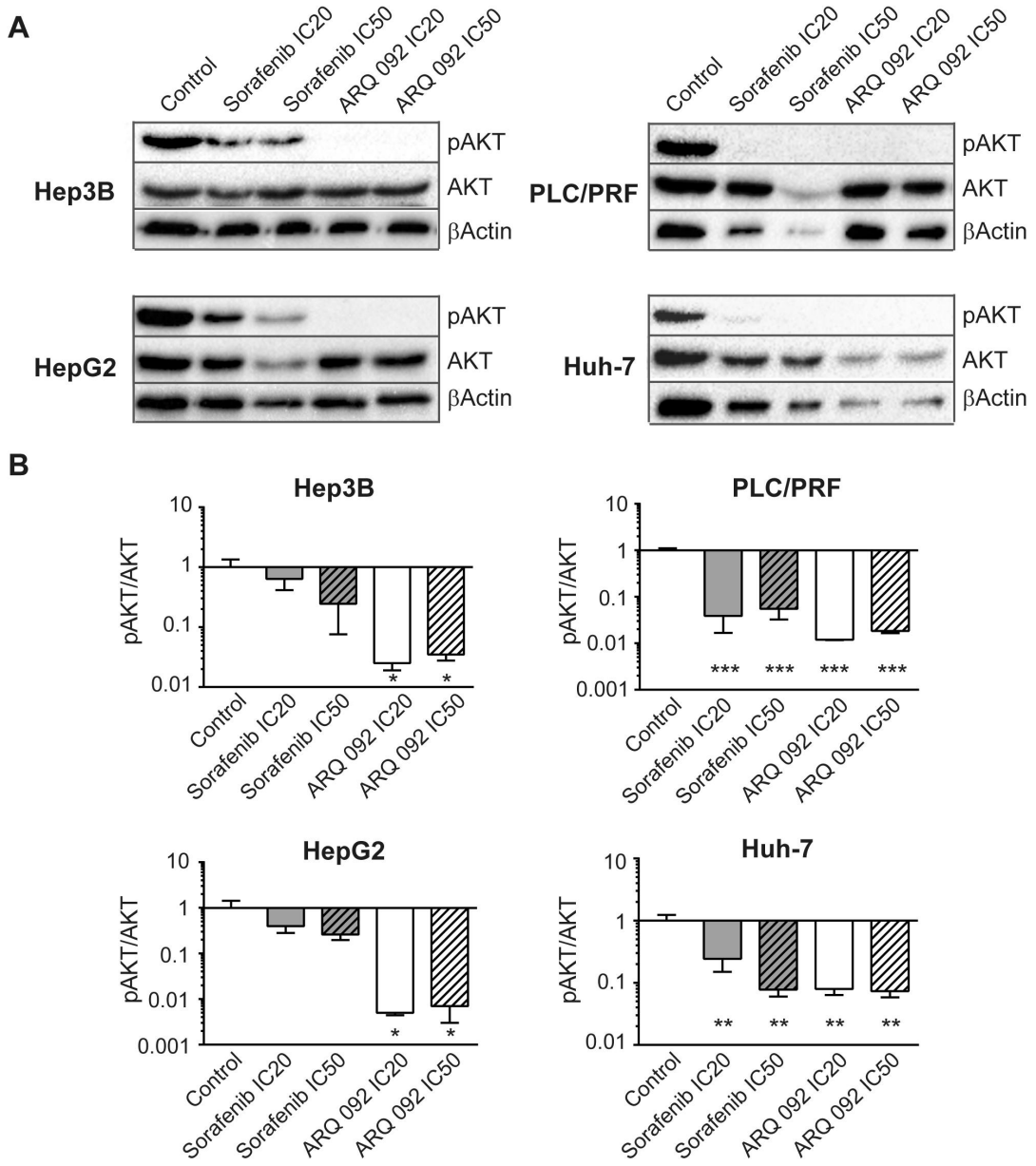

Figure 3.5. Effects of Sorafenib and ARQ 092 on AKT phosphorylation. A) Protein levels of pAKT(Ser473) and AKT after 24 h exposure. Same results were obtained after 2 h and 48 h of exposure - data not shown. B) Quantification of pAKT/AKT ratio in Hep3B (upper left), PLC/PRF (upper right), HepG2 (lower left) and Huh-7 cell lines (lower right). Control was set as 100%, values are expressed as means ± SEM from three independent experiments. *$p \leq 0.05$, **$p \leq 0.01$, ***$p \leq 0.001$ vs. control.

3.1.5. Immunofluorescence Staining

In order to confirm western blot analysis, the p-AKT expression in Hep3B, HepG2, HuH7 and PLC/PRF cell lines was investigated. Immunofluorescence stainings of p-AKT showed no expression or lower expression in ARQ 092 treated cells than Sorafenib treated and untreated cells in demonstrated figure 3.6.

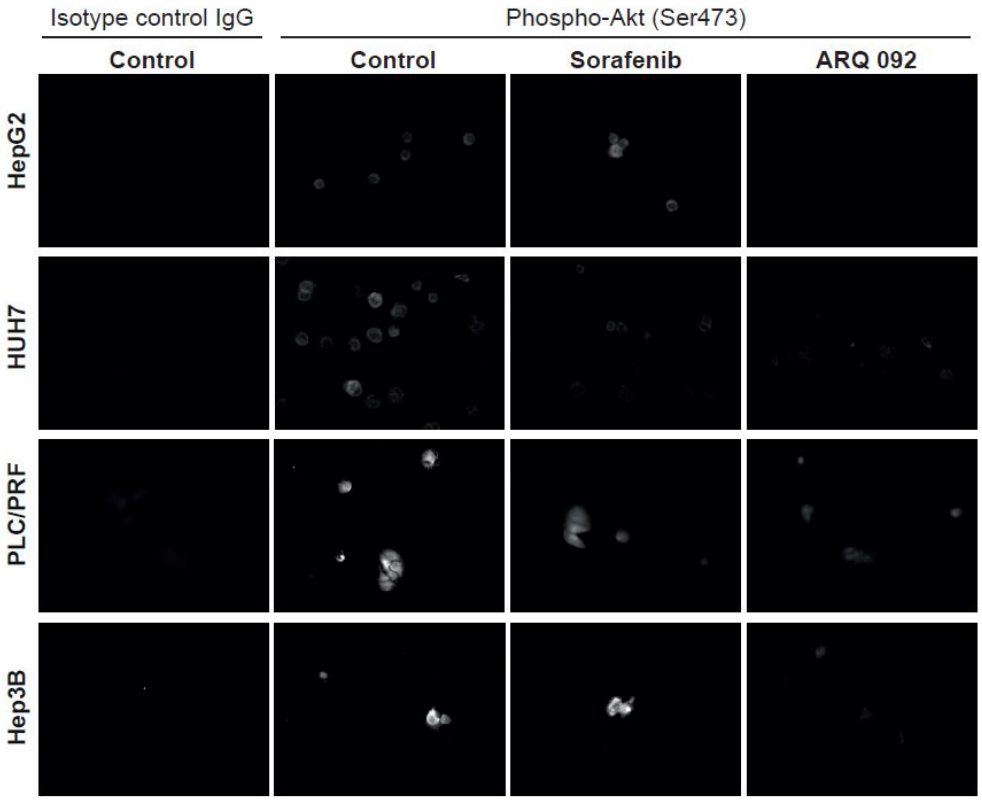

Figure 3.6. Effects of Sorafenib or ARQ 092 on phosphorylation of AKT(Ser473).

3.1.6. Treatment Tolerance

We made three groups of rats: one of them was Sorafenib treated group, the other one was ARQ 092 treated group and third one was untreated group (control). During six week, all the rats were monitored. In the Sorafenib group, dose was reduced to 10 mg/kg/day from 20 mg/kg/day for each rat after one week of treatment because of a significant loss of weight, 6.8% of their initial body weight, and signs of severe

toxicity in two rats with a loss of their initial body weight and with adverse events as diarrhea, strong asthenia, and modifications of their behavior considered as hepatic encephalopathy. They died after 17 and 11 days and their death was considered due to toxicity of the treatment. Sorafenib was also stopped in a third rat after 11 days of treatment because of the same adverse events with a loss of weight . It was reintroduced 7 days later, because of an increase of its weight and a disappearance of signs of toxicity, but it was stopped again 3 days after the reintroduction because the same adverse events reappeared. At the end of the study, the mean loss of weight was 5.8% in the Sorafenib group compared to a gain of 5.9% in the control group. In addition, during treatment, 4 rats (40%) presented episode of diarrhea, 3 rats (30%) presented signs of hepatic encephalopathy and 2 (20%) died due to a severe toxicity as resumed in table 4. In the ARQ-092 group, the mean loss of weight was 0.8% at the end of study. Seven rats (70%) presented a temporary loss of weight superior to 10% as described in table 4. This was rapidly reversible during the week without treatment, and after intensification of the nutritional care. No treatment was stopped and no toxic death occurred. Two rats died after 29 and 35 days because of an intraperitoneal tumoral bleeding from an exophytic hepatic tumor despite a mild radiological tumor progression. At the end of study, the mean weight loss was 5.8 ± 5.5% in the Sorafenib group and 0.8 ± 0.6% in ARQ 092 group compared to a gain of 5.9 ± 3.1% in the control group (p=0.164), table 4.

Table 4. Adverse events in Sorafenib, ARQ-092 and control groups.

Adverse events	Sorafenib (n=10)	ARQ-092 (n=10)	Control (n=6)
Diarrhea	4 (40%)	1 (10%)	0
Hepatic encephalopathy	3 (30%)	0	0
Loss of weight > 10% and <20%	3 (30%)	7 (70%)	0
Loss of weight > 20%	3 (30%)	0	0
Hand-foot skin lesions	2 (20%)	0	0
Dose-reduction	7 (70%)	0	0
Treatment stop	3 (30%)	0	0
Toxic death	2 (20%)	0	0

Blood sample analysis (Table 5) revealed better liver function in ARQ 092 and Sorafenib groups compared to control group, with a significantly lower total bilirubin level (ARQ 092: p=0.0007, Sorafenib: p=0.0002), albumin level was significantly higher in ARQ 092 compared to non-treated rats (p=0.0170) and Sorafenib group (p=0.0098). There was no statistical difference in transaminases, ALP and GGT levels, but serum levels of AFP were significantly decreased by ARQ 092 treatment compared to control (p=0.0328). Glucose, cholesterol and triglyceride blood concentrations were similar to the control group. Assessment of triglycerides in liver and Oil Red O staining did not show any significant difference between groups (p=0.467, p=0.355) (Table 5) (Figure 3.7). Therefore, our results showed that ARQ 092 treatment does not interfere with lipid metabolism and improves liver function.

Table 5. Clinical and Biological Analyses

		Control (n=6)	Sorafenib (n=10)	ARQ 092 (n=10)	ANOVA p-values (Tukey HSD)
Mean Δ body weight (% of initial weight)		+5.9 ± 3.1	-5.8 ± 5.5	-0.8 ± 0.6	*0.164*
Liver tissue	Intrahepatic TG (g/L)	34.8 ± 6.9	28.0 ± 3.0	30.2 ± 1.9	*0.467*
	Oil Red O (%)	10.9 ± 4.4	6.5 ± 1.9	11.2 ± 1.8	*0.355*
Blood samples	Albumin (g/dL)	3.7 ± 0.2	3.7 ± 0.1	4.1 ± 0.3 $^{\#\#}$	*0.006*
	AST (IU/L)	320 ± 29	325 ± 46	357 ± 104	*0.250*
	ALT (IU/L)	303 ± 28	206 ± 28	269 ± 81	*0.171*
	ALP (IU/L)	306 ± 6	212 ± 3 *	230 ± 11	*0.023*
	GGT (IU/L)	147 ± 15	47 ± 8	82 ± 26	*0.087*
	Glucose (mg/dL)	131 ± 3	142 ± 7	153 ± 4	*0.086*
	Cholesterol (g/L)	1.19 ± 0.01	0.99 ± 0.06	1.20 ± 0.07	*0.071*
	TG (g/L)	1.19 ± 0.04	1.31 ± 0.15	1.30 ± 0.21	*0.927*
	Total Bilirubin (mg/L)	4.09 ± 0.58	1.46 ± 0.19 ***	1.75 ± 0.18 ***	*0.0003*
	Direct Bilirubin (mg/L)	2.05 ± 0.29	0.58 ± 0.00 ****	0.58 ± 0.00 ****	*<0.0001*
	Prothrombin time (s)	16.3 ± 0.9	18.7 ± 4.4	16.7 ± 0.5	*0.301*
	AFP (ng/mL)	0.85 ± 0.15	0.44 ± 0.12	0.33 ± 0.09 *	*0.041*

AST, aspartate aminotransferase; ALT, alanine aminotransferase; ALP, alkaline phosphatase; GGT, Gamma-glutamyl transpeptidase; AFP, alphafetoprotein; Values are means ± SE, significant difference compared to control; *: p<0.05 ; **: p<0.01 ; ***: p<0.001 ; ****: p<0.0001. Significant difference between ARQ 092 and sorafenib; ##: p<0.01.

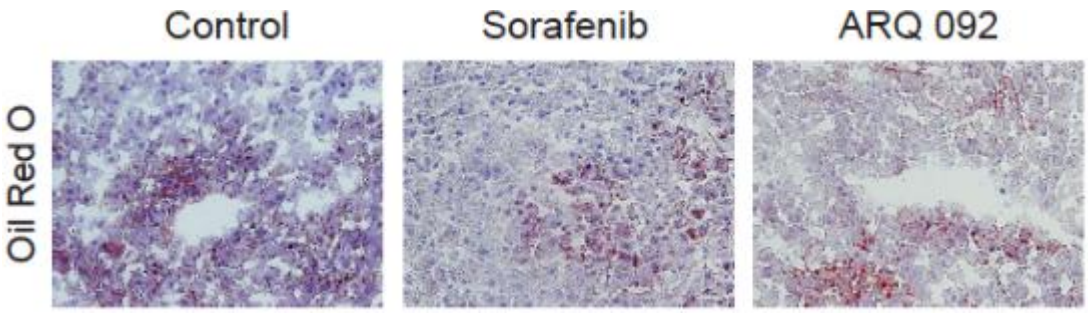

Figure 3.7. Representative pictures of lipids accumulations in rat livers after Oil Red O staining.

3.1.7. Anti-tumor Efficacy

3.1.7.1. Morphological Analysis

On the first MRI (n=26), tumor sizes were comparable between groups with 21.3 ± 1.7 mm, 18.0 ± 1.2 mm and 20.6 ± 2.0 mm in control, Sorafenib and ARQ-092 groups (p=0.424), respectively. As illustrated by Figure 3 8, on the second MRI (n=24), tumor progression was significantly reduced in the Sorafenib (+ 28.5 ± 3.0%; p<0.0001) and ARQ 092 (+ 20.9 ± 3.8% ; p<0.00001) groups compared to control (+ 69.6 ± 9.0%). No statistical difference was found between Sorafenib and ARQ 092 groups (p=0.38) on the third MRI (n=22) where the tumor progression rate was + 57.0 ± 8.1% in ARQ 092 group compared to + 80.2 ± 9.3%, in Sorafenib group (p=0.273) and + 155.3 ± 16.0% in the control group, (p<0.0001) (Figure 3.8). Tumor progression was lower in ARQ-092 group than in Sorafenib group but without statistical difference.

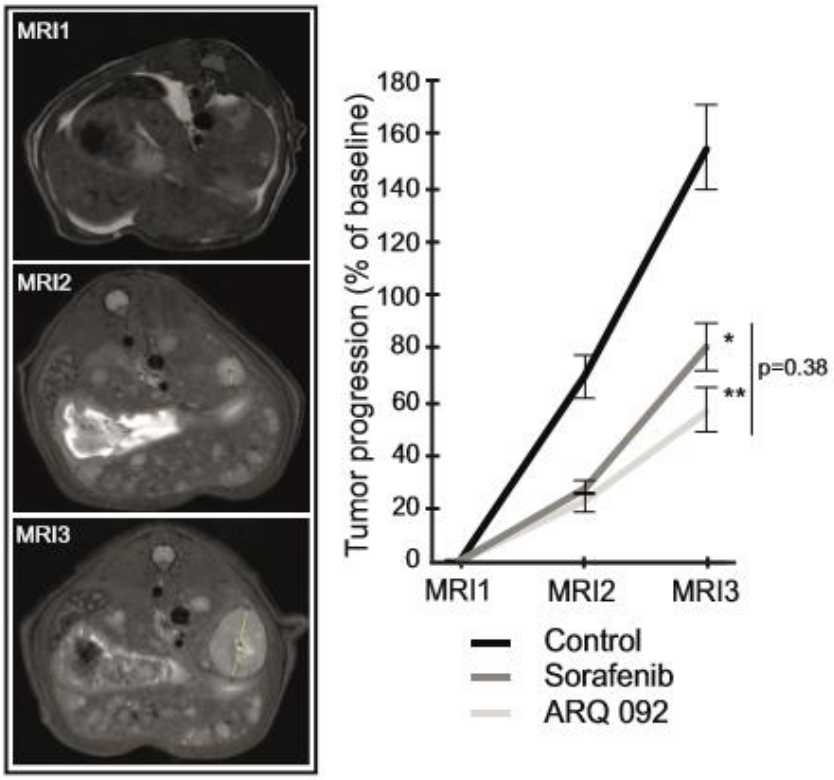

Figure 3.8. Effect of ARQ 092 and Sorafenib on tumor progression and proliferation. MRI morphological analysis with representative T2 turboRARE images and tumor progression assessment by comparison of tumor size on MRI 1, 2 and 3 in control, Sorafenib and ARQ 092 groups (MRI 1 was considered as the baseline in each group and MRI2 and 3 were expressed as a percentage of MRI1).

3.1.7.2. Histopathological Analyses

It was further confirmed by macroscopic examination of the liver as showed Figure 3 9. After the third MRI, rats were euthanized and liver were removed, weighed and macroscopically inspected. Mean tumor volume represented by the sum of diameters of the 5 largest tumors were 28.8 ± 1.8 mm in the ARQ 092 group compared to 37.9 ± 3.1 mm in Sorafenib group ($p=0.092$) and 62.7 ± 4.4 mm in control group ($p<0.0001$) by illustrated figure 3.9.

Rats from the group treated with ARQ 092 also displayed a significantly lower number of tumors (53.9 ± 7.0 tumors) when compared to Sorafenib-treated animals (96.3 ± 13.5 tumors, $p=0.021$) and controls (96.8 ± 9.4 tumors, $p=0.031$) and shown in figure 3.9.

ARQ-092 showed a statistically greater efficiency in the control of tumoral initiation and progression.

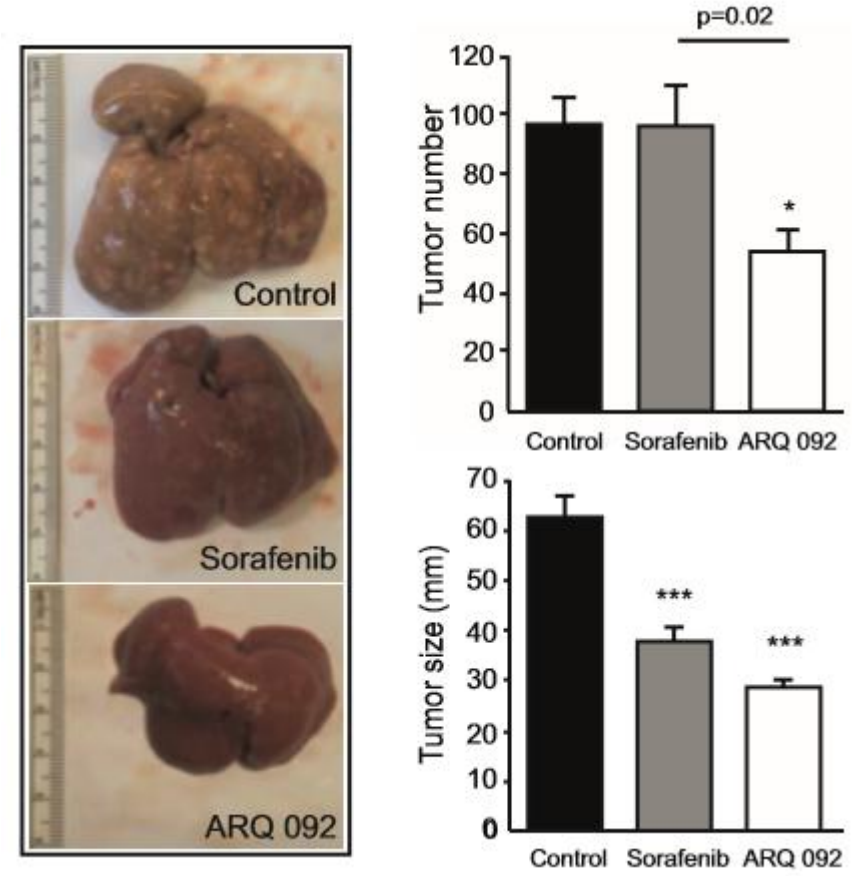

Figure 3.9. Macroscopic examination of livers with assessment of tumor number (upper bar chart) and tumor size (sum of diameter of the five largest tumors) (lower bar chart) at the surface of livers.

3.1.7.3. Immunohistochemical Analyses

Cell proliferation and apoptosis were monitored by Ki67 and TUNEL immunostainings. Figure 3.10 shows that only ARQ 092 significantly decreased proliferation (41.1 ± 13.3 % of control, p=0.042) and induced apoptosis (148.6 ± 7.7% of control, p=0.045), while Sorafenib shows no statistical significance with these parameters (Ki67: 56.9 ± 19.6 % of control, p=0.160 ; TUNEL: 144.2 ± 16.5% of control, p=0.072).

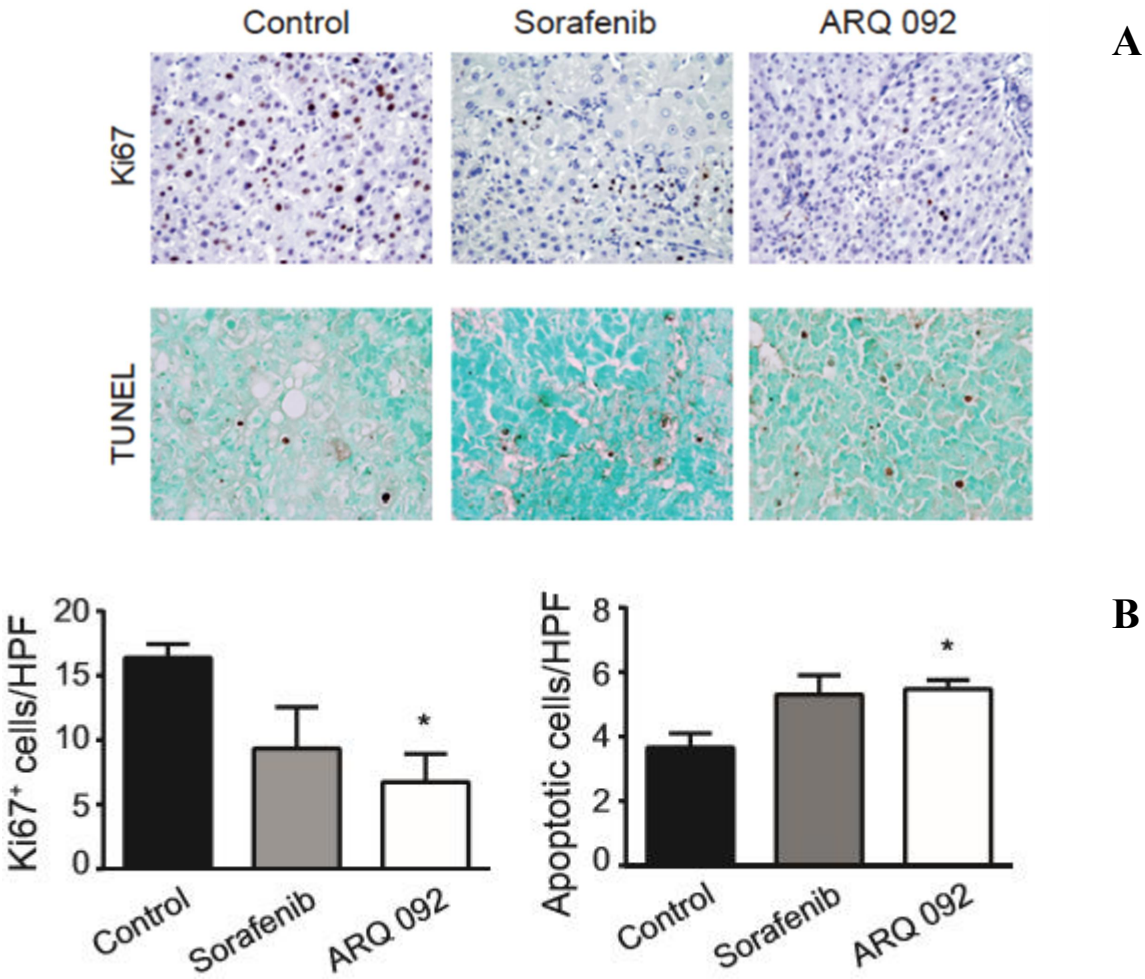

Figure 3.10. (A) Representative pictures of tumor proliferation (Ki67 marker) and apoptosis (TUNEL- staining), respectively. (B) Immunohistochemistry analysis of tumor proliferation (left bar chart), and apoptosis induction (right bar chart) with Ki67 and TUNEL immunostainings, respectively.

3.1.8. Level of Alpha Feto Protein (AFP)

Alpha-fetoprotein (AFP) is a major plasma protein that is produced by the yolk sac and the liver (Lee, Chang et al. 1989). Very high level of APF has been associated to liver damages and hepatocellular carcinoma (Ertle, Heider et al. 2013). Thus, level of AFP was investigated level of AFP in serum. Levels of AFP were significantly decreased by ARQ 092 treatment compared to control (p=0.041) as shown table 5.

Besides this, qPCR analysis of AFP gene expression in tumor liver samples was performed. ARQ 092 treated group significantly decreased the expression of AFP gene. On the other hand, Sorafenib treated group did not show significant decrease (Figure 3.11).

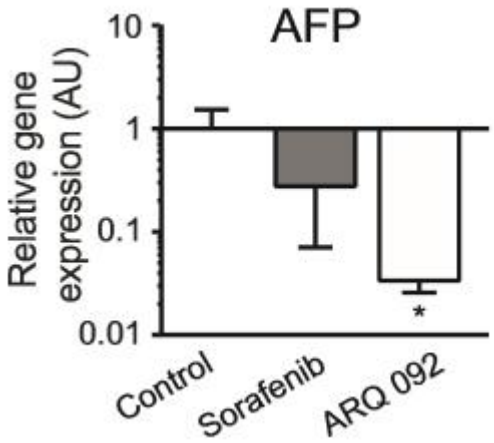

Figure 3.11. RT-qPCR analysis of alpha fetoprotein (AFP) gene expression in tumor liver samples.

3.1.9. Anti-angiogenic Effect

In order to investigate anti-angiogenic effect, dynamic contrast enhanced (DCE) MRI was assessed, as illustrated figure 3.12. At the baseline, i.e.the first MRI, tumor enhancement was comparable between the groups shown in figure 3.13.

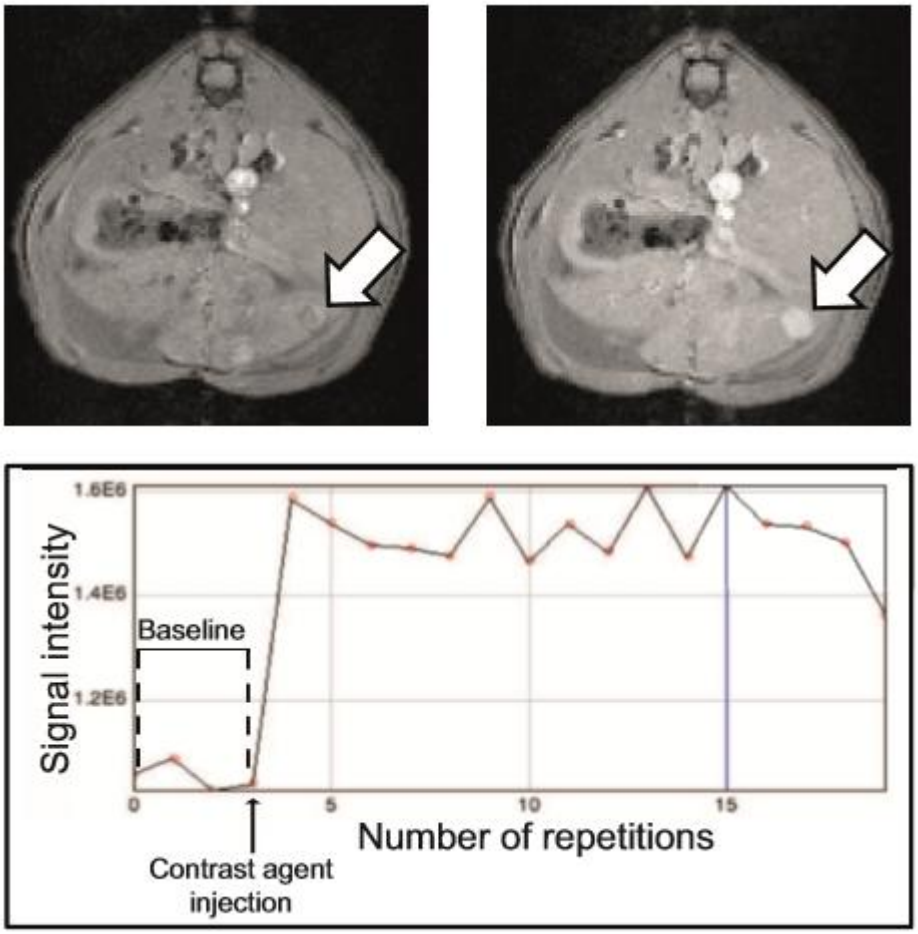

Figure 3.12. Dynamic contrast enhanced (DCE) MRI pictures of a control rat before (left picture) and after (right picture) injection of contrast agent with a typical enhancement curve obtained by analysis of signal intensity on the tumor area illustrated by previous pictures.

On MRI3, tumor enhancement was significantly different between the groups with significantly less tumor enhancement in ARQ 092 group compared to the Sorafenib group. In each group of treatment, comparison between baseline and the end of the treatment (MRI1 and MRI3), revealed that only ARQ 092 treatment was associated with a significant decrease of tumor enhancement (p=0.012; Figure 3.13).

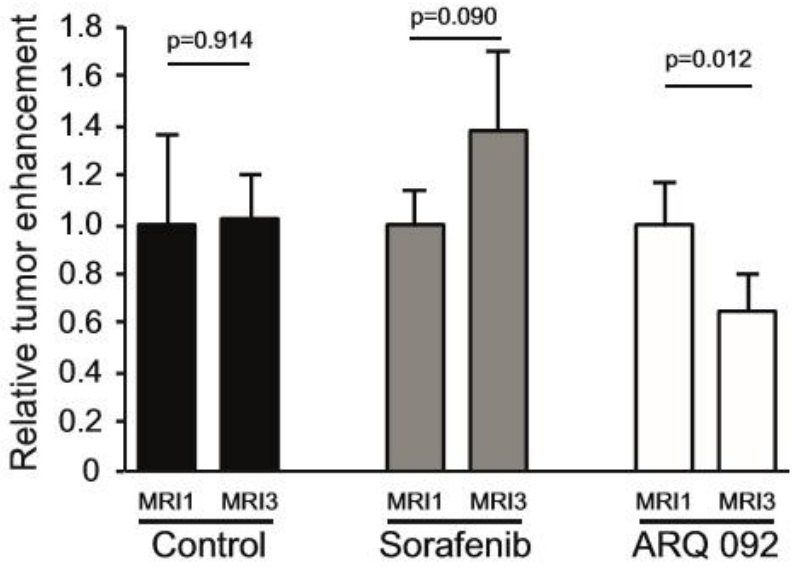

Figure 3.13. Comparison of MRI1 (left) and MRI3 (right) tumor enhancement of ARQ 092, Sorafenib and control groups. Control group was set as 1, ARQ 092 and Sorafenib groups are expressed as a percentage of control.

Secondly, to prove anti-angiogenic effect, tumor vascularization was studied by using a rat specific anti-CD34 antibody to perform immunofluoresence staining of liver tissues. While structural abnormalities of the tumor vasculature were numerous in control animals, normalization of vasculature was observed in both treated groups (Figure 3.14A). The quantification of vascular density revealed that Sorafenib decreased vascular density by 46 % ($p=0.0008$) and ARQ 092, by 68 % ($p<0.0001$) of non-treated rats (Figure 3.14B).

Therefore, MRI results and CD34 staining demonstrate that treatment by ARQ 092 leads to vascular normalization and inhibition of tumor angiogenesis.

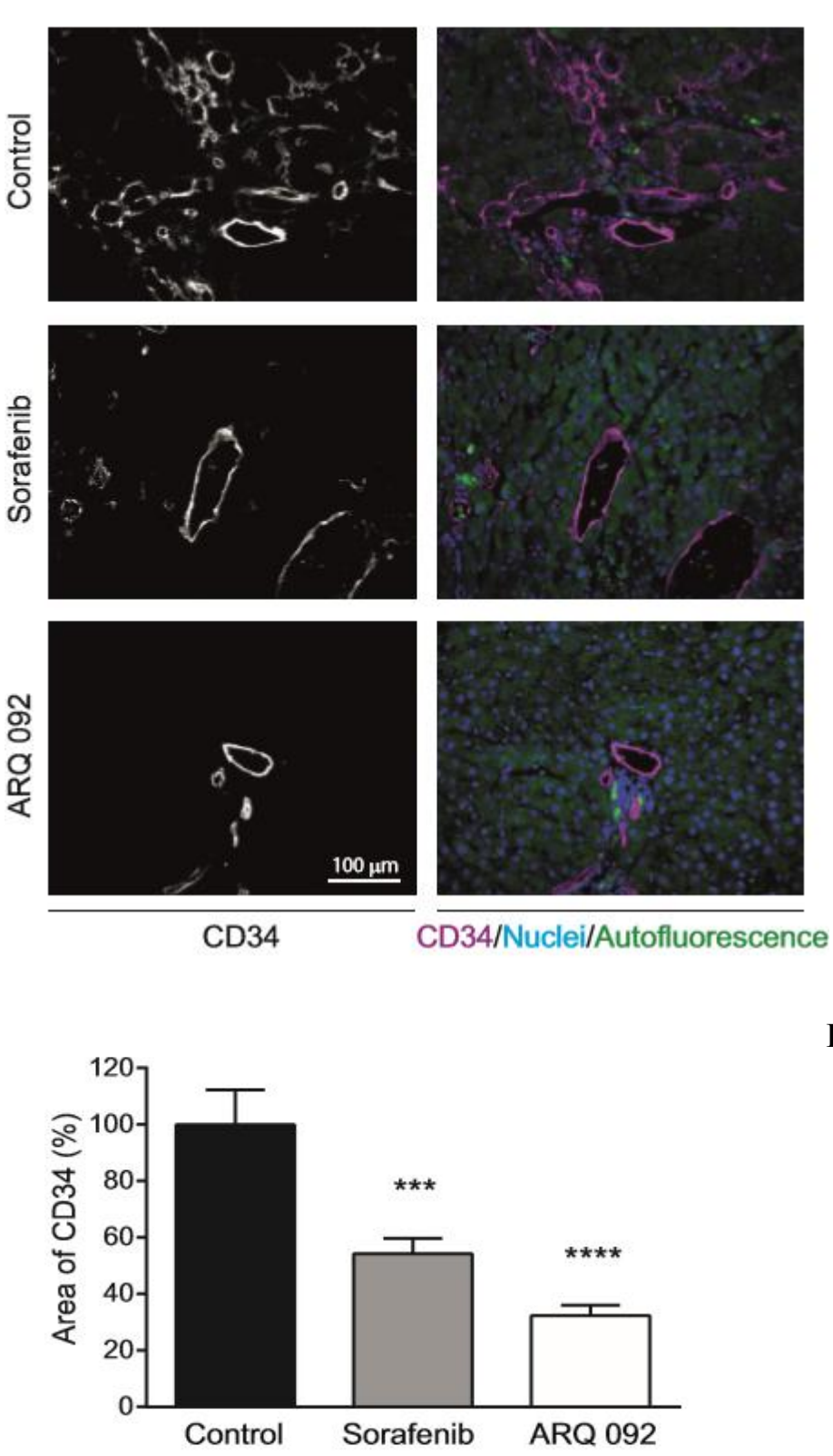

Figure 3.14. (A)Representative pictures of CD34 staining of liver tissue. (B) Quantification of CD34 immunostaining. Control was set as 100%, valuesare means ± SE. **: $p<0.01$; ***: $p<0.001$ vs. control.

3.1.10. Liver Fibrosis Assessment

Sirius red staining is used to observe fibrosis that is known to be increased in cases of inflammation and cancer. Thus, in order to investigate liver fibrosis, sirius red staining was performed. According to figure 3.15, liver fibrosis was significantly reduced in ARQ 092 group compared to the control group (p=0.001) and to the Sorafenib group (p=0.021). Difference between Sorafenib and ARQ 092 groups was not significant (p=0.348).

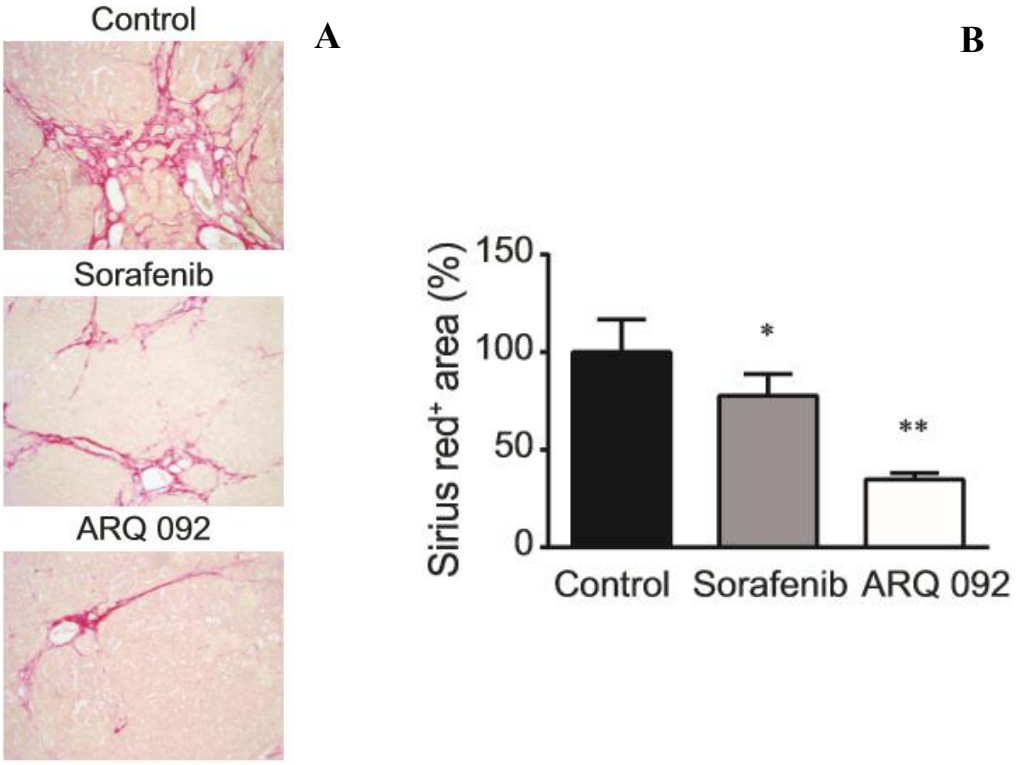

Figure 3.15. (A) Representative histological images of livers stained with Sirius red from control, Sorafenib or ARQ 092 rats,10x magnification. (B) Quantification of fibrosis on 10 random fields/ slide, 1 slide per animal (Sirius red staining area per total area; control was set as 100%).

Improvement of liver fibrosis by ARQ 092 treatment was confirmed by qPCR analysis figure 3.16. The expression of fibrosis markers was downregulated in non-tumor liver samples of ARQ 092 group compared to the control group with significant differences for alpha actin (ACTA)1. (31.7 ± 10.9% of control, p=0.029) and collagen 1 (9.9 ± 2.9% of control, p=0.007), but no significant difference for transforming growth

factor (TGFβ1) (40.1 ± 15.9% of control, p=0.115) was observed. For Sorafenib group, collagen 1 was the only significantly downregulated fibrosis marker (23.0 ± 12.3% of control, p=0.02).

Overall, ARQ 092 significantly decreased hepatic collagen deposition and improved liver fibrosis in DEN-induced cirrhotic rat model of HCC.

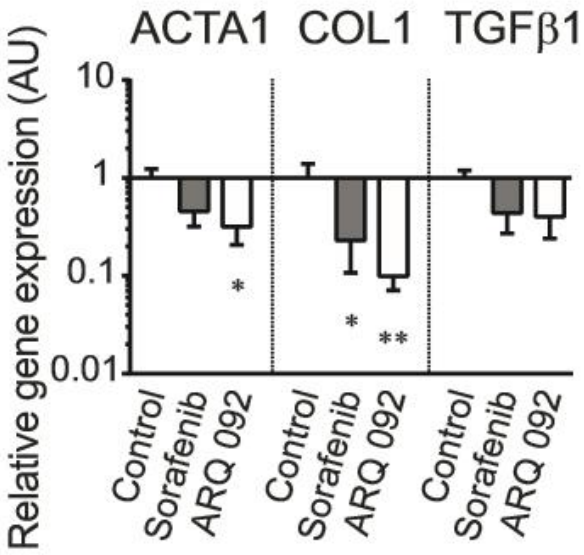

Figure 3.16. Relative gene expression of Actin alpha (ACTA)1, Collagen 1 (COL1) and Transforming growth factor (TGF)β1 in non-tumor liver tissues (n=5). Control was set as 1, values are means ± SE. **p <0.01 vs.

3.1.11. Pathway Analyses

Western blot analyses demonstrated an effect on the AKT pathway as ARQ 092 inhibited phosphorylation of AKT(Ser473) in both tumor and non-tumor liver tissues, (Figure 3.17) with a pAKT/AKT ratio of 29.5 ± 2.27% of control (p=0.002) in tumor samples and 17.2 ± 2.33% of control (p=0.034) in surrounding liver samples. Interestingly, Sorafenib treatment significantly increased pAKT/AKT ratio in tumor samples (p<0.0001) compare to the control group.

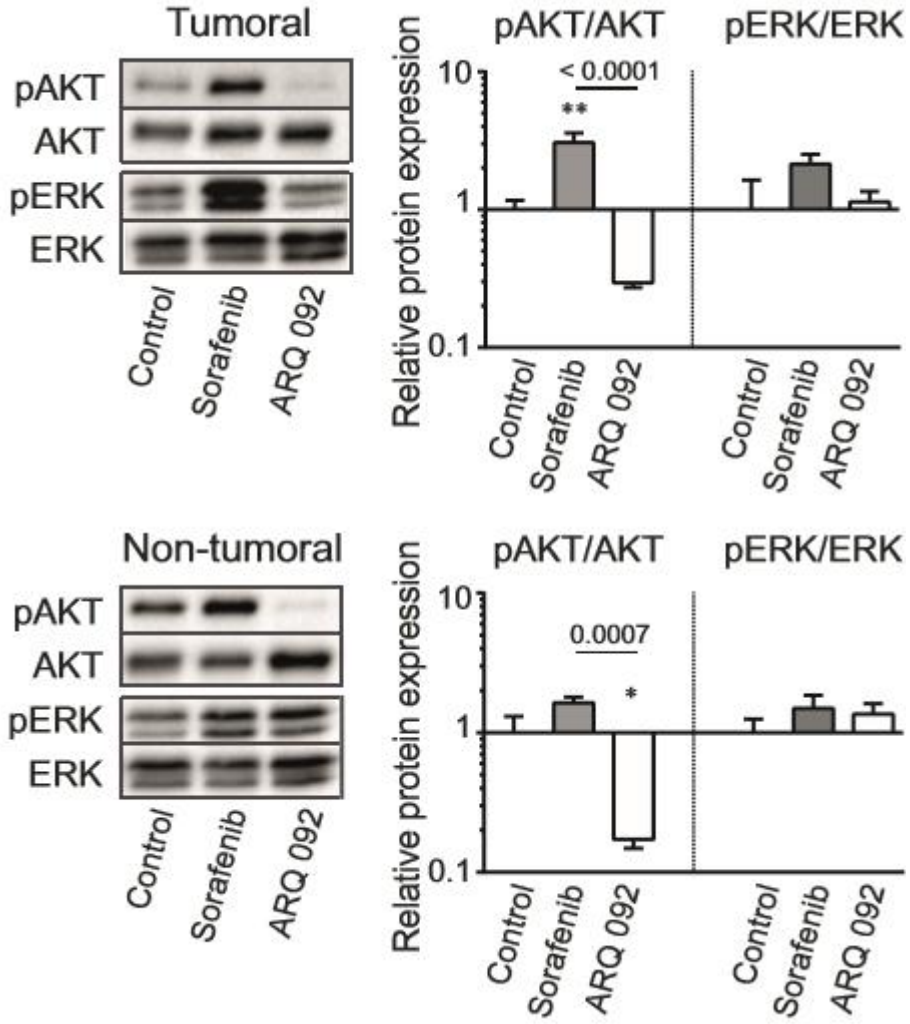

Figure 3.17. Effect of ARQ 092 and Sorafenib on AKT and ERK pathways. Western blot analysis of pAKT/ AKT and pERK/ERK in tumor (above) and non-tumor (below) liver tissue and the quantification of its.

By profiling kinases phosphorylations, it was found that the levels of phosphorylated mTOR, proline-rich Akt/PKB substrate 40 kDa (PRAS 40), phospholipase C (PLC)γ1 and Ribosomal protein S6 kinase (S6K1) were significantly decreased in tumor tissues after ARQ 092 treatment compared to the control (Figure 3.18).

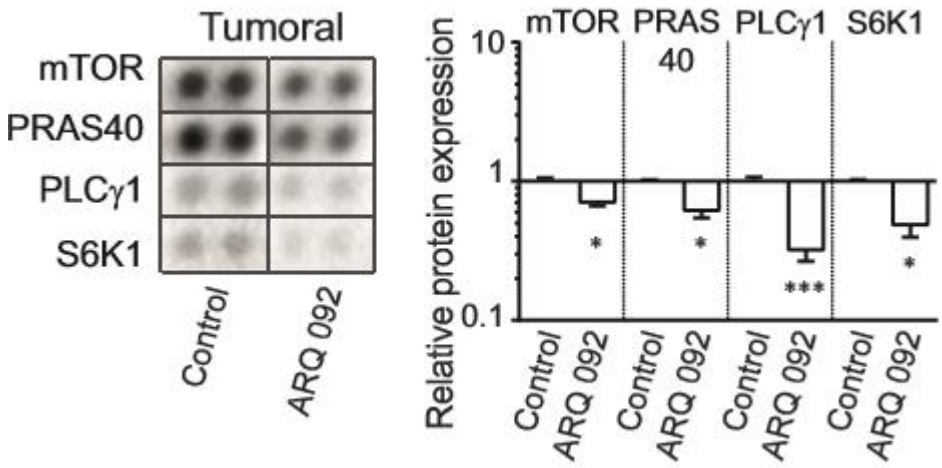

Figure 3.18. Phospho-protein analysis of downstream kinases of AKT pathway in tumor tissue.

As expected, qPCR analyses did not show a significant difference in AKT gene expression, but confirmed that ARQ 092 downregulated AKT pathway downstream actors such as mTORC1 (44.2 ± 11.4% of control, p=0.005) or S6K1 (54.6 ± 11.9% of control, p=0.142), as shown in figure 3.19.

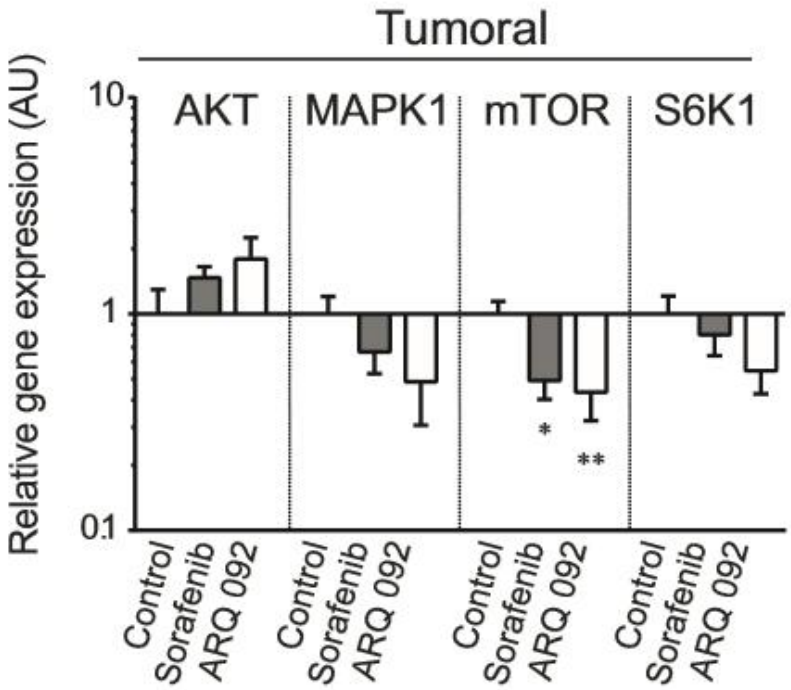

Figure 3.19. RT-qPCR analysis of gene expression in tumor **(cont. on next page)**

(above)and non-tumor (below) liver samples. Control was set as 1, values are means ± SE,*p≤ 0.05, **p≤0.01, ***p ≤ 0.001 vs. control.

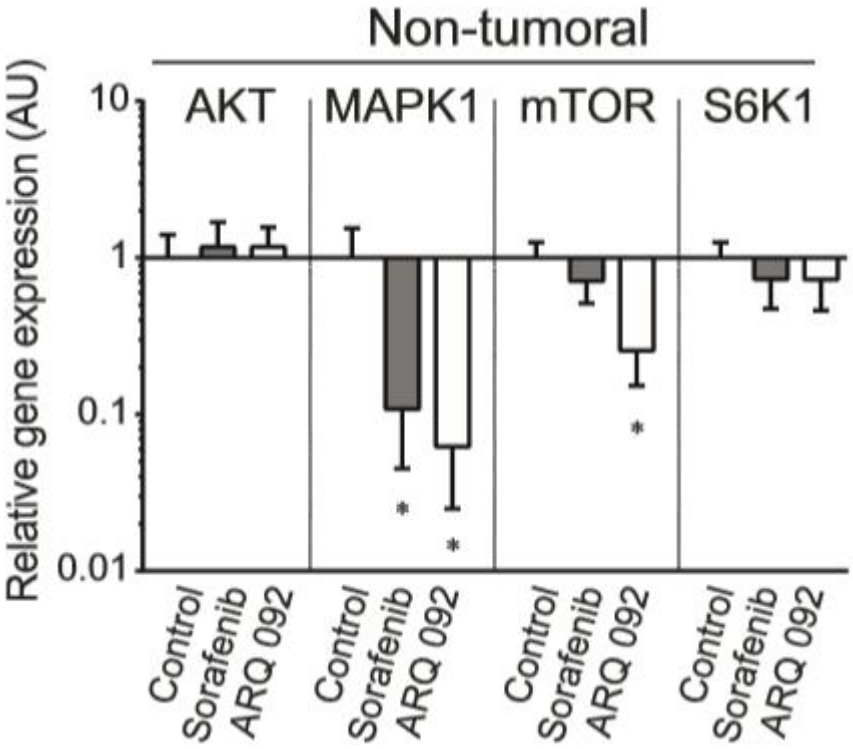

Figure 3.19. (cont.).

On the other hand, regarding the ERK pathway, western blot analyses did not show significant differences in pERK/ERK ratio between the groups. Accordingly, no difference was observed between the groups in gene expression of ERK in tumor samples. Interestingly, the gene expression of ERK was downregulated in non-tumor tissues of both, ARQ 092 and Sorafenib-treated groups compared to the non-treated group (p=0.029 and p=0.039).

3.2. Second Study: Combination Treatment by AKT Inhibitor ARQ 092 and Sorafenib in a Cirrhotic rat model with HCC

3.2.1. Combination Treatment Decreased Cell Viability

In order to determine cell viability of combination treatment of ARQ 092 plus Sorafenib, MTT assay on Hep3B, HepG2, HuH-7 and PLC/PRF/5 cell line was performed. Different concentrations of IC50 values of Sorafenib and IC50 values of ARQ 092 were used, i.e. always same ratio of IC50:IC50 as shown figure 3.20.

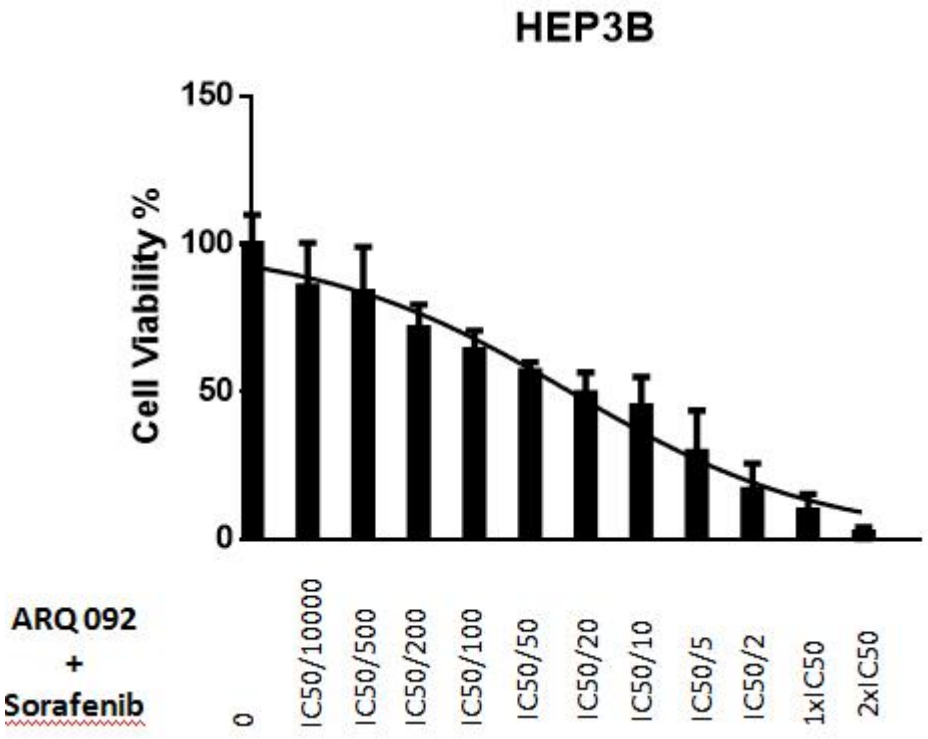

Figure 3.20. MTT assay was used to determine viability of Hep3B, HepG2, HuH7 and PLC/PRF cells treated with combination of different concentrations of IC50 values of Sorafenib and ARQ 092 incubated during 48 hours. All experiments were done in triplicates and repeated three times. Data are presented as mean ± SD. **(cont. on next page).**

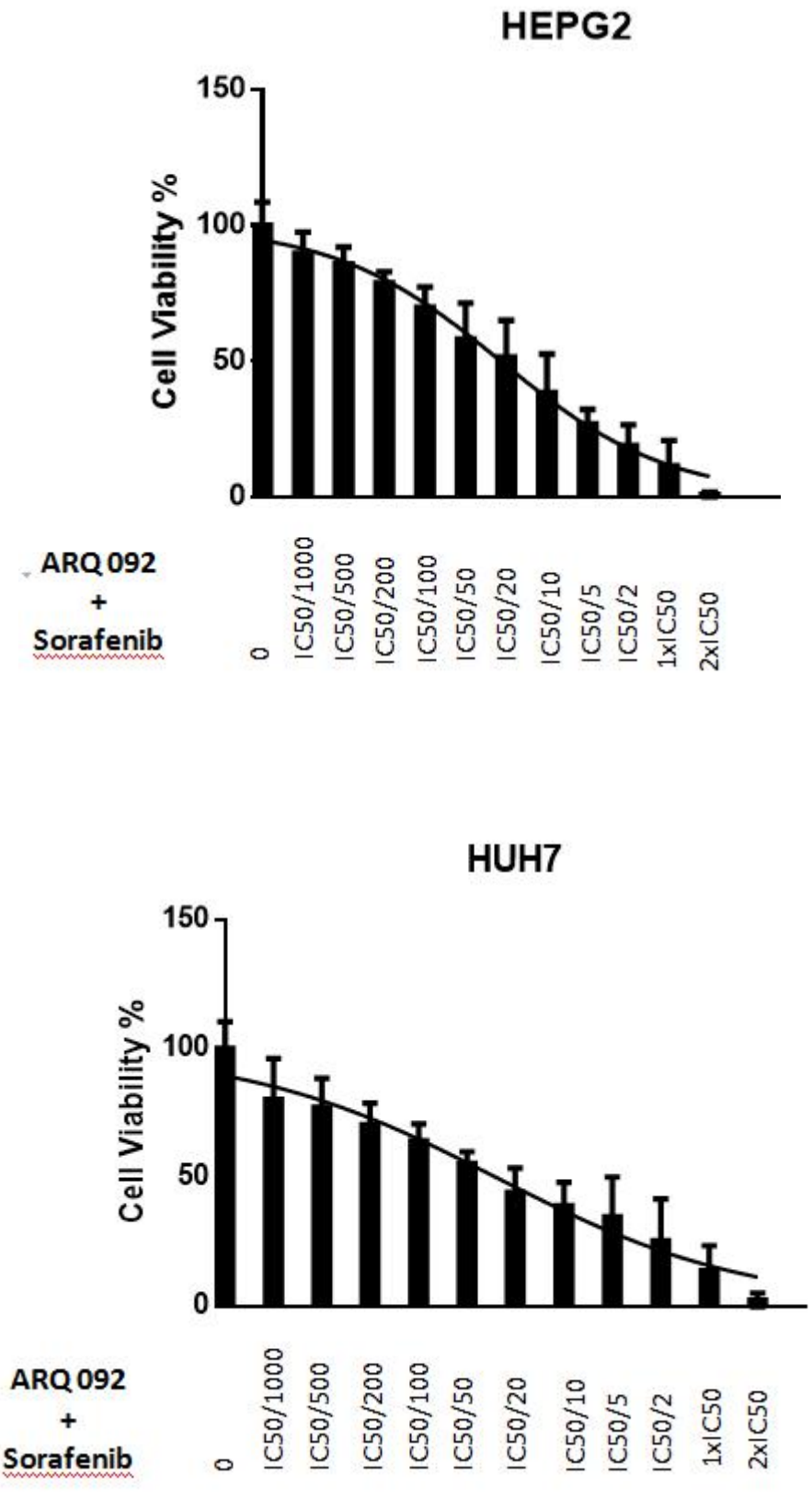

Figure 3.20 (cont. on next page).

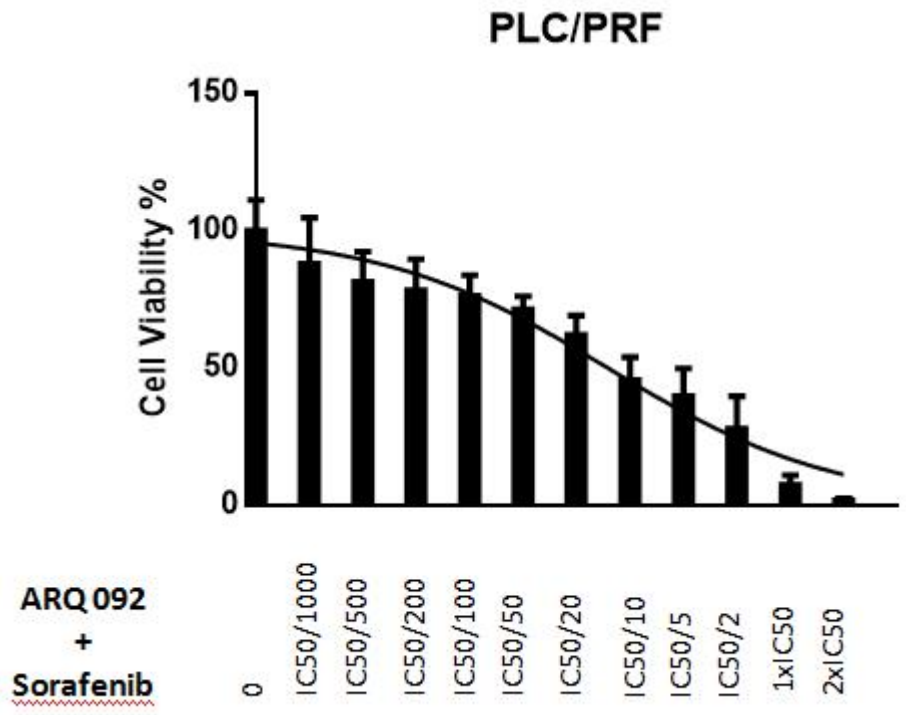

Figure 3.20 (cont.)

Calculated concentrations of IC50 values by the CompuSyn.exe software of Combination treatment (Sorafenib plus ARQ 092) with combination index (CI) values are summarized in the table 6. CI values for combination therapy are lower than 1 which shows strong synergistic effect of combination of Sorafenib and ARQ 092 on inhibition of cell growth in all cancer cell lines.

Table 6. Combination Index values of cell lines treated with combination of different concentrations of IC50 values of Sorafenib and ARQ 092. Three independent experiments were performed in triplicates.

Cell Lines	Potency Ratio	ARQ 092/ Sorafenib (μM)	CI values ED50
Hep3B	IC50/IC50	1:7	0.053
HepG2	IC50/IC50	4:11	0.072
HuH7	IC50/IC50	3:12	0.054
PLC/PRF	IC50/IC50	7:13	0.085

3.2.2. Combination Treatment Induced Apoptosis

Annexin V FITC and 7AAD staining was used to quantify the apoptosis rate in Hep3B, HepG2, HuH-7 and PLC/PRF cancer cells. The ARQ 092 plus Sorafenib were attempted as a combination study. According to the MTT results, two different concentration IC50/200 (approximately 80% alive cell for all cell lines) and IC50/10 (approximately 50% alive cell for all cell lines) were chosen for apoptosis analysis and figure 3.21 was obtained.

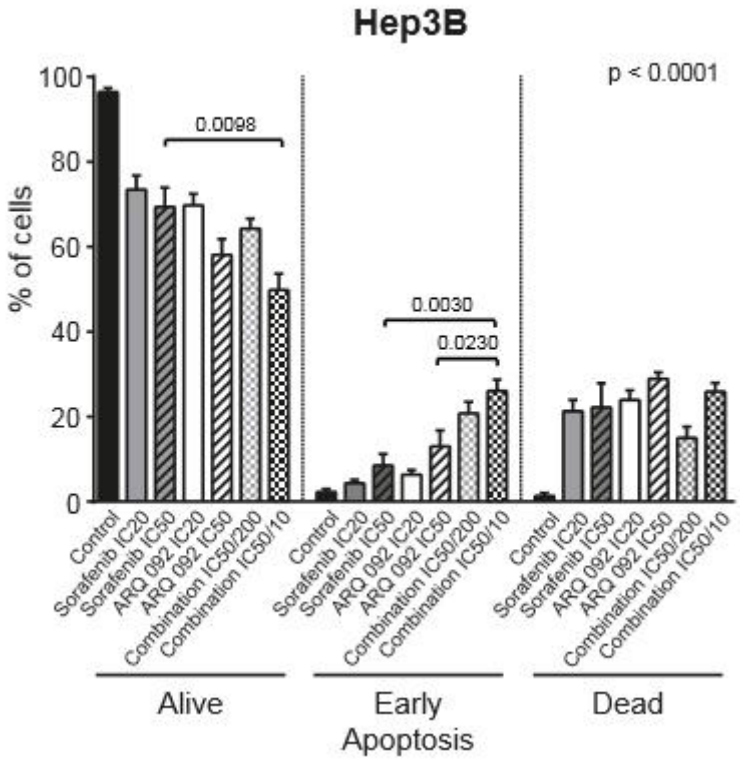

Figure 3.21. Dose-dependent effects of Sorafenib and/or ARQ 092 on apoptosis in Hep3B , HepG2 , Huh-7, PLC/PRF after 48 h exposure. **(cont. on next page).**

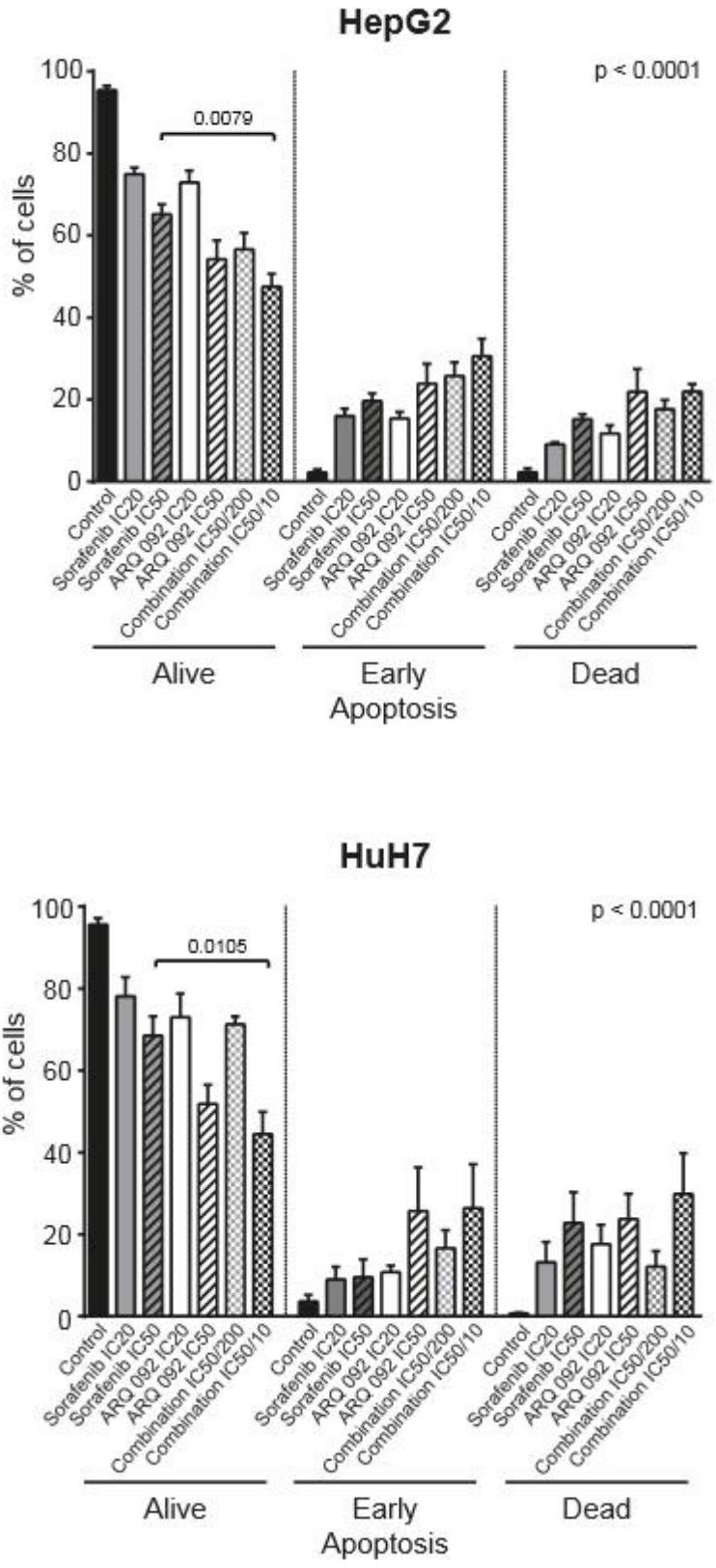

Figure 3.21 (cont. on next page).

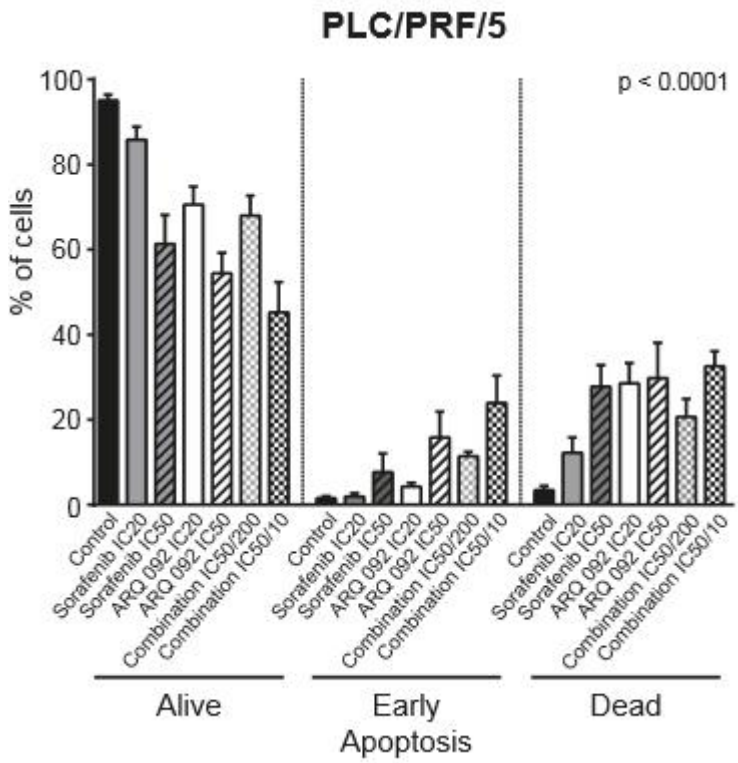

Figure 3.21 (cont.).

In regard to this results, we observed additive effect of combination treatment on the decrease of cell viability in all tested cell lines and on the increase of early apoptotic cells in Hep3B treated by combination IC50/10 compared to IC50 single treatments (Figure 3.21).

3.2.3. Cell Migration Analysis

The migratory behavior of human HCC cell lines was analyzed by scratch assay. After 24h, ARQ 092 and Sorafenib reduced migration of Hep3B, HepG2, HuH7 and PLC/PRF cell lines compared to control with high statistical differences between the groups (Anova $p < 0.0001$) and shown in figure 3.22.

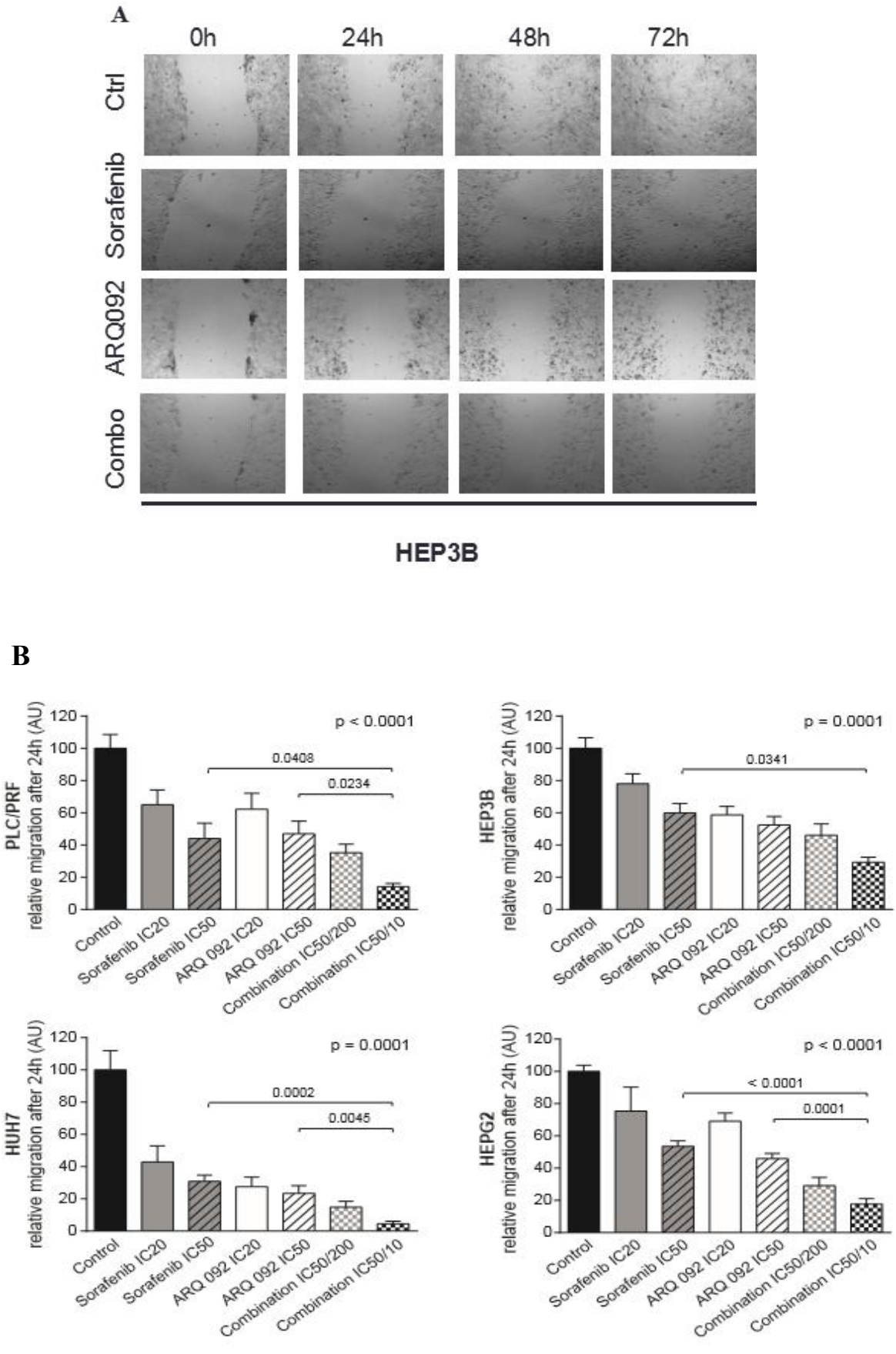

Figure 3.22. Effects of Sorafenib or/and ARQ 092 on migration of HCC cell lines. A) Representative pictures of wound-healing assay at baseline, after 24 h, 48h

and 72 h on Hep3B cell line. B) The quantification of migration (decrease of width of the wound after first 24 h) in all cell lines. For statistical analyses, Anova was used to compare all groups (p value is shown in the corner of each graph) and similarly, IC50 groups were compared by Anova test - p values are shown in graphs.

According to these results, the combination of ARQ 092 and Sorafenib treatments further decreased migration in additive manner compared to single treatments.

3.2.4. Pathway Analysis

Western blot analysis of following proteins, AKT and phoshoylated AKT (pAKT) (Ser473), ERK and phosphorylated ERK (pERK) and β-actin were performed in cell lysates of Hep3B, HepG2, HuH7 and PLC/PRF/5 human cell lines. ARQ 092 treatment completely blocked phosphorylation of AKT as observed in two concentrations of IC20 and IC50 (Figure 3.23). For combination treatment (ARQ 092 and Sorafenib), although low concentration of ARQ 092 (IC50/200 or IC50/10) was used, similar results was found like in single treatment groups. All together, combination treatment completely inhibited phosphorylation of AKT demonstrated in figure 3.23.

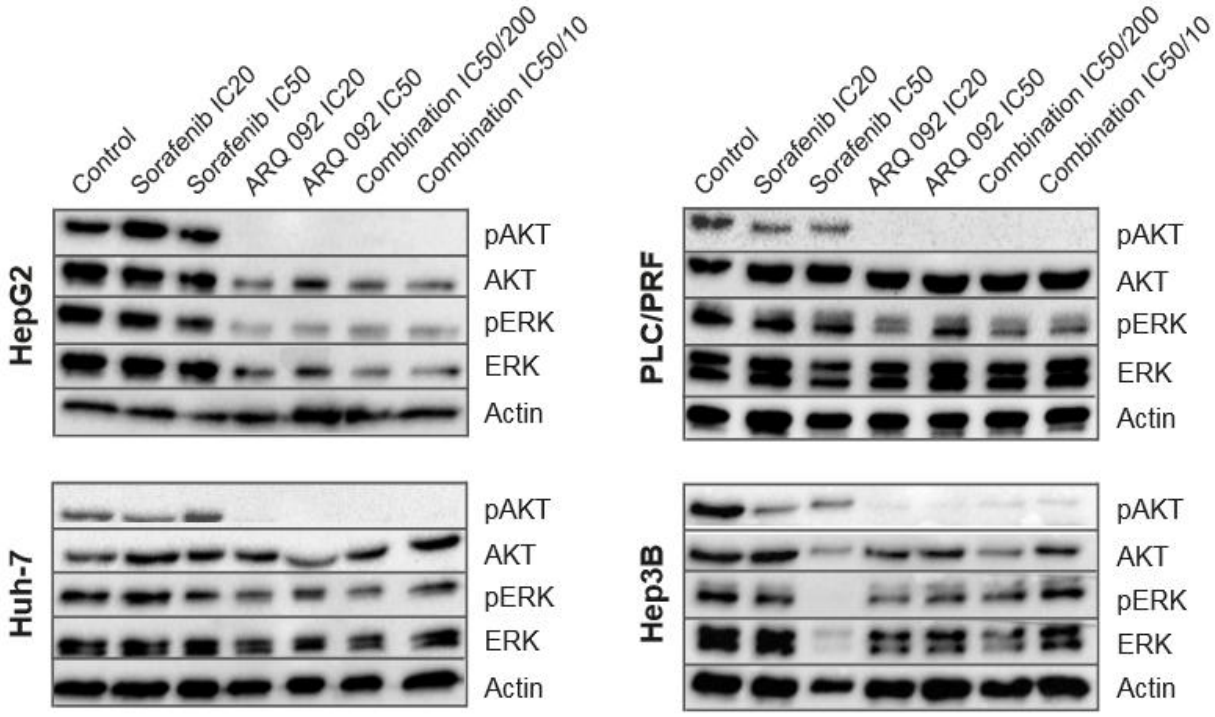

Figure 3.23. Western blot analysis of pAKT, AKT, pERK,ERK and Actin in four different human cell lines. Effect of ARQ 092, Sorafenib and combination of ARQ 092 and Sorafenib on these proteins.

3.2.5. Clinical Safety

In this part, the effect of Sorafenib, ARQ 092 and combination of both treatments on body weight (Figure 3.24A) and liver weight (Figure 3.24B) of rats was investigated.

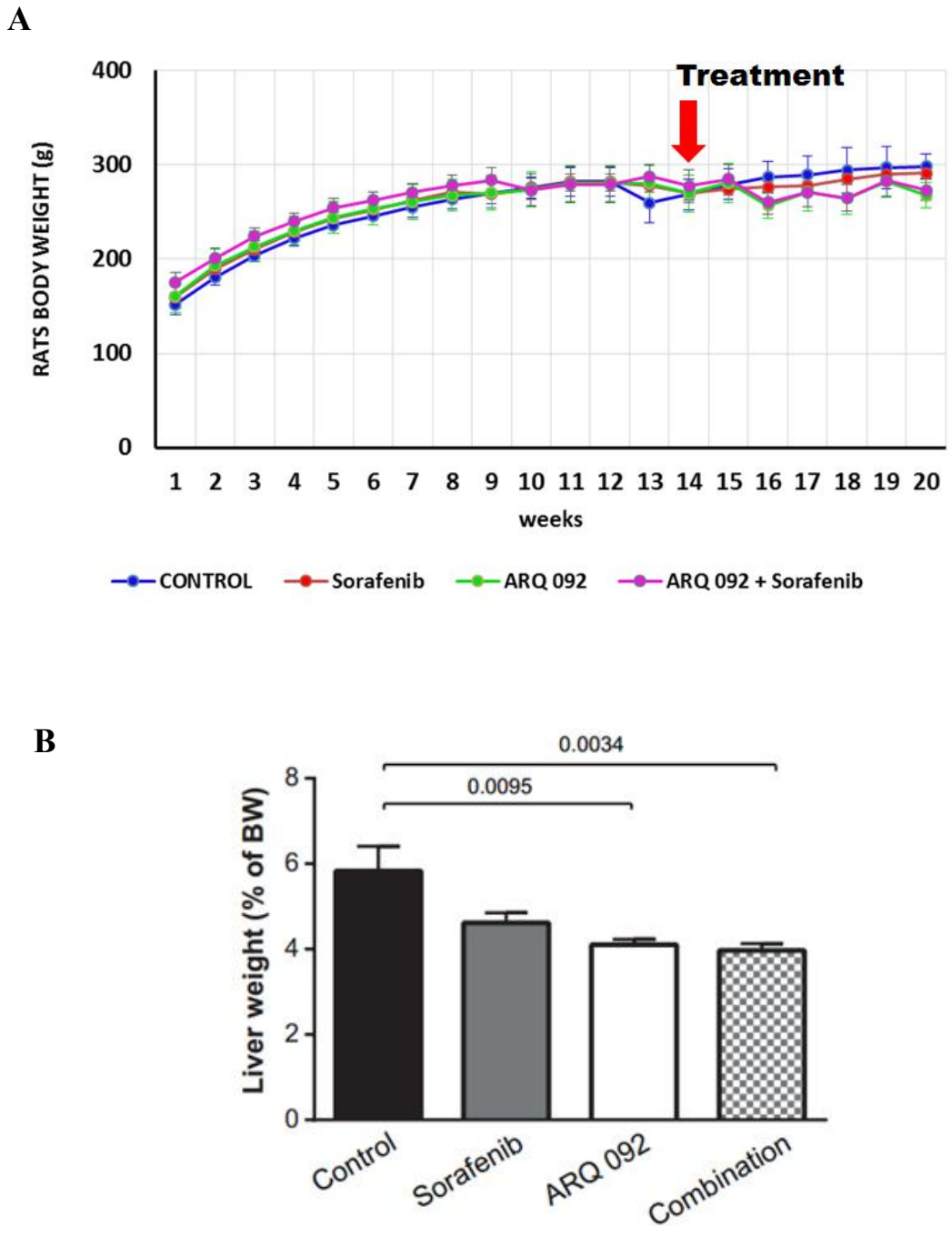

Figure 3.24. Effect of ARQ 092, Sorafenib and Combination of both treatment on (A) body weight (B) liver weight in term of percentage of body weight (BW).

These results showed that there is no major body weight loss during the treatment. Considering liver weight, a significant decrease in liver weight in ARQ 092 ($p=0.0095$) and Combination ($p= 0.0034$) treatment when compared to control was observed.

3.2.6. *In vivo* Efficacy

3.2.6.1. Morphological Analysis

The effect of ARQ 092, Sorafenib and the Combination of both treatments was studied on tumor progression and tumor development. As shown in figure 3.25, tumor progression was significantly reduced in the Sorafenib (33.0 ± 10.3% ; p=0.005) and ARQ 092 (33.8± 10.6% ; p=0.005) groups compared to control. Interestingly, the greatest decrease in tumor progression rate was observed in combination group when compared with control (66.6 ± 10.6%; p<0.0001), Sorafenib (50.1± 13.3%; p=0.006) and ARQ 092 group (49.6 ± 14.1%; p=0.010). No statistical difference was found between Sorafenib and ARQ 092 groups (p=0.9998).

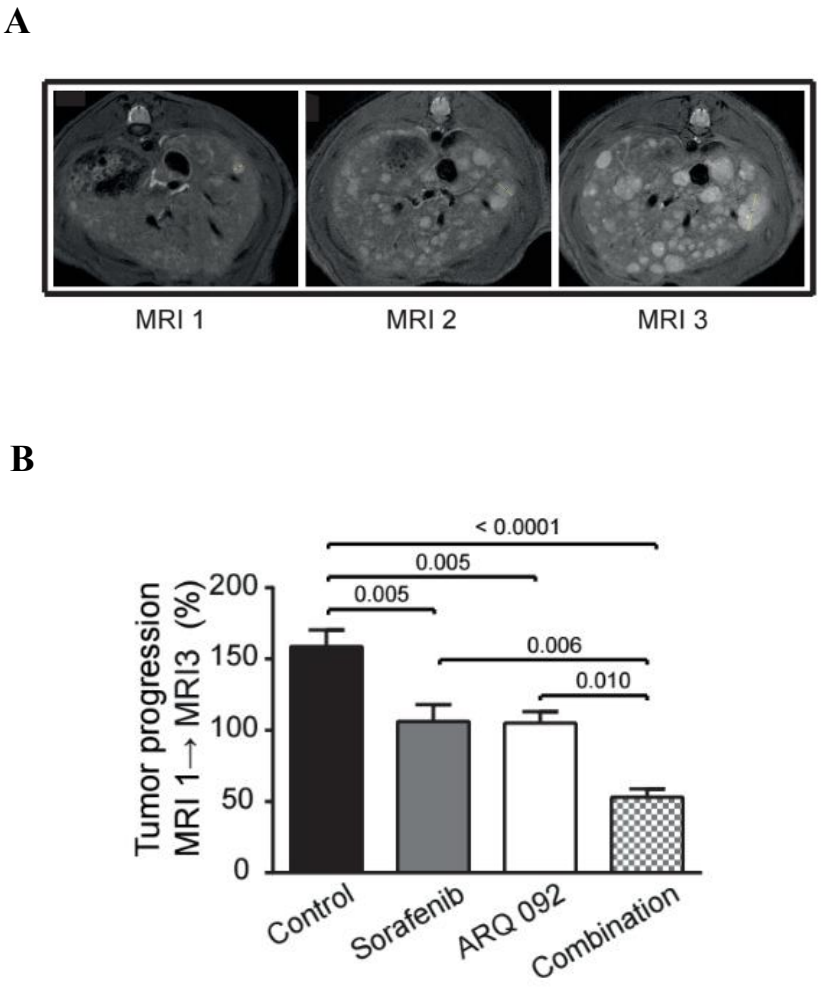

Figure 3.25. Effect of ARQ 092, Sorafenib and combination of both treatments on

tumor progression. (A) representative picture of MRI morphological analysis and (B) tumor progression assessment by comparison of tumor size on MRI 1, 2 and 3 in control, Sorafenib, ARQ 092 and combination group.

3.2.6.2. Histopathological Analyses

It was further confirmed by macroscopic examination of the liver which revealed a tumor size of 9.9 ± 1.1 mm in control compared to 6.3 ± 0.8 mm in Sorafenib ($p=0.0092$), 6.2 ± 0.8 mm in ARQ 092 ($p=0.0101$) and 3.0 ± 1.1 mm in the combination group ($p<0.0001$). Tumor size in combination group was significantly reduced when compared with Sorafenib and ARQ 092 single treatment ($p=0.0187$ and $p=0.0308$). No statistical difference was found between Sorafenib and ARQ 092 treated groups (Figure 3.26A).

Furthermore, rats in the group treated with ARQ 092 and combination displayed a significantly lower number of tumors (31.5 ± 14.8 and 21.21± 14.5 tumors respectively) when compared to Controls (109.5 ± 14.5 tumors, $p<0.0001$ and <0.0001 respectively) and compared to Sorafenib-treated animals (69.21 ± 11.5 tumors, $p=0.0188$ and 0.0016 respectively, Figure 3.26B).

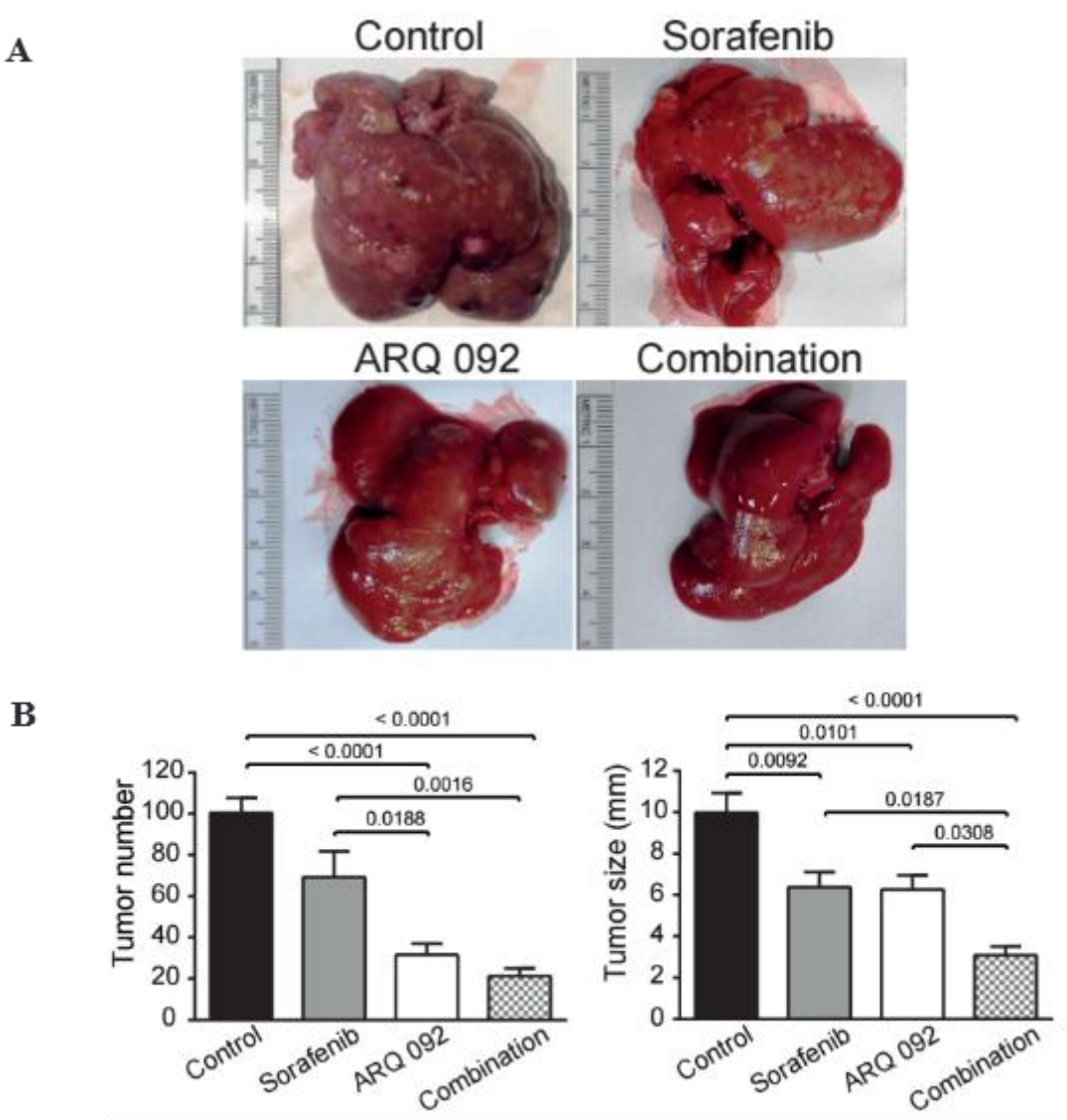

Figure 3.26. Effect of ARQ 092, Sorafenib and combination on tumor proliferation. (A) Representative picture of liver. Macroscopic examination of livers with assessment of (B) tumor size (average of diameter of the five largest tumors) and tumor number at the surface of livers (n=7/group).

Thus, the combination of Sorafenib and ARQ 092 significantly reduced tumor progression and proliferation in DEN induced HCC, and was clearly more effective than Sorafenib and/or ARQ 092 single treatment.

3.2.6.3. Immunohistochemical Analyses

Immunohistochemical analyses were performed by Ki67 immuno-stainig to analyze the HCC proliferation rate and tunnel kit to analyze induced apoptosis. Ki67

protein is associated with cell proliferation. Cell with Ki67 positive nucleus were significantly reduced in combination group (Sorafenib plus ARQ 092) (p= 0.0206) and ARQ 092 group (p= 0.0421) compared to control group. Combination treatment significantly reduced proliferation compared to Sorafenib group (p= 0.0487) as shown figure 3.27.

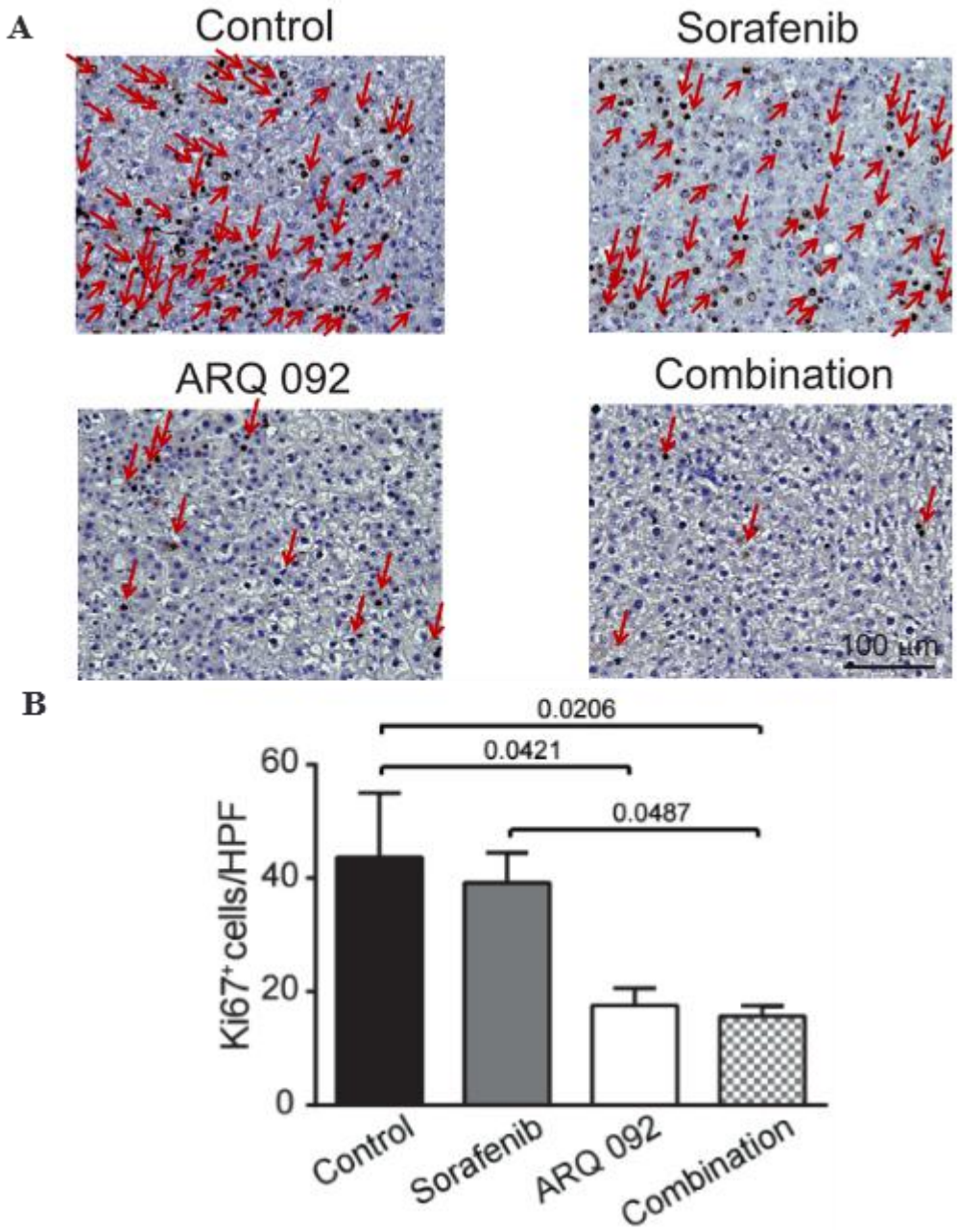

Figure 3.27. (A) Representative histological images of livers stained with Ki67 antibody. Nuclear Ki-67 staining (arrow), 20x magnification (B) quantification of Ki67 staining per high power field (HPF).

In our study, TUNEL immunostaining (Figure 3.28) showed that only combination group significantly induced apoptosis (p=0.0272).

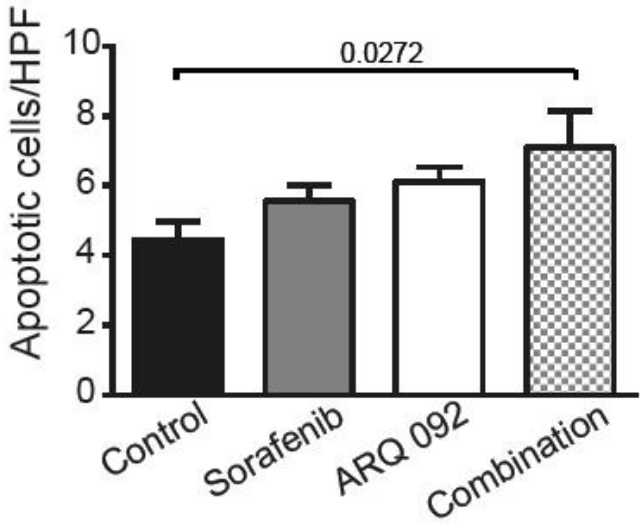

Figure 3.28. Quantification of TUNNEL immuno staining per high power field (HPF).

3.2.7. Alpha Feto Protein Level (AFP)

To investigate the level of AFP, gene expression of APF was quantified. According to figure 3.29, all treated groups displayed a reduced expression of APF gene.

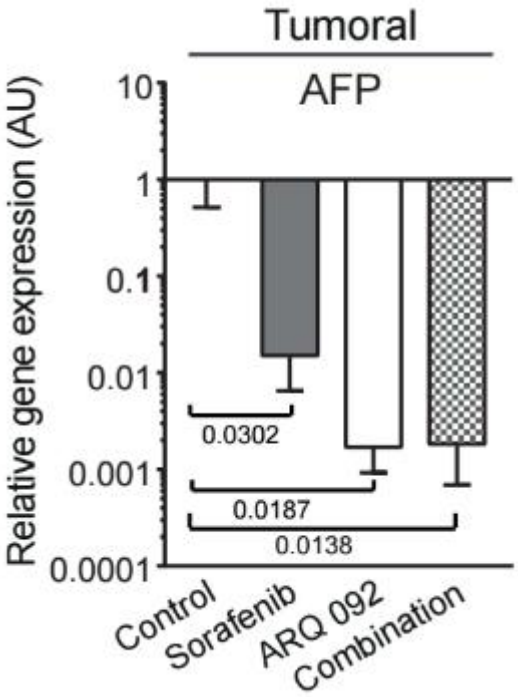

Figure 3.29. qPCR analysis of alpha-feto protein (AFP) gene expression in tumor liver samples. Control was set as 1, values are means ± SE.

3.2.8. Anti-angiogenic Effect

To understand anti angiogenic effect of ARQ 092 or/and Sorafenib, specific anti-rat anti-CD34 antibody was used to perform immunoflorescence staining of liver tissue. While structural abnormalities of the tumor vasculature were numerous in control animals, normalization of vasculature was observed in both treated groups (Figure 3.30A). Quantification of vascular density revealed that combination treatment was associated with a significant decrease of angiogenesis. Sorafenib decreased vascular density by 30 % ($p=0.0012$), ARQ 092 by 58 % ($p<0.0001$) and combination by 75% ($p<0.0001$) compared to non-treated rats (Figure 3.30B).

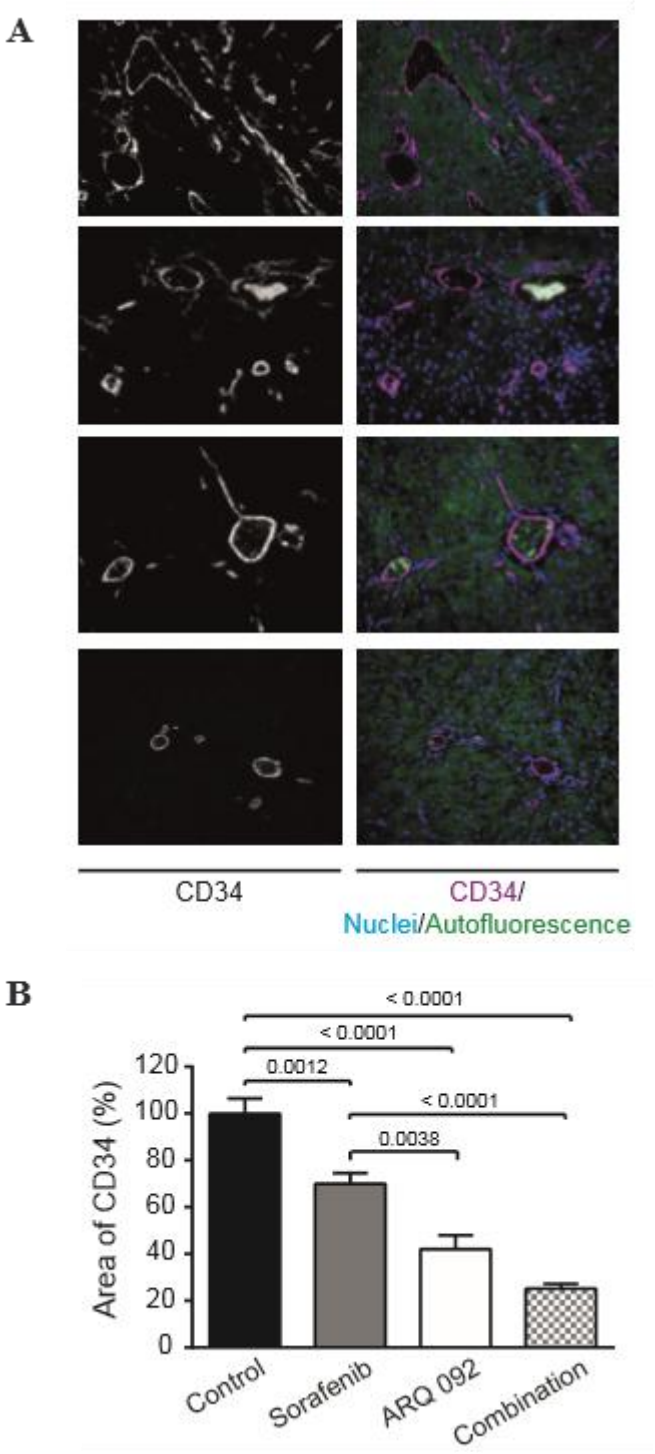

Figure 3.30. Anti-angiogenic effect. (A) Representative pictures of CD34 immunofluorescence staining of liver tissue control, Sorafenib, ARQ 092 and combination, respectively and (B) Quantification of CD34 immunostaining. Control was set as 100, values are means ± SE.

The transcription factor HIF plays an important role in cellular response to systemic oxygen levels in mammals (Brennan, Rexius-Hall et al. 2015) and HIF induces

biological processes such as angiogenesis (Roberts and Der 2007). Thus, the gene expression of HIF was also investigated. To figure 3.31, ll treated groups have a reduced gene expression of HIF with the highest reduction in combination group.

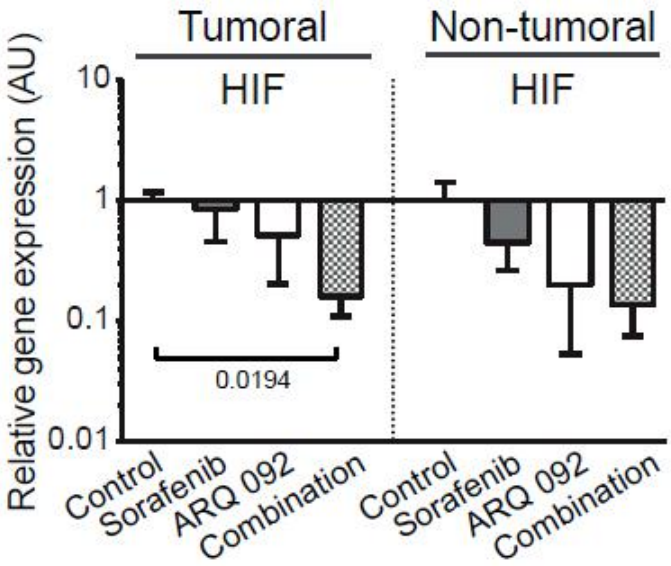

Figure 3.31. RT-qPCR analysis of hypoxia induced factor (HIF) gene expression in tumor an non-tumor liver samples. Control was set as 1, values are means ± SE.

3.2.9. Anti Fibrotic Analysis

Liver fibrosis was analyzed by Sirius red staining. Sirius red stain the collagen of the tissue which is formed due to the accumulation of the extra cellular matrix. Liver fibrosis was significantly reduced in Combination group (Sorafenib plus ARQ 092) (p= 0.0001) and ARQ 092 group (p= 0.0004) compared to control group and to Sorafenib group (p=0.0174 & p= 0.0495), demonstrated in figure 3.32A&B. Furthermore, qPCR results showed that all treated group significantly reduced the gene expression of fibrosis markers called ACTA1, Collagen1 and also the expression of TGFβ1, illustrated in figure 3.32C.

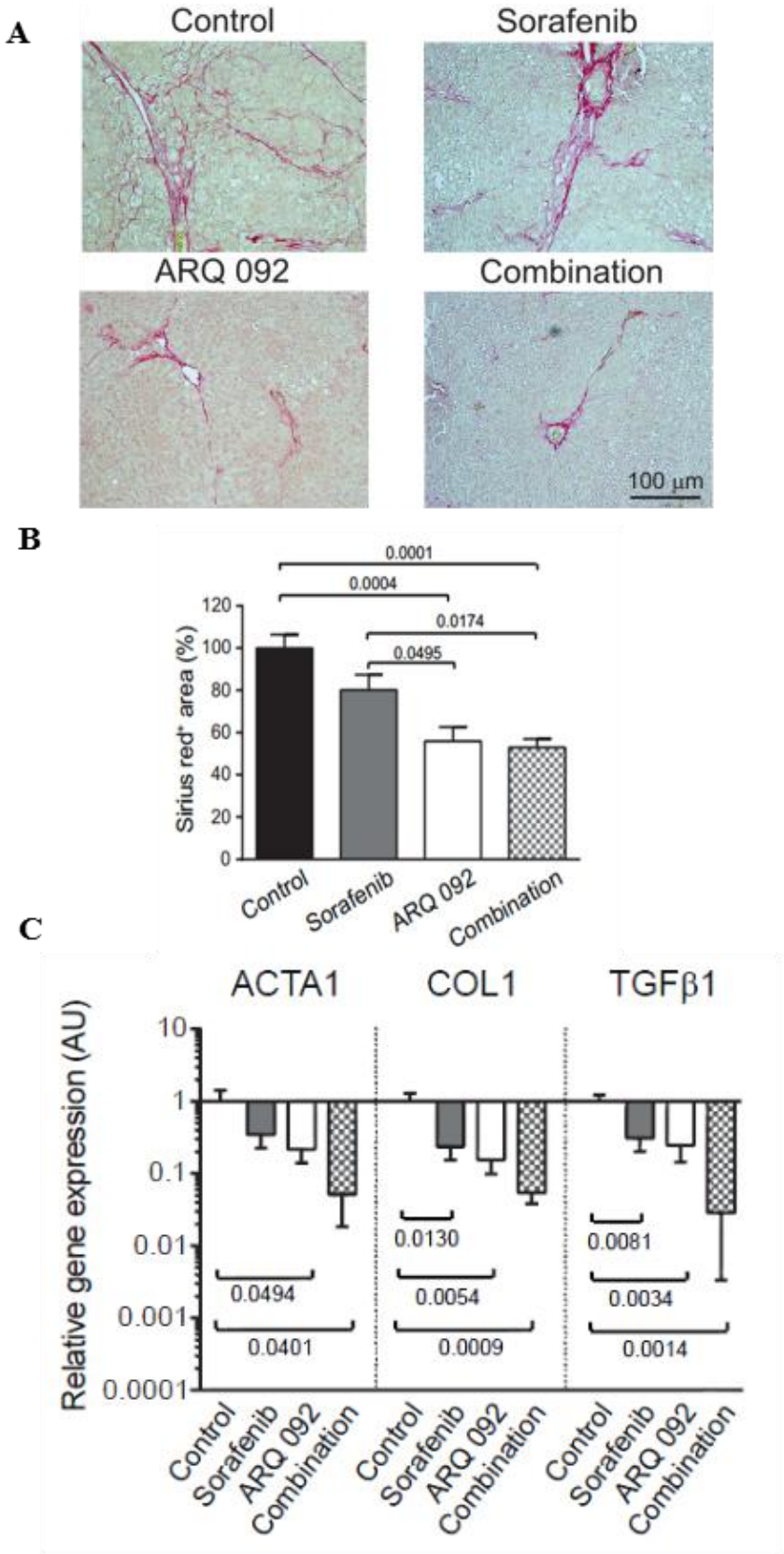

Figure 3.32. Anti-fibrotic effect. (A) Representative histological images of livers stained with Sirius red f, 20x magnification (B) Quantification of fibrosis (C) RT-qPCR analysis of the expression of genes.

3.2.10. Pathway Analyses

Western blot analysis of pAKT/AKT and pERK/ERK were performed on tumor and non-tumor tissues. Western blot analysis showed that ARQ 092 and its Combination with Sorafenib inhibited phosphorylation of AKT in both, tumor and non-tumor tissues (Figure 3.33A&B). Regarding the ERK pathway, western blot analyses did not show significant differences in pERK/ERK ratio between the groups (Figure 3.33A&B).

In this study, qPCR analyses also showed significant difference in AKT gene expressions, and confirmed that ARQ 092 down regulates AKT pathway downstream actors such as mTORC1 or S6K1 in both tumor and non-tumor tissues. On the other hand, MAPK1 gene expression was not found any significant decreased as shown figure 3.33C and D.

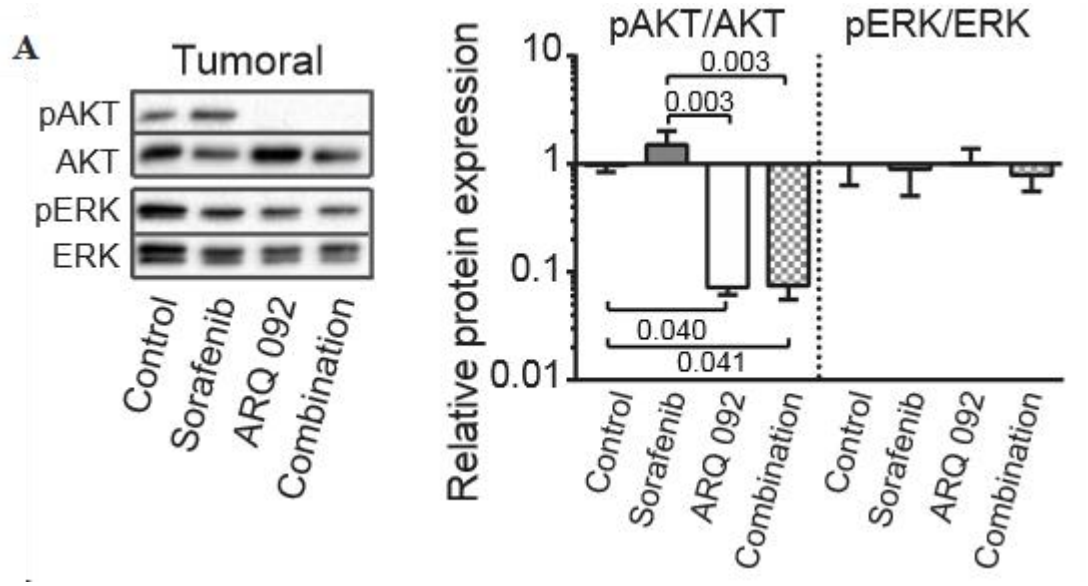

Figure 3.33. Effect of ARQ 092, Sorafenib and their combination on AKT and ERK pathways. Western blot analysis of pAKT/ AKT and pERK/ERK in (A) tumoral and (B) nontumoral liver tissues and the quantification of western blots. RT–qPCR analysis of the expression of AKT, MAPK, mTOR, S6K1 (C) tumoral and (D) nontumoral liver tissue. All of the qPCR results were normalized to the expression of GAPDH and compared with the samples. **(cont. on next page).**

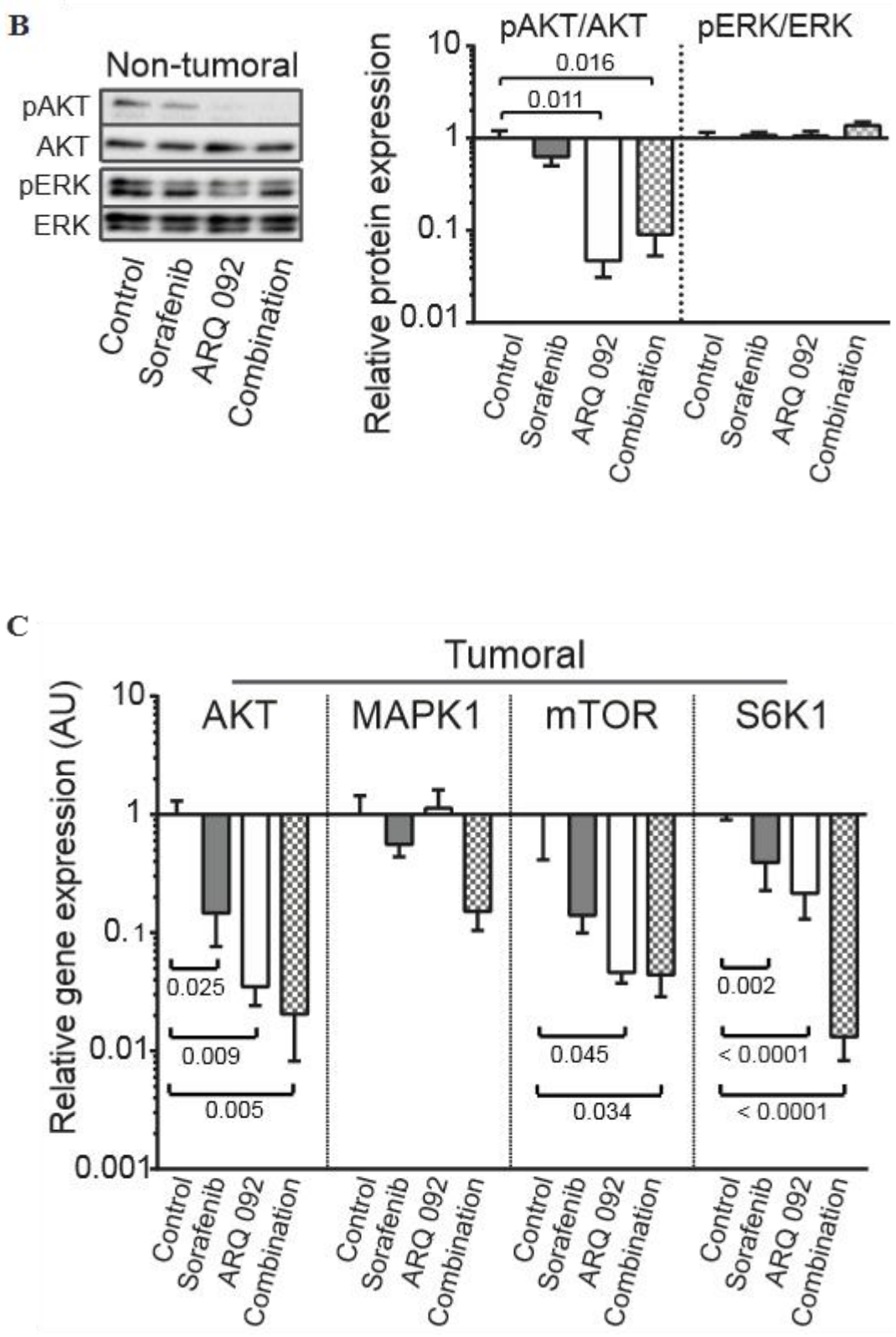

Figure 3.33 (cont. on next page).

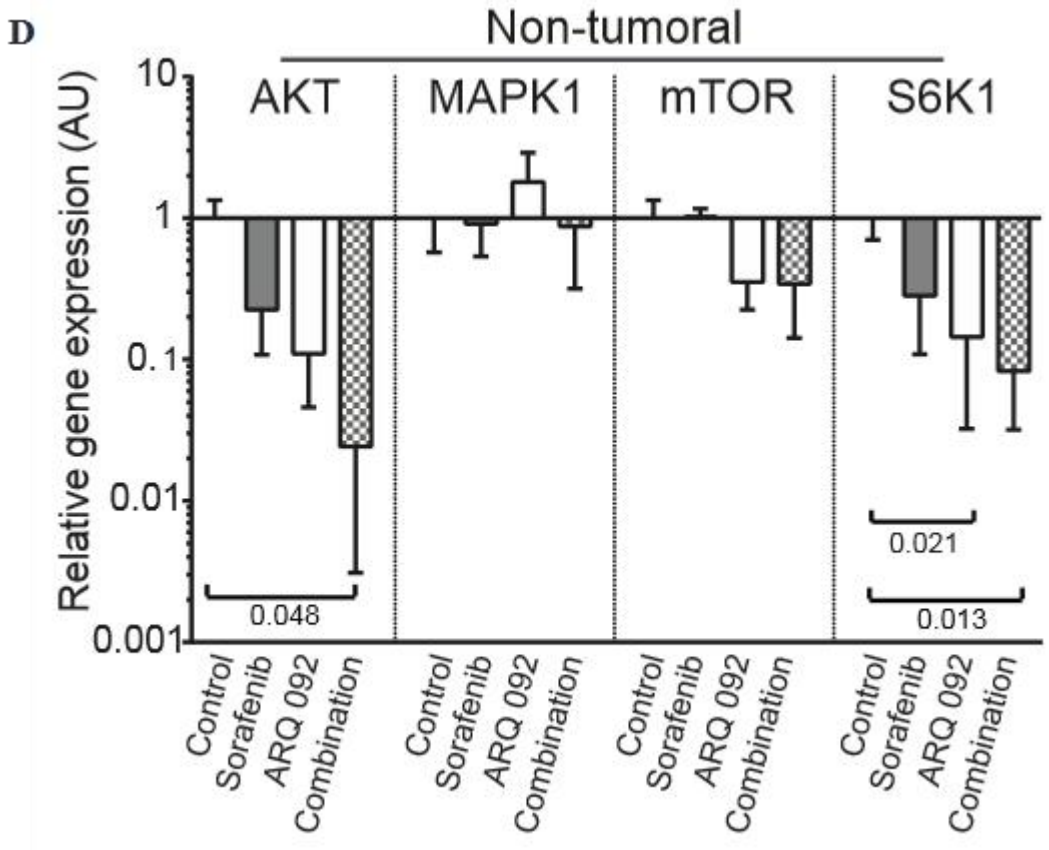

Figure 3.33 (cont.).

3.3. Third Study: Efficacy of AKT Inhibitor ARQ 751 Compared with Sorafenib in Liver Cancer Cells

3.3.1. *In vitro* Cell Viability Analysis

MTT assay was used to analyze the cell viability of Hep3B, HepG2, Huh-7 and PLC/PRF cell-lines treated with next generation of AKT inhibitor, ARQ 751 or Sorafenib, as shown in figure 3.34. IC20 and IC50 values of ARQ 751 and Sorafenib were calculated by Graph Prism software. IC values and potential ratio between IC50 values of ARQ 092, ARQ 751 and Sorafenib are summarize in table 7.

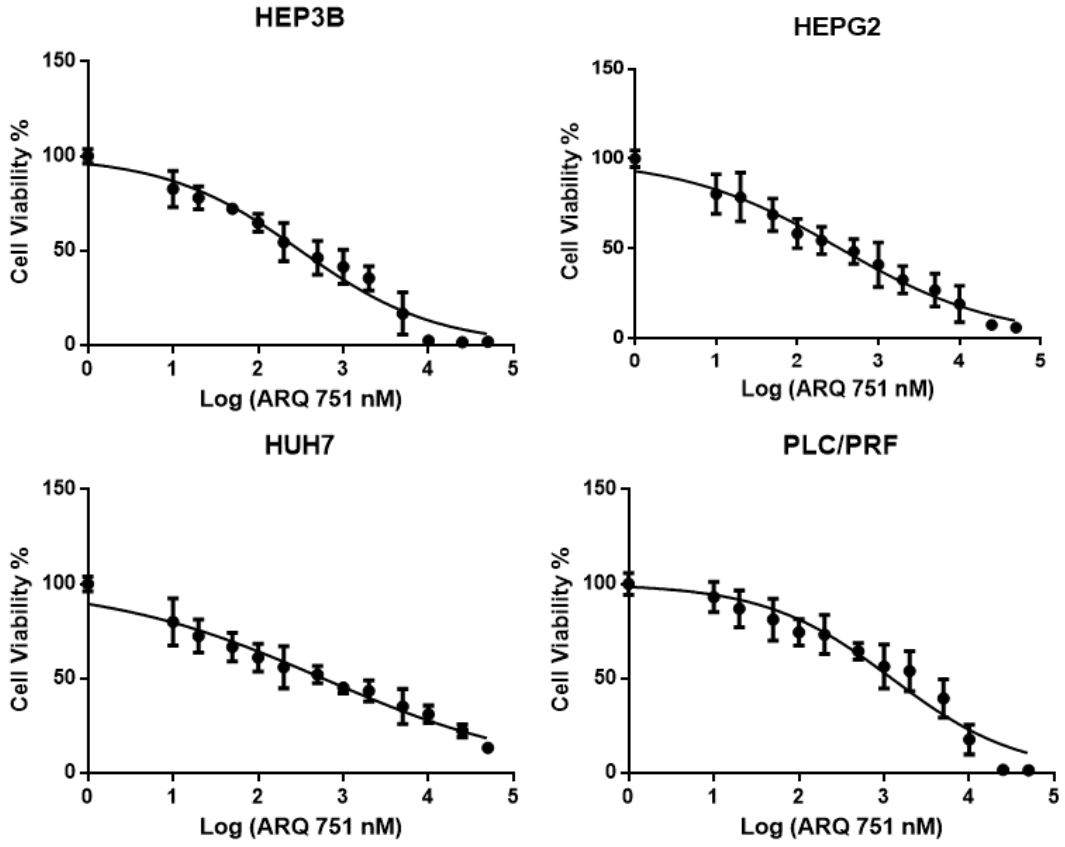

Figure 3.34. MTT assay was used to determine viability of cells treated with different concentrations of ARQ 751 alone incubated during 48 hours. All experiments were done in triplicates and repeated three times. Data are presented as mean ± SD.

Table 7. IC50 values of Hep3B, HepG2, HuH7 and PLC/PRF cells treated with of Sorafenib, ARQ 092 and ARQ 751 alone and potency ratio of Sorafenib/ARQ 092, Sorafenib/ARQ751 and ARQ 092/ARQ 751 after 48 hours of incubation. Values are expressed as the mean ± SEM of three independent experiments performed in triplicate.

	IC50			Potency ratio		
	Sorafenib	ARQ 092	ARQ 751	Sorafenib : 092	Sorafenib : 751	092 : 751
Hep3B	6.68 ± 0.03	1.16 ± 0.06	0.32 ± 0.05	6 X	20X	7X
Huh-7	11.58 ± 0.03	2.88 ± 0.08	0.58 ± 0.05	4X	20X	5X
HepG2	10.53 ± 0.04	3.74 ± 0.03	0.34± 0.02	3X	30X	11X
PLC/PRF	12.69 ± 0.04	6.99 ± 0.08	1.24 ± 0.07	2X	10X	6X

According to table 7, potential ratio of ARQ 751 was found much higher than ARQ 092. It is thought that next generation of allosteric AKT inhibitor ARQ 751 may bind to PH and kinase domain more strongly.

3.3.2. Apoptosis Analysis

Flow cytometry analysis revealed that ARQ 751 had a dose-dependent effect on apoptosis induction as shown in figure 3.35. Its positive effect on apoptosis induction was superior to Sorafenib in every cell lines and this superiority was always significant at IC50 concentration as illustrated by figure 3.35.

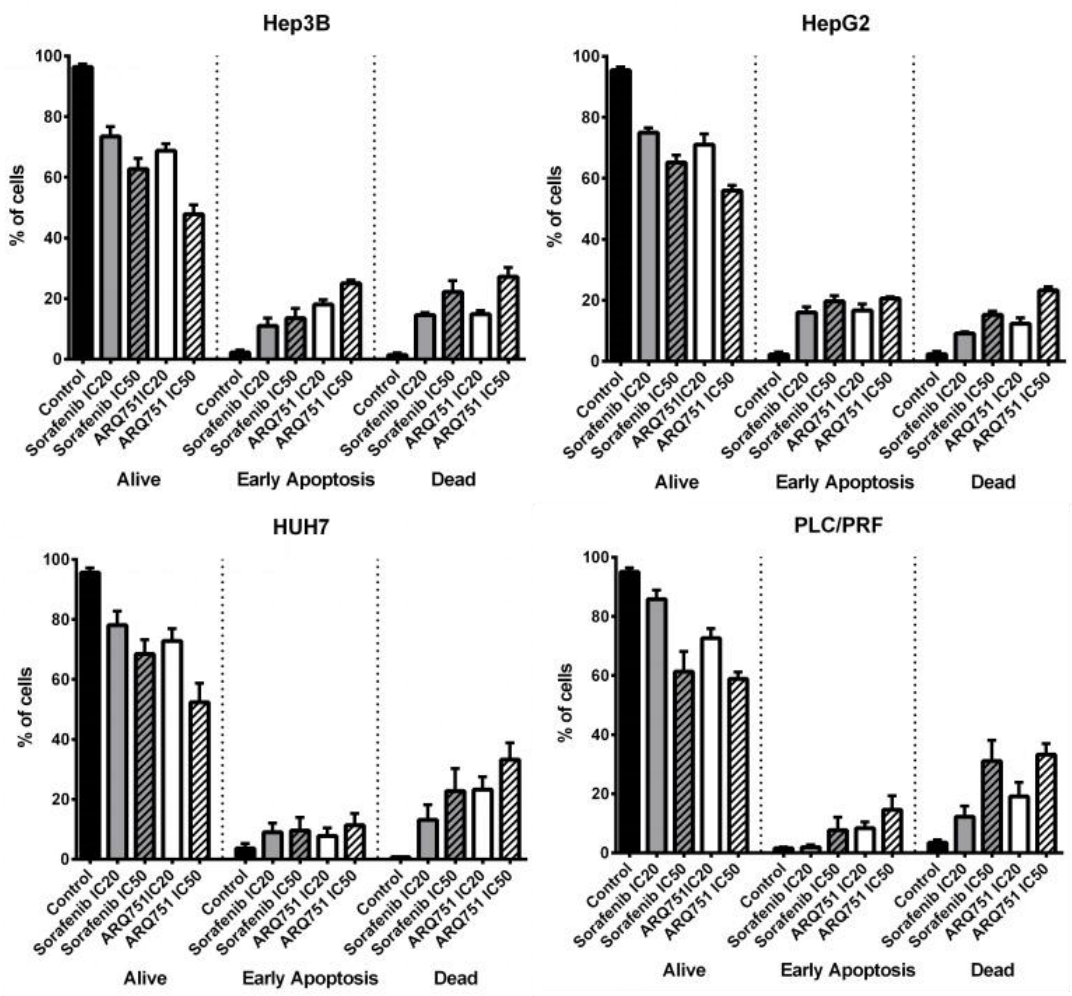

Figure 3.35. Dose-dependent effects of Sorafenib or ARQ 751 on apoptosis in Hep3B (upper left), HepG2 (upper right), Huh-7 (lower left), PLC/PRF (lower righ) after 48 h exposure.

3.3.3. Cell Migration

The migratory behavior of human HCC cell lines was determined by scratch assay. After 24h, ARQ 751 or Sorafenib reduced migration of Hep3B, HepG2, HuH7 and PLC/PRF cell lines compared to control with high statistical differences between the groups (Anova p0.0001), illustrated in figure 3.36.

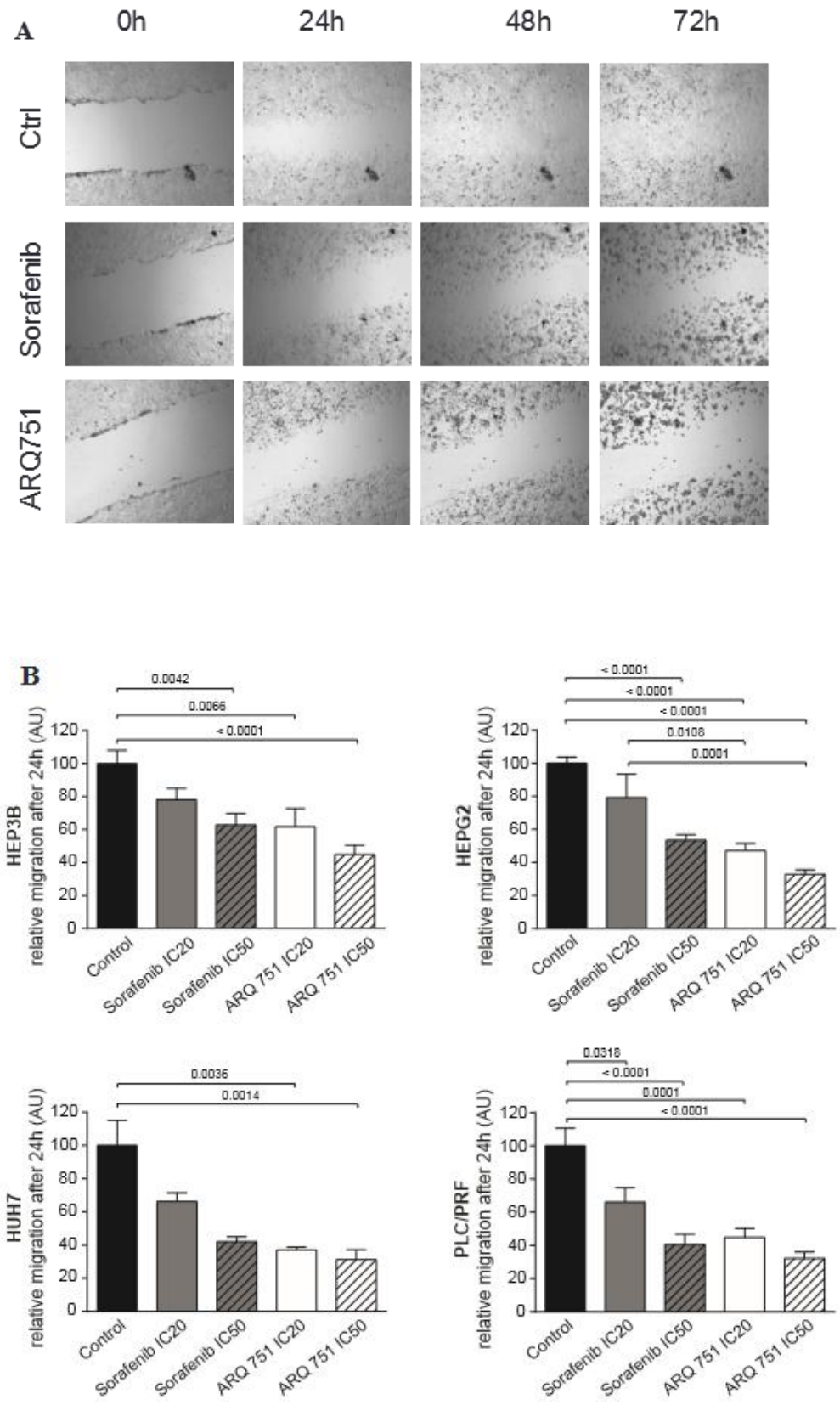

Figure 3.36. Effects of Sorafenib or ARQ 751 on migration of cells. (A) Representative pictures of wound-healing assay at baseline, after 24 h, 48 h and 72 h on Hep3B cell line. (B) The quantification of migration (decrease of width of the wound after first 24 h) in Hep3B (upper left), HepG2 (upper right),

HuH7 (lower left) and PLC/PRF (lower right).

3.3.4. Pathway Analysis

Western blot analysis of following proteins: AKT and phosphorylated AKT (pAKT), ERK and phosphorylated ERK (pERK) and β-actin were performed in cell lysates of Hep3B, HepG2, HuH7 and PLC/PRF human cell lines. ARQ 751 treatments completely blocked phosphorylation of AKT as observed at two concentrations of IC20 and IC50 (Figure 3.37) as expected. Sorafenib inhibited phosphorylated ERK, only in Hep3B cell line but, it did not blocked phosphorylation of ERK in other cell lines.

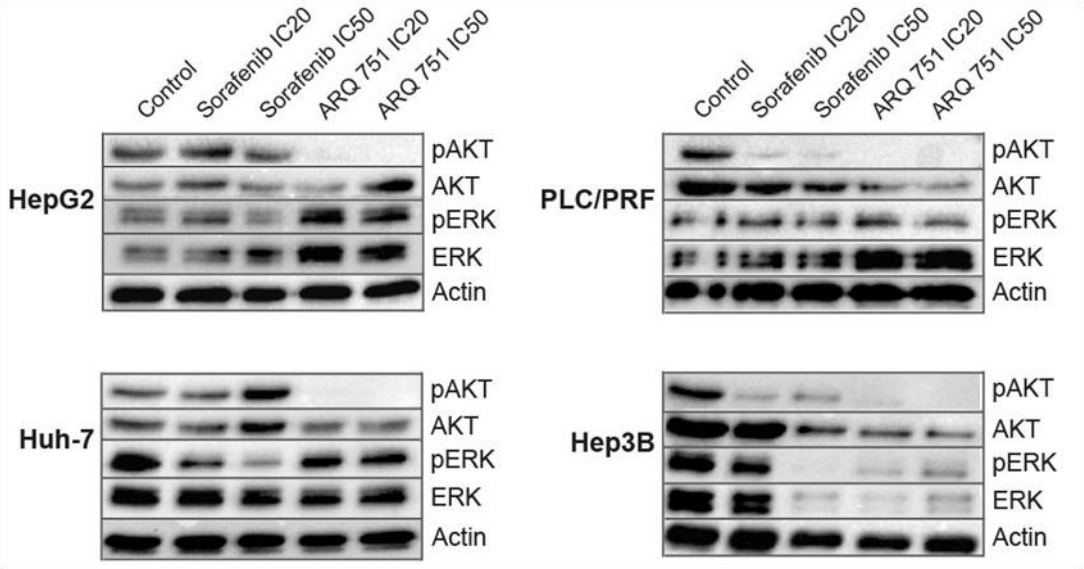

Figure 3.37. Western blot analysis of pAKT/ AKT and pERK/ERK in four different human cancer cell lines. Effect of ARQ 751 and Sorafenib on AKT and ERK pathway.

CHAPTER 4

DISCUSSION

Hepatocellular carcinoma (HCC) is the most common type of primary liver cancer and occurs predominantly in patient with underlying chronic liver diseases and cirrhosis. Since this type of liver tumors are very aggressive and represent the second leading cause of cancer deaths, HCC therapy is a growing challenge. Currently, the only approved systemic treatment for HCC is Sorafenib, a multitargeted tyrosine kinase inhibitor showing a modest improvement in overall survival from 7.9 months to 10.7 months (Llovet and Bruix 2008). Unfortunately, it is only a very short period and furthermore, this treatment often causes side effects altering the quality of patient's life. Therefore, there is an urgent need for new, effective and safe therapies.
PI3K/AKT/MTOR signaling pathway plays an important role in hepatocarcinogenesis (Shen, Hsu et al. 2010). Because of this, it is an attractive candidate as an anticancer drug target for HCC treatment (Reataza and Imagawa 2014) (Courtney, Corcoran et al. 2010). PI3K/AKT/MTOR pathway increases indifferent type of human cancer, including HCC (Kunter, Erdal et al. 2014) supporting the idea of inhibition of this pathway to treat HCC.

AKT is considered as an attractive target for cancer therapy and multiple attempts to identify specific inhibitors with acceptable pharmaceutical properties have been pursued (Nitulescu, Margina et al. 2016). Selectivity is a key issue for many ATP-competitive AKT inhibitors, particularly towards the AGC kinase family. ATP-competitive AKT inhibitors are manly isoquinoline-5-sulfonamides, azepane derivatives, aminofurozans, heterocyclic rings, phenylpyrazole derivatives, thiophenecarboxamide derivatives (Mattmann, Stoops et al. 2011). On the other hand, ATP-competitive inhibitors are non-selective against AKT isozymes, and poorly selective against closely related kinases, as the catalytic domain is highly similar. Efforts to identify AKT-specific and isoform-selective inhibitors have resulted in the discovery of allosteric inhibitors (Wu, Voegtli et al. 2010). Allosteric modulators offer distinct advantages compared to orthosteric ligands that target to active sites, such as greater specificity, reduced side-effects and lower toxicity (Lu, Li et al. 2014). Allosteric AKT inhibitors

are mainly 2,3-diphenylquinoxaline analogues, alkylphospholipids, indole-3-carbinol analogues, sulfonamide derivatives, thiourea derivatives, purine derivatives and other derivatives (BAY 1125976, 3-methyl-xanthine, quinoline-4-carboxamide and 2-[4-(cyclohexa-1,3-dien-1-yl)-1H-pyrazol-3-yl]phenol, 3-oxo-tirucallic acid, 3α- and 3β-acetoxy-tirucallic acids, acetoxy-tirucallic acid) (Nitulescu, Margina et al. 2016).

In order to identify specific adverse effects that could be related to the background of cirrhosis, the newly developed drugs should be preclinically tested in an appropriate animal model. One of the models that most faithfully reproduces human cirrhosis is dietary nitrosamine injured rats (DEN). While most of HCC models have background of normal surrounding liver or moderately fibrotic liver, we used a rat model that develops extensive fibrosis, compensated cirrhosis, decompensated cirrhosis and HCC after chronic administration of diethly nitrosamin (DEN) (Schiffer, Housset et al. 2005).

ARQ 092 and the next generation compound ARQ 751 are potent and highly selective allosteric AKT inhibitors (Yu, Savage et al. 2015). ARQ 092 was identified searching for inhibitors which use the intrinsic negative regulatory function of hydrophobic clusters in the ATP-binding cleft. ARQ 092 binds to inactive, unphosphorylated AKT1 with subnanomolar affinity and inhibits all three isoforms. ARQ 092 and its congener, ARQ 751, have been shown to inhibit proliferation across multiple tumor types and were most potent in cancer cells (Nitulescu, Margina et al. 2016).

In the present study, ARQ 092 and ARQ 751 were investigated not only *in vitro* but also by *in vivo* analyses.

We performed *in vitro* analysis with AKT inhibitors -ARQ 092, ARQ 751 and combination of ARQ 092 and Sorafenib on four different human cell lines Hep3B, HepG2, HuH7 and PLC/PRF. Our results showed a high potency ratio for AKT inhibitor ARQ 092 and ARQ 751 compared to Sorafenib (Table 7) in cell viability analysis by MTT assay. ARQ 092 was highly efficient in these cell lines with a 2 to 6 times, ARQ 751 a 10 to 30 times more potent effect on cell viability than Sorafenib. Combination of ARQ 092 and Sorafenib based on the potency ratio showed a strong synergistic effect in cell viability analysis by MTT assay (Table 6). Similarly, the cells treated with ARQ 092 or ARQ 751 induced apoptosis more than Sorafenib (Figure 3.3 & 3.35). After treatment with combination of ARQ 092 and Sorafenib more apoptotic cells were found as compared to single treatments (Figure 3.21). Interestingly, even

lower concentrations of combination treatment showed strong tumor grown inhibition. In accordance with our results, the combination of Sorafenib with another AKT inhibitor (non-specific AKT-inhibitor Bufalin) has been already tested in vitro by Zhai et al. and showed synergistic effects (Zhai, Hu et al. 2015). By migration analysis, we confirmed that ARQ 092, ARQ 751 and combination of ARQ 092 and Sorafenib significantly decreased cell migration compared to control and was more effective than Sorafenib.

In these studies, we used DEN-induced cirrothic rat model with HCC to test safety and efficacy of a new allosteric inhibitors (ARQ 092&ARQ 751) and combination of AKT inhibitor (ARQ 092) and Sorafenib compared with Sorafenib and control (not treated). AKT inhibitor showed anti-tumor, anti-angiogenic and anti-fibrotic effects with significantly better efficacy than Sorafenib in terms of tumor number, as well as tumor contrast enhancement, and the level of liver fibrosis.

For the first study, ARQ 092 was easily managed in rats with a mean weight loss of only 0.8 % at the end of first study. The most frequent side effects of mTOR inhibitors are diabetes and hyperlipidemia. In our hands, with ARQ 092, there was only small and not significant increase in glucose, and no differences in cholesterol and triglyceride blood levels as well as liver triglyceride levels compared to control and Sorafenib-treated rats (Table 5).

The dose strategy for ARQ 092 in the first *in vivo* study was based on a previous toxicity study (unpublished data). The “one week ON/one week OFF” schedule probably contributed to the good tolerability of the tested regimen. In the second study, where combination with Sorafenib was tested, 5 days ON/9 days OFF schedule was used for ARQ 092 treatment, to decrease possible side effects of treatment. This difference in dosage may explain the slight differences in anti-tumor effect of single.

ARQ 092 treatment that were observed between first and second study. In fact, ARQ 092 single treatment was more intensive in first study and therefore the anti-tumor effect was stronger in comparison with the single treatment of ARQ 092 in the second study. Another difference in treatment, that may affect our results, was the start of treatment. In the first study, ARQ 092 treatment started with one week ON and finished with one week OFF. Therefore, we observed only modest effect of treatment on gene expression, as rats were not treated for one week before the euthanasia. In the second study, ARQ 092 treatment started with one week OFF and finished with week ON. This

may account for our observation of a very strong effect of ARQ 092 treatment on gene expression in the second study as compared to first study.

Previous publications have demonstrated the effect of Sorafenib on HCC in noncirrhotic rats with a good tolerability at doses between 10 mg/Kg in association with another drug (Sieghart, Pinter et al. 2012) and 30 mg/Kg when given alone (Gu, Li et al. 2011) (Yan, Tan et al. 2013). With the cirrhotic rat model, we initially tested a 20 mg/Kg Sorafenib dose, but due to an important weight loss and other symptoms after first days of Sorafenib administration, we had to stop the study. Therefore, we decreased to 10 mg/Kg for Sorafenib. This underlines that new HCC-drugs have to be tested in fibrotic/cirrhotic animal models to better assess side effects of treatment that can be very different between noncirrhotic and cirrhotic livers. Therefore, for the second study, we retained 10 mg/kg Sorafenib treatment.

Another particularity of this study consists in the observation of the kinetic of tumor progression through three sequential MRI scans per individual rat. The dramatic increase of tumor size after 6 weeks in control rats (+ 155.3 ± 16.0%) confirmed the high level of aggressiveness of the DEN-model. Similar results were obtained in both studies. Tumor progression between MRI 1 and MRI 3 was significantly reduced in all groups of treatment compared to control and was the lowest in combination group.

Similarly, according to histological examination, both Sorafenib and ARQ 092 significantly reduced the tumor size compared to the control, but combination treated rats displayed the smallest tumor size. However, only ARQ 092 and combination treated rats displayed a significantly lower number of tumors at the surface of the liver. This suggests that ARQ 092 and combination treatments inhibit the development of new tumors. To be confirmed, this hypothesis needs further experiments with an earlier introduction of ARQ 092 and/or combination treatment that should be performed during the DEN-induction phase. Such an experiment could demonstrate inhibiting effect of ARQ 092 and combination treatment on tumor initiation in context of advanced fibrosis and cirrhosis.

To confirm anti-tumor activity of AKT inhibition on the liver tissue, we performed Ki67 and TUNNEL immunostainings. The inhibition of AKT by ARQ 092 and combination treatments induced basal apoptotic machinery in liver tissue and reduced number of $Ki67^{+}$ cells compare to Sorafenib and control.

The anti-angiogenic effect of ARQ 092 treatment demonstrated by dynamic contrast enhanced MRI2 showed that ARQ 092 induced significantly a lower tumor

enhancement. Besides this, CD34 immunofluorescence staining demonstrated normalization of vasculature in treated groups.

In hepatic fibrosis, excessive connective tissue accumulates in the liver; this tissue represents scarring in response to chronic, repeated liver cell injury. Commonly, fibrosis progresses, disrupting hepatic architecture and eventually function, as regenerating hepatocytes and usually occur cirrhosis then HCC (Bataller and Brenner 2005). Thus, anti-fibrotic effect of ARQ 092 is important to treat HCC. Sirius red staining indicated that liver fibrosis significantly decreased in ARQ 092 and combination groups compare to control and Sorafenib groups. Improvement of liver fibrosis by ARQ 092 and combination groups was confirmed by qPCR analysis. The expression of fibrosis markers such as ACTA 1, TGFβ 1 and Collagen 1, were down-regulated in tumor samples of ARQ 092 and combination group compare to Sorafenib and control.

Our *in vivo* and *in vitro* analyses showed that ARQ 092 and combination treatments strongly and selectively affects AKT pathway. In fact, ARQ 092 is a highly selective allosteric inhibitor that suppresses pan-AKT activity by blocking its phosphorylation and by preventing the inactive form from localizing into plasma membrane which together leads to strong and specific downregulation of downstream targets of AKT (Yu, Savage et al. 2015). Such high specificity was missing in action of catalytic AKT inhibitors that have been previously developed (Rodon, Dienstmann et al. 2013).

However, in Sorafenib-treated rats, the absence of downregulation of the ERK pathway on qPCR and western blot analyses can be surprising, since it has been previously shown that Sorafenib downregulates pERK in rat HCC (Sieghart, Pinter et al. 2012).

This observation is probably due to the DEN-induced strongly aggressive type of HCC and also multiple resistance mechanisms in this model. Higher pAKT in this group is a surrogate marker of such resistance.

In summary we have indicated that two allosteric inhibitor (ARQ 092 and ARQ 751) alone or in combination with Sorafenib potently inhibit AKT pathway both *in vitro* and *in vivo*. Despite difficult conditions with an aggressive model of cancer in cirrhotic rats, single treatment ARQ 092 showed its efficacy in controlling tumor progression, and demonstrated a good safety profile that makes this experimental drug promising in the treatment of HCC in cirrhotic patients. Moreover, the combination with Sorafenib

further increased antitumor efficacy of treatment and can be considered as novel combination strategy of HCC treatment.

As a conclusion, the results presented here confirm the importance of targeting AKT in HCC development and progression. The high potency and high selectivity of these compound warrant further clinical investigation in patient with HCC.

REFERENCES

Alexia, C., G. Fallot, M. Lasfer, G. Schweizer-Groyer and A. Groyer (2004). "An evaluation of the role of insulin-like growth factors (IGF) and of type-I IGF receptor signalling in hepatocarcinogenesis and in the resistance of hepatocarcinoma cells against drug-induced apoptosis." Biochemical Pharmacology **68**(6): 1003-1015.

Andersen, J. B., B. Spee, B. R. Blechacz, I. Avital, M. Komuta, A. Barbour, E. A. Conner, M. C. Gillen, T. Roskams, L. R. Roberts, V. M. Factor and S. S. Thorgeirsson (2012). "Genomic and Genetic Characterization of Cholangiocarcinoma Identifies Therapeutic Targets for Tyrosine Kinase Inhibitors." Gastroenterology **142**(4): 1021-1031.e1015.

Ang, S. F., E. S.-H. Ng, H. Li, Y.-H. Ong, S. P. Choo, J. Ngeow, H. C. Toh, K. H. Lim, H. Y. Yap, C. K. Tan, L. L. P. J. Ooi, A. Y. F. Chung, P. K. H. Chow, K. F. Foo, M.-H. Tan and P. C. Cheow (2015). "The Singapore Liver Cancer Recurrence (SLICER) Score for Relapse Prediction in Patients with Surgically Resected Hepatocellular Carcinoma." PLoS ONE **10**(4): e0118658.

Avila, M. A., C. Berasain, B. Sangro and J. Prieto (2006). "New therapies for hepatocellular carcinoma." Oncogene **25**(27): 3866-3884.

Bataller, R. and D. A. Brenner (2005). "Liver fibrosis." J Clin Invest **115**(2): 209-218.

Bergers, G. and L. E. Benjamin (2003). "Tumorigenesis and the angiogenic switch." Nat Rev Cancer **3**(6): 401-410.

Blankenberg, F. G. and H. W. Strauss (2001). "Will imaging of apoptosis play a role in clinical care? A tale of mice and men." Apoptosis **6**(1): 117-123.

Brennan, M. D., M. L. Rexius-Hall and D. T. Eddington (2015). "A 3D-Printed Oxygen Control Insert for a 24-Well Plate." PLoS ONE **10**(9): e0137631.

Brown, D. B., J. F. Geschwind, M. C. Soulen, S. F. Millward and D. Sacks (2006). "Society of Interventional Radiology position statement on chemoembolization of hepatic malignancies." J Vasc Interv Radiol **17**(2 Pt 1): 217-223.

Bruix, J. and M. Sherman (2011). "Management of hepatocellular carcinoma: An update." Hepatology (Baltimore, Md.) **53**(3): 1020-1022.

Carracedo, A., L. Ma, J. Teruya-Feldstein, F. Rojo, L. Salmena, A. Alimonti, A. Egia, A. T. Sasaki, G. Thomas, S. C. Kozma, A. Papa, C. Nardella, L. C. Cantley, J. Baselga and P. P. Pandolfi (2008). "Inhibition of mTORC1 leads to MAPK pathway activation through a PI3K-dependent feedback loop in human cancer." The Journal of Clinical Investigation **118**(9): 3065-3074.

Cheng, A.-L., Y.-K. Kang, Z. Chen, C.-J. Tsao, S. Qin, J. S. Kim, R. Luo, J. Feng, S. Ye, T.-S. Yang, J. Xu, Y. Sun, H. Liang, J. Liu, J. Wang, W. Y. Tak, H. Pan, K. Burock, J. Zou, D. Voliotis and Z. Guan (2009). "Efficacy and safety of sorafenib in patients in the Asia-Pacific region with advanced hepatocellular carcinoma: a phase III randomised, double-blind, placebo-controlled trial." The Lancet Oncology **10**(1): 25-34.

Chou, T.-C. (2006). "Theoretical Basis, Experimental Design, and Computerized Simulation of Synergism and Antagonism in Drug Combination Studies." Pharmacological Reviews **58**(3): 621-681.

Cillo, U., A. Vitale, M. Bassanello, P. Boccagni, A. Brolese, G. Zanus, P. Burra, S. Fagiuoli, F. Farinati, M. Rugge and D. F. D'Amico (2004). "Liver Transplantation for the Treatment of Moderately or Well-Differentiated Hepatocellular Carcinoma." Annals of Surgery **239**(2): 150-159.

Courtney, K. D., R. B. Corcoran and J. A. Engelman (2010). "The PI3K Pathway As Drug Target in Human Cancer." Journal of Clinical Oncology **28**(6): 1075-1083.

Dienstmann, R., J. Rodon, V. Serra and J. Tabernero (2014). "Picking the Point of Inhibition: A Comparative Review of PI3K/AKT/mTOR Pathway Inhibitors." Molecular Cancer Therapeutics **13**(5): 1021-1031.

El-Serag, H. B. (2012). "Epidemiology of Viral Hepatitis and Hepatocellular Carcinoma." Gastroenterology **142**(6): 1264-1273.e1261.

Ertle, J. M., D. Heider, M. Wichert, B. Keller, R. Kueper, P. Hilgard, G. Gerken and J. F. Schlaak (2013). "A combination of alpha-fetoprotein and des-gamma-carboxy prothrombin is superior in detection of hepatocellular carcinoma." Digestion **87**(2): 121-131.

Evan, G. I. and K. H. Vousden (2001). "Proliferation, cell cycle and apoptosis in cancer." Nature **411**(6835): 342-348.

Finn, R. S. (2013). "Emerging targeted strategies in advanced hepatocellular carcinoma." Semin Liver Dis **33 Suppl 1**: S11-19.

Forner, A., J. M. Llovet and J. Bruix (2012). "Hepatocellular carcinoma." The Lancet **379**(9822): 1245-1255.

Gomez, P. and M. E. Lacouture (2011). "Clinical Presentation and Management of Hand–Foot Skin Reaction Associated with Sorafenib in Combination with Cytotoxic Chemotherapy: Experience in Breast Cancer." The Oncologist **16**(11): 1508-1519.

Gu, F. M., Q. L. Li, Q. Gao, J. H. Jiang, X. Y. Huang, J. F. Pan, J. Fan and J. Zhou (2011). "Sorafenib inhibits growth and metastasis of hepatocellular carcinoma by (2012) blocking STAT3." World J Gastroenterol **17**(34): 3922-3932.

Guertin, D. A., D. M. Stevens, C. C. Thoreen, A. A. Burds, N. Y. Kalaany, J. Moffat, M. Brown, K. J. Fitzgerald and D. M. Sabatini (2006). "Ablation in Mice of the mTORC Components raptor, rictor, or mLST8 Reveals that mTORC2 Is Required for Signaling to Akt-FOXO and PKCα, but Not S6K1." Developmental Cell **11**(6): 859-871.

Guichard, C., G. Amaddeo, S. Imbeaud, Y. Ladeiro, L. Pelletier, I. B. Maad, J. Calderaro, P. Bioulac-Sage, M. Letexier, F. Degos, B. Clément, C. Balabaud, E. Chevet, A. Laurent, G. Couchy, E. Letouzé, F. Calvo and J. Zucman-Rossi (2012). "Integrated analysis of somatic mutations and focal copy-number (2013) changes identifies key genes and pathways in hepatocellular carcinoma. (2014) " Nature Genetics **44**(6): 694-698.

Hanahan, D. and R. A. Weinberg (2000). "The Hallmarks of Cancer." Cell **100**(1): 57-70.

Hanahan, D. and Robert A. Weinberg (2011). "Hallmarks of Cancer: The Next Generation." Cell **144**(5): 646-674.

Hann, B. and A. Balmain (2001). "Building 'validated' mouse models of human cancer." Current Opinion in Cell Biology **13**(6): 778-784.

Haybaeck, J., N. Zeller, M. J. Wolf, A. Weber, U. Wagner, M. O. do Kurrer, J. Bremer, G. Iezzi, R. Graf, P.-A. Clavien, R. Thimme, H. Blum, S. A. Nedospasov, K. Zatloukal, M. Ramzan, S. Ciesek, T. Pietschmann, P. N. Marche, M. Karin, M. Kopf, J. L. Browning, A. Aguzzi and M. Heikenwalder (2009). "A lymphotoxin-driven pathway to hepatocellular carcinoma." Cancer cell **16**(4): 295-308.

Hayflick, L. (1997). "Mortality and immortality at the cellular level. A review. " Biochemistry (Mosc) **62**(11): 1180-1190.

Heindryckx, F., I. Colle and H. Van Vlierberghe (2009). "Experimental mouse models for hepatocellular carcinoma research." International Journal of Experimental

Pathology **90**(4): 367-386.

Höpfner, M., D. Schuppan and H. Scherübl (2008). "Growth factor receptors and related signalling pathways as targets for novel treatment strategies of hepatocellular cancer." World Journal of Gastroenterology : WJG **14**(1): 1-14.

Hulkower, K. I. and R. L. Herber (2011). "Cell Migration and Invasion Assays as Tools for Drug Discovery." Pharmaceutics **3**(1): 107.

Hussain, S. P., J. Schwank, F. Staib, X. W. Wang and C. C. Harris (2007). "TP53 mutations and hepatocellular carcinoma: insights into the etiology and pathogenesis of liver cancer." Oncogene **26**(15): 2166-2176.

Jemal, A., F. Bray, M. M. Center, J. Ferlay, E. Ward and D. Forman (2011). "Global cancer statistics." CA Cancer J Clin **61**(2): 69-90.

Jiang, X., K. Feng, Y. Zhang, Z. Li, F. Zhou, H. Dou and T. Wang (2015). "Sorafenib and DE605, a novel c-Met inhibitor, synergistically suppress hepatocellular carcinoma." Oncotarget **6**(14): 12340-12356.

Josephs, D. H. and D. Sarker (2015). "Pharmacodynamic Biomarker Development for PI3K Pathway Therapeutics." Translational Oncogenomics **7**(Suppl 1): 33-49.

Kitamoto, T., A. Kitamoto, M. Yoneda, H. Hyogo, H. Ochi, T. Nakamura, H. Teranishi, S. Mizusawa, T. Ueno, K. Chayama, A. Nakajima, K. Nakao, A. Sekine and K. Hotta (2013). "Genome-wide scan revealed that polymorphisms in the PNPLA3, SAMM50, and PARVB genes are associated with development and progression of nonalcoholic fatty liver disease in Japan." Human Genetics **132**(7): 783-792.

Kunter, I., E. Erdal, D. Nart, F. Yilmaz, S. Karademir, O. Sagol and N. Atabey (2014). "Active form of AKT controls cell proliferation and response to apoptosis in hepatocellular carcinoma." Oncology reports **31**(2): 573-580.

Lapierre, J.-M., S. Eathiraj, D. Vensel, Y. Liu, C. O. Bull, S. Cornell-Kennon, S. Iimura, E. W. Kelleher, D. E. Kizer, S. Koerner, S. Makhija, A. Matsuda, M. Moussa, N. Namdev, R. E. Savage, J. Szwaya, E. Volckova, N. Westlund, H. Wu and B. Schwartz (2016). "Discovery of 3-(3-(4-(1-Aminocyclobutyl)phenyl)-5-phenyl-3H-imidazo[4,5-b]pyridin-2-yl)pyridin-2-amine (ARQ 092): An Orally Bioavailable, Selective, and Potent Allosteric AKT Inhibitor." Journal of Medicinal Chemistry **59**(13): 6455-6469.

Laplante, M. and D. M. Sabatini (2012). "mTOR signaling." Cold Spring Harbor Perspectives in Biology **4**(2): 10.1101/cshperspect.a011593 a011593.

Lee, J.-S., I.-S. Chu, A. Mikaelyan, D. F. Calvisi, J. Heo, J. K. Reddy and S. S. Thorgeirsson (2004). "Application of comparative functional genomics to identify best-fit mouse models to study human cancer." Nat Genet **36**(12): 1306-1311.

Lee, P. I., M. H. Chang, D. S. Chen and C. Y. Lee (1989). "Serum alpha-fetoprotein levels in normal infants: a reappraisal of regression analysis and sex difference. " J Pediatr Gastroenterol Nutr **8**(1): 19-25.

Li, S. and M. Mao (2013). "Next generation sequencing reveals genetic landscape of hepatocellular carcinomas." Cancer Letters **340**(2): 247-253.

Li, Y., Z.-H. Gao and X.-J. Qu (2015). "The Adverse Effects of Sorafenib in Patients with Advanced Cancers." Basic & Clinical Pharmacology & Toxicology **116**(3): 216-221.

Lim, I. K. (2002). "Spectrum of molecular changes during hepatocarcinogenesis induced by DEN and other chemicals in Fischer 344 male rats." Mechanisms of ageing and development **123**(12): 1665-1680.

Liu, L., Y. Cao, C. Chen, X. Zhang, A. McNabola, D. Wilkie, S. Wilhelm, M. Lynch and C. Carter (2006). "Sorafenib Blocks the RAF/MEK/ERK Pathway, Inhibits Tumor Angiogenesis, and Induces Tumor Cell Apoptosis in Hepatocellular Carcinoma Model PLC/PRF/5." Cancer Research **66**(24): 11851-11858.

Llovet, J. M. and J. Bruix (2008). "Molecular Targeted Therapies in Hepatocellular Carcinoma." Hepatology (Baltimore, Md.) **48**(4): 1312-1327.

Llovet , J. M., S. Ricci , V. Mazzaferro , P. Hilgard , E. Gane , J.-F. Blanc , A. C. de Oliveira , A. Santoro , J.-L. Raoul , A. Forner , M. Schwartz , C. Porta , S. Zeuzem , L. Bolondi , T. F. Greten , P. R. Galle , J.-F. Seitz , I. Borbath , D. Häussinger , T. Giannaris , M. Shan , M. Moscovici , D. Voliotis and J. Bruix (2008). "Sorafenib in Advanced Hepatocellular Carcinoma." New England (2009) Journal of Medicine **359**(4): 378-390.

Lozano, G. M., I. Bejarano, J. Espino, Gonz, Aacute, D. Lez, Ortiz, Aacute, gueda, Garc, Iacute, J. F. A, Rodr, Iacute, A. B. Guez, J. Pariente, eacute and A (2009). "Relationship between Caspase Activity and Apoptotic Markers in Human Sperm in Response to Hydrogen Peroxide and Progesterone." Journal of Reproduction and Development **55**(6): 615-621.

Lu, S., S. Li and J. Zhang (2014). "Harnessing allostery: a novel approach to drug discovery." Med Res Rev **34**(6): 1242-1285.

Macek Jilkova, Z., S. Afzal, H. Marche, T. Decaens, N. Sturm, E. Jouvin-Marche, B. Huard and P. N. Marche (2016). "Progression of fibrosis in patients with chronic viral hepatitis is associated with IL-17+ neutrophils." Liver International **36**(8): 1116-1124.

Matter, M. S., T. Decaens, J. B. Andersen and S. S. Thorgeirsson (2014). "Targeting the mTOR pathway in hepatocellular carcinoma: Current state and future trends." Journal of hepatology **60**(4): 855-865.

Mattmann, M. E., S. L. Stoops and C. W. Lindsley (2011). "Inhibition of Akt with small molecules and biologics: historical perspective and current status of the patent landscape." Expert opinion on therapeutic patents **21**(9): 1309-1338.

Miraglia, R., G. Pietrosi, L. Maruzzelli, I. Petridis, S. Caruso, G. Marrone, G. Mamone, G. Vizzini, A. Luca and B. Gridelli (2007). "Efficacy of transcatheter embolization/chemoembolization (TAE/TACE) for the treatment of single hepatocellular carcinoma." World Journal of Gastroenterology : WJG **13**(21): 2952-2955.

Mosmann, T. (1983). "Rapid colorimetric assay for cellular growth and survival: Application to proliferation and cytotoxicity assays." Journal of Immunological Methods **65**(1): 55-63.

Nault, J. C., M. Mallet, C. Pilati, J. Calderaro, P. Bioulac-Sage, C. Laurent, A. Laurent, D. Cherqui, C. Balabaud and J. Z. Rossi (2013). "High frequency of telomerase reverse-transcriptase promoter somatic mutations in hepatocellular carcinoma and preneoplastic lesions." Nature Communications **4**: 2218.

Nitulescu, G. M., D. Margina, P. Juzenas, Q. Peng, O. T. Olaru, E. Saloustros, C. Fenga, D. A. Spandidos, M. Libra and A. M. Tsatsakis (2016). "Akt inhibitors in cancer treatment: The long journey from drug discovery to clinical use (Review)." International Journal of Oncology **48**(3): 869-885.

Obed, A., T.-Y. Tsui, A. A. Schnitzbauer, M. Obed, H. J. Schlitt, H. Becker and T. Lorf (2008). "Liver transplantation as curative approach for advanced hepatocellular (2009) carcinoma: is it justified?" Langenbeck's Archives of Surgery **393**(2): (2010) 141-147.

Oda, H., Y. Imai, Y. Nakatsuru, J.-i. Hata and T. Ishikawa (1996). "Somatic Mutations of the APC Gene in Sporadic Hepatoblastomas." Cancer Research **56**(14): 3320-3323.

Ogawa, K. (2009). "Molecular pathology of early stage chemically induced hepatocarcinogenesis." Pathology International **59**(9): 605-622.

Peterson, C., N. Park, N. Hall and M. E. P. Seligman (2009). "Zest and work." Journal of Organizational Behavior **30**(2): 161-172.

Polakis, P. (2000). "Wnt signaling and cancer." Genes Dev **14**(15): 1837-1851.

Poynard, T., P. Bedossa and P. Opolon (1997). "Natural history of liver fibrosis progression in patients with chronic hepatitis C." The Lancet **349**(9055): 825-832.

Ravi, S. and A. K. Singal (2014). "Regorafenib: an evidence-based review of its potential in patients with advanced liver cancer." Core Evidence **9**: 81-87.

Reataza, M. and D. K. Imagawa (2014). "Advances in managing hepatocellular carcinoma." Front Med **8**(2): 175-189.

Roberts, P. J. and C. J. Der (2007). "Targeting the Raf-MEK-ERK mitogen-activated protein kinase cascade for the treatment of cancer." Oncogene **26**(22): 3291-3310.

Rodon, J., R. Dienstmann, V. Serra and J. Tabernero (2013). "Development of PI3K inhibitors: lessons learned from early clinical trials." Nat Rev Clin Oncol **10**(3): 143-153.

Salih, D. A. M. and A. Brunet (2008). "FoxO transcription factors in the maintenance of cellular homeostasis during aging." Current opinion in cell biology **20**(2): 126-136.

Sanz-Cameno, P., M. Trapero-Marugán, M. Chaparro, E. A. Jones and R. Moreno-Otero (2010). "Angiogenesis: From Chronic Liver Inflammation to Hepatocellular Carcinoma." Journal of Oncology **2010**: 7.

Scheid, M. P. and J. R. Woodgett (2003). "Unravelling the activation mechanisms of protein kinase B/Akt." FEBS Lett **546**(1): 108-112.

Schiffer, E., C. Housset, W. Cacheux, D. Wendum, C. Desbois-Mouthon, C. Rey, F. Clergue, R. Poupon, V. Barbu and O. Rosmorduc (2005). "Gefitinib, an EGFR inhibitor, prevents hepatocellular carcinoma development in the rat liver with cirrhosis." Hepatology **41**(2): 307-314.

Shaib, Y. and H. B. El-Serag (2004). "The epidemiology of cholangiocarcinoma." Semin Liver Dis **24**(2): 115-125.

Shen, Y. C., C. Hsu and A. L. Cheng (2010). "Molecular targeted therapy for advanced hepatocellular carcinoma: current status and future perspectives." J Gastroenterol

45(8): 794-807.

Shibata, T. and H. Aburatani (2014). "Exploration of liver cancer genomes." Nat Rev Gastroenterol Hepatol **11**(6): 340-349.

Shiloh, Y. and Y. Ziv (2013). "The ATM protein kinase: regulating the cellular response to genotoxic stress, and more." Nat Rev Mol Cell Biol **14**(4): 197-210.

Siegel, R., J. Ma, Z. Zou and A. Jemal (2014). "Cancer statistics, 2014." CA: A Cancer Journal for Clinicians **64**(1): 9-29.

Sigel, R. L., K. D. Miller and A. Jemal (2016). "Cancer statistics, 2016." CA: A Cancer Journal for Clinicians **66**(1): 7-30.

Sieghart, W., M. Pinter, B. Dauser, N. Rohr-Udilova, A.-C. Piguet, G. Prager, H. Hayden, H.-P. Dienes, J.-F. Dufour and M. Peck-Radosavljevic (2012). "Erlotinib and sorafenib in an orthotopic rat model of hepatocellular carcinoma." Journal of Hepatology **57**(3): 592-599.

Taguchi, K., H. Motohashi and M. Yamamoto (2011). "Molecular mechanisms of the Keap1–Nrf2 pathway in stress response and cancer evolution." Genes to Cells **16**(2): 123-140.

Van Zijl, F., G. Krupitza and W. Mikulits (2011). "Initial steps of metastasis: Cell invasion and endothelial transmigration." Mutation Research **728**(1-2): 23-34.

Vivanco, I. and C. L. Sawyers (2002). "The phosphatidylinositol 3-Kinase-AKT pathway in human cancer." Nat Rev Cancer **2**(7): 489-501.

Vucur, M., C. Roderburg, K. Bettermann, F. Tacke, M. Heikenwalder, C. Trautwein and T. Luedde (2010). "Mouse models of hepatocarcinogenesis: What can we learn for the prevention of human hepatocellular carcinoma?" Oncotarget **1**(5): 373-378.

Wallin, J. J., K. A. Edgar, J. Guan, M. Berry, W. W. Prior, L. Lee, J. D. Lesnick, C. Lewis, J. Nonomiya, J. Pang, L. Salphati, A. G. Olivero, D. P. Sutherlin, C. O'Brien, J. M. Spoerke, S. Patel, L. Lensun, R. Kassees, L. Ross, M. R. Lackner, D. Sampath, M. Belvin and L. S. Friedman (2011). "GDC-0980 Is a Novel Class I PI3K/mTOR Kinase Inhibitor with Robust Activity in Cancer Models Driven by the PI3K Pathway." Molecular Cancer Therapeutics **10**(12): 2426-2436.

Wang, T., J. Zeng, C. B. Lowe, R. G. Sellers, S. R. Salama, M. Yang, S. M. Burgess, R. K. Brachmann and D. Haussler (2007). "Species-specific endogenous retroviruses shape the transcriptional network of the human tumor suppressor protein p53." Proceedings of the National Academy of Sciences **104**(47): 18613-

18618.

Weigelt, B. and J. Downward (2012). "Genomic Determinants of PI3K Pathway Inhibitor Response in Cancer." Frontiers in Oncology **2**: 109.

Wendel, H.-G., E. d. Stanchina, J. S. Fridman, A. Malina, S. Ray, S. Kogan, C. Cordon-Cardo, J. Pelletier and S. W. Lowe (2004). "Survival signalling by Akt and eIF4E in oncogenesis and cancer therapy." Nature **428**(6980): 332-337.

Whittaker, S., R. Marais and A. X. Zhu (2010). "The role of signaling pathways in the development and treatment of hepatocellular carcinoma." Oncogene **29**(36): 4989-5005.

Wilhelm, S. M., L. Adnane, P. Newell, A. Villanueva, J. M. Llovet and M. Lynch (2008). "Preclinical overview of sorafenib, a multikinase inhibitor that targets (2009) both Raf and VEGF and PDGF receptor tyrosine kinase signaling." (2010) Molecular Cancer Therapeutics **7**(10): 3129-3140.

Wilhelm, S. M., C. Carter, L. Tang, D. Wilkie, A. McNabola, H. Rong, C. Chen, X. Zhang, P. Vincent, M. McHugh, Y. Cao, J. Shujath, S. Gawlak, D. Eveleigh, B. Rowley, L. Liu, L. Adnane, M. Lynch, D. Auclair, I. Taylor, R. Gedrich, A. Voznesensky, B. Riedl, L. E. Post, G. Bollag and P. A. Trail (2004). "BAY 43-9006 Exhibits Broad Spectrum Oral Antitumor Activity and Targets the RAF/MEK/ERK Pathway and Receptor Tyrosine Kinases Involved in Tumor Progression and Angiogenesis." Cancer Research **64**(19): 7099-7109.

Wu, W.-I., W. C. Voegtli, H. L. Sturgis, F. P. Dizon, G. P. A. Vigers and B. J. Brandhuber (2010). "Crystal Structure of Human AKT1 with an Allosteric Inhibitor Reveals a New Mode of Kinase Inhibition." PLoS ONE **5**(9): e12913.

Yan, J., C. Tan, F. Gu, J. Jiang, M. Xu, X. Huang, Z. Dai, Z. Wang, J. Fan and J. Zhou (2013). "Sorafenib delays recurrence and metastasis after liver transplantation in (2014) a rat model of hepatocellular carcinoma with high expression of (2015) phosphorylated extracellular signal-regulated kinase." Liver (2016) Transplantation **19**(5): 507-520.

Yang, L., G. Qiao, H. Ying, J. Zhang and F. Yin (2010). "TCR-Induced Akt Serine 473 Phosphorylation Is Regulated by Protein Kinase C-Alpha." Biochemical and biophysical research communications **400**(1): 16-20.

Yu, Y., R. E. Savage, S. Eathiraj, J. Meade, M. J. Wick, T. Hall, G. Abbadessa and B. Schwartz (2015). "Targeting AKT1-E17K and the PI3K/AKT Pathway with an Allosteric AKT Inhibitor, ARQ 092." PLoS ONE **10**(10): e0140479.

Yuzugullu, H., K. Benhaj, N. Ozturk, S. Senturk, E. Celik, A. Toylu, N. Tasdemir, M.

Yilmaz, E. Erdal, K. C. Akcali, N. Atabey and M. Ozturk (2009). "Canonical Wnt signaling is antagonized by noncanonical Wnt5a in hepatocellular carcinoma cells." Molecular Cancer **8**: 90-90.

Zender, L., A. Villanueva, V. Tovar, D. Sia, D. Y. Chiang and J. M. Llovet (2010). "Cancer Gene Discovery in Hepatocellular Carcinoma." Journal of hepatology **52**(6): 921-929.

Zhai, B., F. Hu, X. Jiang, J. Xu, D. Zhao, B. Liu, S. Pan, X. Dong, G. Tan, Z. Wei, H. Qiao, H. Jiang and X. Sun (2014). "Inhibition of Akt Reverses the Acquired Resistance to Sorafenib by Switching Protective Autophagy to Autophagic Cell Death in Hepatocellular Carcinoma." Molecular Cancer Therapeutics **13**(6): 1589-1598.

Zhai, B., F. Hu, H. Yan, D. Zhao, X. Jin, T. Fang, S. Pan, X. Sun and L. Xu (2015). "Bufalin Reverses Resistance to Sorafenib by Inhibiting Akt Activation in Hepatocellular Carcinoma: The Role of Endoplasmic Reticulum Stress." PLoS ONE **10**(9): e0138485.

Zhai, B. and X.-Y. Sun (2013). "Mechanisms of resistance to sorafenib and the corresponding strategies in hepatocellular carcinoma." World Journal of Hepatology **5**(7): 345-352.

Zhang, C., X. Guo, G. Jiang, L. Zhang, Y. Yang, F. Shen, M. Wu and L. Wei (2008). "CpG island methylator phenotype association with upregulated telomerase activity in hepatocellular carcinoma." International Journal of Cancer **123**(5): 998-1004.

Zhou, L., J. Liu and F. Luo (2006). "Serum tumor markers for detection of hepatocellular carcinoma." World Journal of Gastroenterology : WJG **12**(8): 1175-1181.

Zimmer, V. and F. Lammert (2011). "Genetics in liver disease: new concepts." Current Opinion in Gastroenterology **27**(3): 231-239.

APPENDIX A

MEDIAS

A.1. MEM Growth Medium

Minimum Essential Medium Eagle growth medium, fethal bovine serum (FBS) and gentamicine sulfate were obtained from Gibco, BRL.

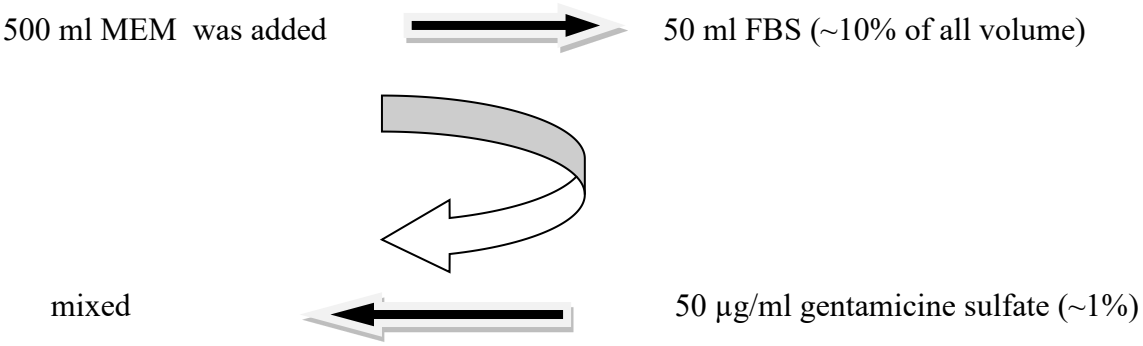

A.2. DMEM Growth Medium

Dulbecco's modified Eagle'S medium (DMEM) growth medium, fethal bovine serum (FBS) and gentamicine sulfate were obtained from Gibco, BRL.

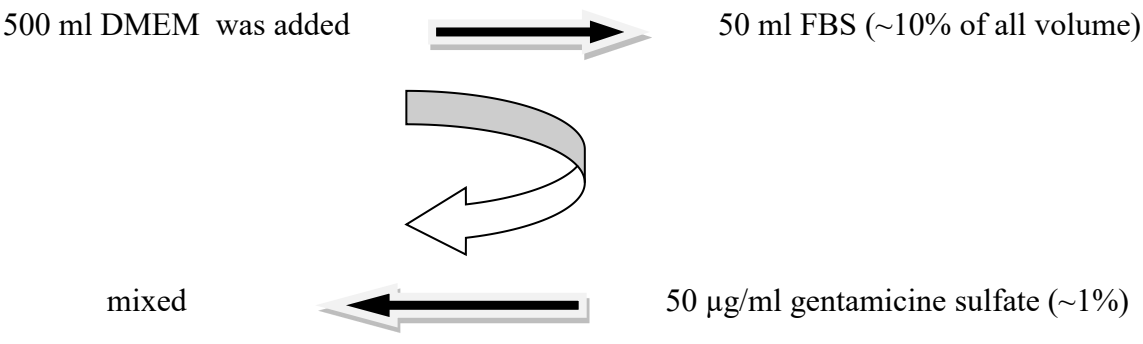

APPENDIX B

CHEMICALS, REAGENTS AND SOLUTIONS

B.1. Cell Lines

Hep3B, HepG2, HuH7 and PLC/PRF cell lines were provided by Prof. Dr. Thomas Deacen in Institute for Advance Biosciences, Grenoble/France.

Table.1.B. Chemicals and Reagents Used in Experiments

No	CHEMICALS	COMPANY
1	Dimethly Sulfoxide (DMSO)	Sigma
2	Trypan Blue Dye	Sigma
3	Phosphate Buffered Saline (PBS)	Invitrogen
4	Gentamicine Sulfate	Gibco
5	Fetal Bovine Serum (FBS)	Gibco
6	MTT Reagent	Sigma
7	0,5M Tris-HCl, pH 6,8	AppliChem
8	Annexin-V Apoptosis Detection Kit I	BD Pharmingen
9	Bovine Serum Albumine (BSA)	Sigma

(cont. on next page)

Table1.B. (cont.)

10	Coomassie Brilliant Blue G-250	AppliChem
11	Absolute Ethanol	AppliChem
12	Phosphoric Acid	AppliChem
13	Ethylenediaminetetraacetic acid (EDTA)	Sigma
14	Protease inhibitor	Roche
15	Glycerol	AppliChem
16	Bromophenol Blue (%0.5)	AppliChem
17	CHAPS (%2)	AppliChem
18	Marcaptoethanol	AppliChem
19	SDS	AppliChem
20	phosphoric acid	AppliChem
21	Acrylamide	AppliChem
22	Bisacrylamide	AppliChem
23	1.5 M Tris – HCl pH = 8.8	AppliChem
24	Ammoniun Persulfate (APS)	Sigma
25	Tetramethylethylenediamine (TEMED)	Sigma

(cont. on next page)

Table1.B. (cont.)

26	Trypsin	Sigma
27	Triton X-100	Sigma
28	RNase	Thermo